

AFFDL-TR-78-124

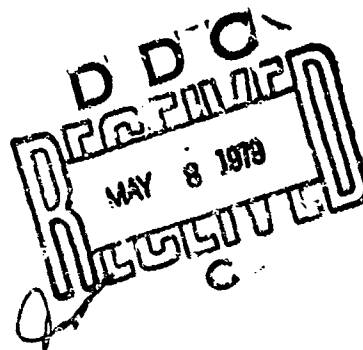
**LEVEL**

(2)

AD A068324

**THE EFFECT OF WINGLETS ON THE KC-135A AIRCRAFT**

George W. Loptier  
Flight Vehicle Branch  
Aeromechanics Division



November 1978

TECHNICAL REPORT AFFDL-TR-78-124

Final Report for Period June 1975 - October 1977

Approved for public release; distribution unlimited.

AIR FORCE FLIGHT DYNAMICS LABORATORY  
AIR FORCE WRIGHT AERONAUTICAL LABORATORIES  
AIR FORCE SYSTEMS COMMAND  
WRIGHT-PATTERSON AIR FORCE BASE, OHIO 45433

DDC FILE COPY

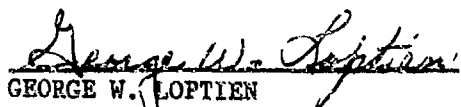
79 05 07 019

NOTICE

When Government drawings, specifications, or other data are used for any purpose other than in connection with a definitely related Government procurement operation, the United States Government thereby incurs no responsibility nor any obligation whatsoever; and the fact that the government may have formulated, furnished, or in any way supplied the said drawings, specifications, or other data, is not to be regarded by implication or otherwise as in any manner licensing the holder or any other person or corporation, or conveying any rights or permission to manufacture, use, or sell any patented invention that may in any way be related thereto.

This report has been reviewed by the Information Office (OI) and is releasable to the National Technical Information Service (NTIS). At NTIS, it will be available to the general public, including foreign nations.

This technical report has been reviewed and is approved for publication.

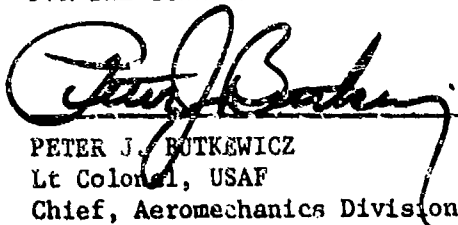


GEORGE W. LOPTIEN  
Project Engineer  
Flight Vehicle Branch  
Aeromechanics Division



CHARLES J. COSENZA  
Chief, Flight Vehicle Branch  
Aeromechanics Division

FOR THE COMMANDER



PETER J. BUTKEWICZ  
Lt Colonel, USAF  
Chief, Aeromechanics Division

"If your address has changed, if you wish to be removed from our mailing list, or if the addressee is no longer employed by your organization please notify AFFDL/FKS, W-PAFB, OH 45433 to help us maintain a current mailing list".

Copies of this report should not be returned unless return is required by security considerations, contractual obligations, or notice on a specific document.

SECURITY CLASSIFICATION OF THIS PAGE (When Data Entered)

REPORT DOCUMENTATION PAGE		READ INSTRUCTIONS BEFORE COMPLETING FORM
1. REPORT NUMBER AFFDL-TR-78-124	2. GOVT ACCESSION NO.	3. RECIPIENT'S CATALOG NUMBER
4. AUTHOR(s) THE EFFECT OF WINGLETS ON THE KC-135 AIRCRAFT	5. TYPE OF REPORT & PERIOD COVERED Final Report June 1975 - October 1977	6. PERFORMING ORG. REPORT NUMBER
7. AUTHOR(s) George W. Loptien	8. CONTRACT OR GRANT NUMBER(s) 62201F	
9. PERFORMING ORGANIZATION NAME AND ADDRESS Air Force Flight Dynamics Laboratory (AFFDL/FXS) Air Force Wright Aeronautical Laboratories Wright-Patterson Air Force Base, Ohio 45433	10. PROGRAM ELEMENT, PROJECT, TASK AREA & WORK UNIT NUMBERS Project 2404, Task 240416, Work Unit 24041603	
11. CONTROLLING OFFICE NAME AND ADDRESS Air Force Flight Dynamics Laboratory (AFFDL/FXS) Air Force Wright Aeronautical Laboratories Wright-Patterson Air Force Base, Ohio 45433	12. REPORT DATE November 1978	
14. MONITORING AGENCY NAME & ADDRESS (if different from Controlling Office) 12 118p.	13. NUMBER OF PAGES 118	
	15. SECURITY CLASS. (of this report) Unclassified	
	15a. DECLASSIFICATION/DOWNGRADING SCHEDULE	
16. DISTRIBUTION STATEMENT (of this Report) Approved for public release; distribution unlimited.		
17. DISTRIBUTION STATEMENT (of the abstract entered in Block 20, if different from Report) 16 16		
18. SUPPLEMENTARY NOTES		
19. KEY WORDS (Continue on reverse side if necessary and identify by block number) KC-135, Winglets, Drag Reduction, Fuel Savings		
20. ABSTRACT (Continue on reverse side if necessary and identify by block number) To investigate the effects of winglets on the aerodynamic characteristics of the KC-135 aircraft, semispan and full-span wind tunnel models with winglets have been investigated in the NASA/LRC 8-Foot Transonic Pressure Tunnel. At cruise conditions, the full-span tests indicated a total drag reduction of 5.3 percent for the model with the Boeing and NASA upper plus lower winglet configurations and 6.5 percent for the model with the NASA upper winglet configuration. A wing-tip-extension configuration tested on the semispan model (over)		

DD FORM 1 JAN 73 1473 EDITION OF 1 NOV 65 IS OBSOLETE

SECURITY CLASSIFICATION OF THIS PAGE (When Data Entered)

012 070 *Gen*

20. Abstract (Continued)

had a drag reduction of about 3 percent compared to about 5 to 7 percent for the winglet configurations, however, the tip extension was not optimized for drag reduction. At cruise conditions, the wing tip extension produced the greatest increase in the wing root bending moment and the upper winglets the least. The increase in wing root bending moment at cruise conditions varied from about 2.5 percent with the Boeing winglets, to about 3.5 percent with the tip extension. At cruise flight conditions, winglets on the KC-135A aircraft were estimated to reduce the drag about 8.2 percent and increase the maximum lift-drag ratio about 9.5 percent.

ACCESSION for	
NTIS	WFO Section <input checked="" type="checkbox"/>
DDC	RII Section <input type="checkbox"/>
UNANNOUNCED	<input type="checkbox"/>
DESTINATION	
BY	
DISTRIBUTION	
A	

FOREWORD

This report was prepared by Mr. George W. Loptien of the Flight Vehicle Branch, Aeromechanics Division, Air Force Flight Dynamics Laboratory, Wright-Patterson Air Force Base, Ohio, under Project 2404, Aerodynamic Synthesis and Flight Research, Task 240416, Unified Flight Mechanics Technology, Work Unit 24041603, Analysis and Evaluation of Aero Configuration Advancements.

Winglets appear to offer significant improvement in aerodynamic efficiency and fuel and operating cost savings. This Report summarizes basic information concerning winglets and is part of an overall plan to develop winglet technology for flight test demonstration.

Winglets have been investigated using semispan and full span KC-135A models in the NASA/LaRC 8-Foot Transonic Pressure Tunnel. Basic results from this investigation are presented in this Report. Mr. Stuart G. Flechner, NASA/LaRC, was the project engineer.

## TABLE OF CONTENTS

SECTION	PAGE
INTRODUCTION	1
MODEL AND TEST APPARATUS	2
DISCUSSION	5
Winglets	5
Results of Boeing Investigations	7
Aerodynamic Data	8
Winglet Configuration	9
Wing Root Bending Moment	13
Winglet Incidence	14
Winglet Cant	15
Wing Tip Extensions	16
Flap and Horizontal Tail Deflection	17
Lateral-Directional Stability	18
Aileron Deflection	18
Winglet Loss	19
Full-Scale Winglet Performance	20
CONCLUSIONS	21
APPENDIX A - Effect of Wing Tip Removal on Basic KC-135A Wing	25
APPENDIX B - Characteristics of Basic KC-135A Model	28
APPENDIX C - Comparison of Full-Span and Semispan Model Data	30
REFERENCES	102

## ILLUSTRATIONS

FIGURE		PAGE
1	Semispan KC-135A Model in the NASA/LaRC 8-Foot Transonic Pressure Tunnel	32
2	Basic Dimensions of KC-135A Semispan Model	33
3	NASA Winglet Configurations	34
4	Boeing Winglet Configuration	35
5	Leading and Trailing Edge Flaps for Semispan KC-135A Model	36
6	Full Span 0.035 Scale KC-135A Model With Low Speed Wing and Winglets	37
7	Wing Flap and Aileron Geometry of Full-Span KC-135A Model	38
8	Effect of Winglet Length at Zero Cant $C_{L\_CONFIG} = 0.426$	39
9	Effect of Winglet Cant Angle - Variable Span $C_{L\_CONFIG} = 0.426$	40
10	Equal Area Tip Extension Geometry Investigated in Reference 1	41
11	Comparison of Induced Drag and Wing Root Bending Moment Increments Between Zero Cant Winglets and Tip Extensions	42
12	Comparison of Pitching Moment Increment Between Zero Cant Winglets and Tip Extensions	43
13	Effect of Winglet Configuration on Semispan KC-135A Model Drag. $M = 0.78$ . $\delta_F = 0$	44
14	Effect of Winglet Configuration on Semispan KC-135A Model Drag. $M = 0.30$ . $\delta_F = 25$ Degrees	45
15	Effect of Winglet Configuration on Full-Span KC-135A Model Drag. $M = 0.30$ . $\delta_F = 0$	46
16	Effect of Winglet Configuration on Full-Span KC-135A Model Drag. $M = 0.50$ . $\delta_F = 0$	47

## ILLUSTRATIONS (CONTINUED)

FIGURE		PAGE
17	Effect of Winglet Configuration on Full-Span KC-135A Model Drag. $M = 0.70$ . $\delta_F = 0$	48
18	Effect of Winglet Configuration on Full-Span KC-135A Model Drag. $M = 0.75$ . $\delta_F = 0$	49
19	Effect of Winglet Configuration on Full-Span KC-135A Model Drag. $M = 0.78$ . $\delta_F = 0$	50
20	Effect of Winglet Configuration on Full-Span KC-135A Model Drag. $M = 0.80$ . $\delta_F = 0$	51
21	Effect of Winglet Configuration on Full-Span KC-135A Model Drag for Different Mach Numbers. $C_L = 0.426$	52
22	Effect of Winglet Configuration on Full-Span KC-135A Model Lift. $M = 0.30$ . $\delta_F = 0$	53
23	Effect of Winglet Configuration on Full-Span KC-135A Model Lift. $M = 0.50$ . $\delta_F = 0$	53
24	Effect of Winglet Configuration on Full-Span KC-135A Model Lift. $M = 0.70$ . $\delta_F = 0$	54
25	Effect of Winglet Configuration on Full-Span KC-135A Model Lift. $M = 0.75$ . $\delta_F = 0$	54
26	Effect of Winglet Configuration on Full-Span KC-135A Model Lift. $M = 0.78$ . $\delta_F = 0$	55
27	Effect of Winglet Configuration on Full-Span KC-135A Model Lift. $M = 0.80$ . $\delta_F = 0$	55
28	Effect of Winglet Configuration on Full-Span KC-135A Model Lift for Different Mach Numbers. $C_L = 0.426$	56
29	Effect of Winglet Configuration on Full-Span KC-135A Model Lift Curve Slope for Different Mach Numbers	57
30	Effect of Winglet Configuration on Full-Span KC-135A Model Angle of Attack Near Cruise Conditions	57
31	Effect of Winglet Configuration on Full-Span KC-135A Model Untrimmed Maximum Lift-Drag Ratio for Different Mach Numbers	58



## ILLUSTRATIONS (CONTINUED)

FIGURE		PAGE
32	Effect of Winglet Configuration on Full-Span KC-135A Model Pitching Moment. $M = 0.30$ . $\delta_F = 0$	59
33	Effect of Winglet Configuration on Full-Span KC-135A Model Pitching Moment. $M = 0.50$ . $\delta_F = 0$	59
34	Effect of Winglet Configuration on Full-Span KC-135A Model Pitching Moment. $M = 0.70$ . $\delta_F = 0$	60
35	Effect of Winglet Configuration on Full-Span KC-135A Model Pitching Moment. $M = 0.75$ . $\delta_F = 0$	60
36	Effect of Winglet Configuration on Full-Span KC-135A Model Pitching Moment. $M = 0.78$ . $\delta_F = 0$	61
37	Effect of Winglet Configuration on Full-Span KC-135A Model Pitching Moment. $M = 0.80$ . $\delta_F = 0$	61
38	Effect of Winglet Configuration on Full-Span KC-135A Model Pitching Moment for Different Mach Numbers. $C_L = 0.426$	62
39	Effect of Winglet Configuration on Full-Span KC-135A Model Drag. $M = 0.30$ , $\delta_F = 50$ Degrees. $i_H = -10$ Degrees	63
40	Effect of Winglet Configuration on Full-Span KC-135A Model Lift. $M = 0.30$ , $\delta_F = 50$ Degrees $i_H = -10$ Degrees	64
41	Effect of Winglet Configuration on Full-Span KC-135A Model Pitching Moment. $M = 0.30$ . $\delta_F = 50$ Degrees. $i_H = -10$ Degrees	64
42	Effect of Winglet Configuration on Semispan KC-135A Model Wing Root Bending Moment. $M = 0.78$ , $\delta_F = 0$	65
43	Effect of NASA Upper Plus Lower Winglet Configuration on Semispan KC-135A Model Wing Root Bending Moment. $M = 0.30$ , $\delta_F = 0$	65

## ILLUSTRATIONS (CONTINUED)

FIGURE		PAGE
44	Effect of Upper Winglet Incidence on KC-135A Model Drag Near Cruise Conditions. NASA Upper Winglet Configuration. $C_L = 0.426$	66
45	Effect of Upper Winglet Incidence on KC-135A Model Drag Near Cruise Conditions. Boeing Winglet Configuration. $C_L = 0.426$	66
46	Effect of Upper Winglet Incidence on KC-135A Model Drag Near Cruise Conditions. $C_L = 0.426$	67
47	Effect of Lower Winglet Incidence on KC-135A Model Drag Near Cruise Conditions. NASA Upper Plus Lower Winglet Configuration. $C_L = 0.426$	67
48	Effect of Lower Winglet Incidence on KC-135A Model Drag Near Cruise Conditions. $C_L = 0.426$	68
49	Effect of Upper Winglet Cant on KC-135A Model Drag. $M = 0.78$ . $C_L = 0.426$ . $\delta_F = 0$	69
50	Effect of Upper Winglet Cant on KC-135A Model Drag. $M = 0.78$ . $C_L = 0.426$ . $\delta_F = 0$	69
51	Effect of Lower Winglet Cant on KC-135A Model Drag. $M = 0.78$ . $C_L = 0.426$ . $\delta_F = 0$	70
52	Effect of Lower Winglet Cant on KC-135A Model Drag. $M = 0.78$ . $C_L = 0.426$ . $\delta_F = 0$	70
53	Comparison of Semispan KC-135A Model Drag with Winglets and Tip Extension. $M = 0.78$ . $\delta_F = 0$	71
54	Comparison of Semispan KC-135A Model Wing Root Bending Moment with Winglets and Tip Extension $M = 0.78$ . $\delta_F = 0$	72
55	Comparison of Semispan KC-135A Model Lift with Winglets and Tip Extension. $M = 0.78$ . $\delta_F = 0$	72
56	Comparison of Semispan KC-135A Model Pitching Moment with Winglets and Tip Extension. $M = 0.78$ . $\delta_F = 0$	73
57	Effect of Flap and Horizontal Tail Deflection on KC-135A Model Drag. $M = 0.30$ . $C_L = 1.0$	74

## ILLUSTRATIONS (CONTINUED)

FIGURE		PAGE
58	Effect of Flap and Horizontal Tail Deflection on KC-135A Model Lift. $M = 0.30$ . $C_L = 1.0$	75
59	Effect of Flap and Horizontal Tail Deflection on KC-135A Model Lift Curve Slope. $M = 0.30$	75
60	Effect of Flap and Horizontal Tail Deflection on KC-135A Model Lift-Drag Ratio. $M = 0.30$	76
61	Effect of Flap and Horizontal Tail Deflection on KC-135A Model Pitching Moment. $M = 0.30$ . $C_L = 1.0$	76
62	Effect of Winglet Configuration on Full-Span KC-135A Model Yawing Moment. $M = 0.30$ . $\delta_F = 50$ Degrees. $i_H = -10$ Degrees	77
63	Effect of Winglet Configuration on Full-Span KC-135A Model Rolling Moment. $M = 0.30$ . $\delta_F = 50$ Degrees. $i_H = -10$ Degrees	77
64	Effect of Aileron Deflection on Rolling Moment $M = 0.30$ . $\delta_F = 30$ Degrees. $i_H = -10$ Degrees	78
65	Effect of Aileron Deflection on Rolling Moment $M = 0.30$ . $\delta_F = 50$ Degrees. $i_H = -10$ Degrees	78
66	Effect of Aileron Deflection on Yawing Moment $M = 0.30$ . $\delta_F = 30$ Degrees. $i_H = -10$ Degrees. $\delta_A = -10/+10$ Degrees	79
67	Effect of Aileron Deflection on Yawing Moment. $M = 0.30$ . $\delta_F = 30$ Degrees. $i_H = -10$ Degrees. $\delta_A = -20/20$ Degrees	79
68	Effect of Aileron Deflection on Yawing Moment. $M = 0.30$ . $\delta_F = 50$ Degrees. $i_H = -10$ Degrees. $\delta_A = -10/10$ Degrees	80
69	Effect of Aileron Deflection on Yawing Moment. $M = 0.30$ . $\delta_F = 50$ Degrees. $i_H = -10$ Degrees. $\delta_A = -20/+20$ Degrees	80

## ILLUSTRATIONS (CONTINUED)

FIGURE		PAGE
70	Effect of Winglet Loss on KC-135A Model Yawing Moment. $M = 0.30$ . $\delta_F = 50$ Degrees. $i_H = -10$ Degrees	81
71	Effect of Winglet Loss on KC-135A Model Rolling Moment. $M = 0.30$ . $\delta_F = 50$ Degrees. $i_H = -10$ Degrees	82
72	Effect of Winglet Loss on KC-135A Model Yawing Moment Slope. $M = 0.30$ . $\delta_F = 50$ Degrees. $i_H = -10$ Degrees	82
73	Effect of Winglet Loss on KC-135A Model Rolling Moment Slope. $M = 0.30$ . $\delta_F = 50$ Degrees. $i_H = -10$ Degrees	83
74	Effect of Winglet Loss on KC-135A Model Lift $M = 0.30$ . $\delta_F = 50$ Degrees. $i_H = -10$ Degrees	83
75	Effect of Winglet Loss on KC-135A Model Drag $M = 0.30$ . $\delta_F = 50$ Degrees. $i_H = -10$ Degrees	84
76	Effect of Winglet Loss on KC-135A Model Pitching Moment. $M = 0.30$ . $\delta_F = 50$ Degrees. $i_H = -10$ Degrees	84
77	Effect of Winglets on KC-135A Aircraft Drag at Cruise Flight Conditions	85
78	Effect of Winglets on KC-135A Aircraft Lift-Drag Ratio at Cruise Flight Conditions	85
79	Variation of Lift of Basic KC-135A Model with Angle of Attack. $M = 0.30$ . $\delta_F = 0$	86
80	Variation of Lift of Basic KC-135A Model with Angle of Attack and Flap Deflection. $M = 0.30$ . $i_H = -10$ Degrees	87
81	Variation of Lift of Basic KC-135A Model with Angle of Attack Near Cruise Conditions. $\delta_F = 0$	88
82	Variation of Drag of Basic KC-135A Model with Lift. $M = 0.30$ . $\delta_F = 0$	89
83	Variation of Drag of Basic KC-135A Model with Lift and Flap Deflection. $M = 0.30$ . $i_H = -10$ Degrees	90

## ILLUSTRATIONS (CONTINUED)

FIGURE		PAGE
84	Variation of Drag of Basic KC-135A Model with Lift Near Cruise Condition. $\delta_F = 0$	91
85	Variation of Pitching Moment of Basic KC-135A Model with Lift. $M = 0.30$ . $\delta_F = 0$	92
86	Variation of Pitching Moment of Basic KC-135A Model with Lift and Flap Deflection. $M = 0.30$ . $i_H = -10$ Degrees	93
87	Variation of Pitching Moment of Basic KC-135A Model with Lift Near Cruise Conditions. $\delta_F = 0$	94
88	Variation of Yawing Moment of Basic KC-135A Model with Lift and Flap Deflection. $M = 0.30$ . $\beta = 0$	95
89	Variation of Rolling Moment of Basic KC-135A Model with Lift and Flap Deflection. $M = 0.30$ . $\beta = 0$	95
90	Variation of Yawing Moment Slope Parameter of Basic KC-135A Model with Lift and Flap Deflection. $M = 0.30$	96
91	Variation of Rolling Moment Slope Parameter of Basic KC-135A Model with Lift and Flap Deflection. $M = 0.30$	96
92	Variation of Yawing Moment Slope Parameter of Basic KC-135A Model with Lift Near Cruise Conditions. $\delta_F = 0$	97
93	Variation of Rolling Moment Slope Parameter of Basic KC-135A Model with Lift Near Cruise Condition. $\delta_F = 0$	97
94	Comparison of Full-Span and Semispan Model Incremental Lift. $M = 0.70$	98
95	Comparison of Full-Span and Semispan Model Incremental Lift. $M = 0.78$	99
96	Comparison of Full-Span and Semispan Model Incremental Drag. $M = 0.70$	100
97	Comparison of Full-Span and Semispan Model Incremental Drag. $M = 0.78$	101

## SYMBOLS

$$\Delta C_L = C_{L \text{ WITH WINGLET}} - C_{L \text{ WITHOUT WINGLET}}$$

Incremental lift coefficient

$$\Delta C_D = C_{D \text{ WITH WINGLET}} - C_{D \text{ WITHOUT WINGLET}}$$

Incremental drag coefficient

$$\Delta C_m = C_{m \text{ WITH WINGLET}} - C_{m \text{ WITHOUT WINGLET}}$$

Incremental pitching moment coefficient

$$\Delta C_b = C_{b \text{ WITH WINGLET}} - C_{b \text{ WITHOUT WINGLET}}$$

Incremental wing root bending moment coefficient

$$\Delta C_n = C_{n \text{ WITH WINGLET}} - C_{n \text{ WITHOUT WINGLET}}$$

Incremental yawing moment coefficient

$$\Delta C_l = C_{l \text{ WITH WINGLET}} - C_{l \text{ WITHOUT WINGLET}}$$

Incremental rolling moment coefficient

$$\Delta \alpha = \alpha_{\text{WITH WINGLET}} - \alpha_{\text{WITHOUT WINGLET}}$$

Incremental angle of attack

$$C_L = \frac{L}{qS}$$

Lift coefficient

$$C_D = \frac{D}{qS}$$

Drag coefficient

$$C_m = \frac{M\alpha}{qSc}$$

Pitching moment coefficient

$$C_b = \frac{B}{qSb}$$

Wing root bending moment coefficient

$$C_n = \frac{N}{qSb}$$

Yawing moment coefficient

$$C_l = \frac{R}{qSb}$$

Rolling moment coefficient

L

Lift

## SYMBOLS (CONTINUED)

D	Drag
$M_x$	Pitching moment, about an axis perpendicular to plane of symmetry and through the quarter chord position of the wing mean aerodynamic chord, positive nose up
B	Wing root bending moment (rolling moment of one-half of model), about a longitudinal axis parallel to plane of symmetry at the wing-fuselage juncture, positive up
N	Yawing moment, about a vertical axis parallel to plane of symmetry, positive nose right
R	Rolling moment, about a longitudinal axis parallel to plane of symmetry, positive right wing down
q	Free stream dynamic pressure
S	Wing reference area <ul style="list-style-type: none"> <li><math>S = 5.003 \text{ ft}^2</math> (semispan model, exposed basic wing, NASA winglets)</li> <li><math>S = 5.038 \text{ ft}^2</math> (semispan model, exposed basic wing, Boeing winglets)</li> <li><math>S = 2.91 \text{ ft}^2</math> (full span model)</li> </ul>
$\bar{c}$	Wing reference chord <ul style="list-style-type: none"> <li><math>\bar{c} = 15.74 \text{ in.}</math> (semispan model, exposed basic wing, NASA winglets)</li> <li><math>\bar{c} = 15.69 \text{ in.}</math> (semispan model, exposed basic wing, Boeing winglets)</li> <li><math>\bar{c} = 8.28 \text{ in.}</math> (full span model)</li> </ul>

## SYMBOLS (CONTINUED)

$b$	Wing reference span $b = 54.60$ in. (full span model)
$b'$	Exposed basic wing semispan $b' = 48.92$ in. (semispan model, NASA wing) $b' = 49.56$ in. (semispan model, Boeing wing)
$l$	Winglet length or span
$M$	Mach number
$R, ft$	Reynolds number per foot
$\alpha$	Angle of attack, angle between fuselage centerline and flow direction, positive nose up
$\beta$	Angle of sideslip, angle between fuselage centerline and flow direction, positive nose left
$i_u$	Upper winglet incidence angle, angle between upper winglet root chord and plane of symmetry, positive nose toward plane of symmetry (toe in)
$i_L$	Lower winglet incidence angle, angle between lower winglet root chord and plane of symmetry, positive nose away from plane of symmetry (toe out)
$\phi_U$	Upper winglet cant angle, angle between upper winglet and vertical, positive cant outward
$\phi_L$	Lower winglet cant angle, angle between lower winglet and vertical, positive cant outward
$i_H$	Horizontal tail incidence angle, angle between horizontal tail chord line and fuselage centerline, positive nose up



SYMBOLS (CONTINUED)

$\delta_F$

Wing flap deflection angle, angle between flap chord and wing chord, positive flaps down

$\delta_A$

Aileron deflection angle, angle between aileron chord and wing chord, positive trailing edge down

Aileron deflection is designated by two numbers separated by a slash mark, e.g.,  $\delta_A = 0/0$ . The number to the left of the slash mark indicates left aileron deflection and the number to the right, the right aileron deflection.

Subscripts:

WING

Semispan model wing without winglets

B

Basic KC-135A model without winglets (Wing tips clipped to accommodate mounting winglets)

## INTRODUCTION

The USAF is interested in reducing the fuel requirements and operational costs of existing and future aircraft. Methods for improving aircraft efficiency are continually being investigated and innovative aerodynamic drag reduction technologies are constantly being sought. A method suitable for retrofit to existing fleet aircraft is highly desirable.

The winglet concept, developed by NASA/LRC, appears to offer significant improvement in aircraft efficiency by reducing aircraft drag, fuel requirements, and operating costs. Winglets represent the latest state-of-the-art aerodynamic drag reduction technology and offer significant improvement in aircraft efficiency. Total drag reductions up to 8 percent have been estimated for the KC-135A aircraft at cruise.

The feasibility of winglets on the KC-135 aircraft has been investigated by the Boeing Commercial Airplane Company under Air Force contract (Reference 1). This investigation has indicated no basic aerodynamic, structural, or dynamic problems from winglets on the KC-135. The investigation has indicated a fuel savings of 68,000 gallons per aircraft per year, which results in a fleet fuel savings of 44 million gallons per year at a cost savings of 17.5 million dollars (40¢/gallon). A KC-135 winglet retrofit investigation indicated the cost for retrofitting winglets to be \$66,000 (1977 dollars) per aircraft, or a fleet retrofit cost of about 42.5 million dollars.

The aerodynamic characteristics of semispan and full-span KC-135A wind tunnel models with different winglet concepts have been investigated in the

NASA/LRC 8-Foot Transonic Pressure Tunnel. Data from these investigations have been provided to the Air Force Flight Dynamics Laboratory and some basic results are presented in this Report.

#### MODEL AND TEST APPARATUS

##### Semispan Model.

An 0.070-scale semispan wind tunnel model was constructed by NASA/LRC (Figures 1 and 2).<sup>\*</sup> A semispan model configuration was selected to obtain maximum Reynolds number on the winglets.

The 0.070-scale semispan model consisted of the right half of the KC-135A aircraft. The wing was constructed basically of aluminum and was designed to deflect under airloads to simulate aeroelastic deflection. The wing was designed so that the tip deflected approximately the same as the tip of the full-scale airplane at cruise conditions. The model included the wing, flow-through nacelles, and fuselage (no tail), although only the wing and nacelles were attached to the balance system. The basic KC-135A aircraft wing has a sweep angle at the quarter chord of 35 degrees, an aspect ratio of 7.035, a taper ratio of 0.33, a 7-degree dihedral, two degrees positive incidence at the root, and no geometric twist. The thickness/chord ratio varies non-linearly from 15 percent at the wing-fuselage juncture to 9 percent at the trailing edge break station and then remains constant at 9 percent to the tip.

To accommodate mounting the winglets, a small portion of the model wing tip was cut off, reducing the aspect ratio of the basic wing slightly. In addition, the NASA and Boeing winglets were mounted at slightly different spanwise locations so that the span of the basic wing was slightly different.

<sup>\*</sup>Figures are located at end of report.

The exposed model wing semispan was 43.92 inches for the NASA basic wing (Figure 2) and 49.56 for the Boeing basic wing. The aspect ratio of the KC-135A wing was reduced from 7.035 to 6.86 for the NASA basic wing and 6.98 for the Boeing basic wing. The slightly different spanwise location of the winglets should have only minimal effect on the aerodynamic characteristics. A simple analysis (Appendix A) indicated a loss in aircraft lift-drag ratio of about -0.07, or about 0.4 percent, with removal of the tip portion of the basic wing.

The original NASA winglet concept was composed of upper and lower winglet fins (Figure 3); however, both upper winglets (only) and upper plus lower winglet combinations were investigated. The Boeing winglet configuration tested (Figure 4) was slightly different from the configuration investigated analytically (Reference 1) because of an error in model fabrication. As a result, the winglet configuration tested had a cant angle of 6 degrees instead of 20 degrees. The wing tip extension model (Figure 2) was an extension of the basic wing sized to produce approximately the same increase in wing root bending moment as the NASA upper plus lower winglet configuration. The span of the tip extension was 3.0 inches.

Fixed-position leading and trailing edge flap configurations were investigated on the semispan KC-135A model (Figure 5). These flaps were only representative and did not conform to the flap geometry of the KC-135A airplane. The trailing edge flaps were located just inboard of the nacelle centerlines and had a chord of 10% of the wing chord. Flap deflection for the leading edge flaps was 70 degrees and for the trailing edge flaps 25 degrees.

Full Span Model.

The basic 0.035 scale full span KC-135A model for the low speed investigation ( $M = 0.3$ ) (Figure 6) was equipped with a wing having flaps and ailerons. The wings were constructed from steel and were not designed to deflect aeroelastically. Three wing flap deflections 0, 30, and 50 degrees, and three aileron deflections 0,  $\pm 10$ , and  $\pm 20$  degrees could be set (Figure 7). The model had four strut-mounted, flow-through nacelles attached to the wings. To accommodate mounting the winglets, a small portion of the model wing tips were cut off, reducing the aspect ratio of the basic wing from 7.035 to 6.98. A variable incidence horizontal tail could be set at incidence angles of 0, -4, and -10 degrees.

Because of the basic KC-135A model body construction, the strain gage balance was located so far aft that the balance pitching moment limit was exceeded at very low lift values at high speed. Consequently, the KC-135A model body was replaced with a body that located the balance further forward. This body was slightly larger than the KC-135A model body and was circular instead of oval in cross section; however, these slight differences should have only minimal effect on the aerodynamic characteristics. Because of the construction of the body, the horizontal and vertical tails could not be attached, and all high-speed tests were made without horizontal and vertical tails. The wing for the high-speed model was constructed from steel and was not designed to deflect aeroelastically. The wing was constructed without flaps or ailerons and had a portion of the wing tips cut off to accommodate mounting the winglets. Four strut-mounted, flow-through nacelles were attached to the wings.

### Test Apparatus.

The experimental investigation was conducted in the NASA/LRC 8 Foot Transonic Pressure Tunnel, a continuous-flow, single-return, variable-pressure facility with a closed slotted test section. The Mach number range is from about 0.3 to 1.35.

The 0.070-scale semispan KC-135A model was attached to a balance system located outside the left wall of the tunnel test section and was mounted in the upright position. Only the wing, nacelles, and winglets were attached to the balance. The fuselage was attached to a turntable in the left wall of the test section and pitched with the wing, however, the fuselage was completely isolated and no fuselage loads were recorded by the balance. The fuselage had a slot through which the wing passed.

The 0.035-scale full-span KC-135A model was mounted in the center of the tunnel test section on a sting-supported six-component strain gage balance system. Aerodynamic forces and moments were read out on magnetic tape which was computer processed.

## DISCUSSION

### Winglets

Winglets are small, cambered fins located at the wing tips (Figures 1 and 6). Two winglet configurations developed by NASA/LRC and the Boeing Commercial Airplane Company are shown in Figures 3 and 4. The original NASA winglet configuration had fins both above and below the wing plane (Figure 3). The upper fin was larger and was located rearward on the tip chord; the trailing edge of the root chord section was located at the wing tip trailing edge. The Boeing Company configuration was developed analytically and had

only an upper fin (Figure 4) located rearward on the tip chord. A basic difference is the leading-edge strake which is intended to reduce the twist required at the winglet root and facilitate blending the winglet into the wing. The NASA upper winglets had a trapezoidal planform with an area 3.8% of the exposed basic wing area, a root chord 65% of the wing tip chord, a tip chord 21% of the wing tip chord, a height equal to the wing tip chord, and a leading edge sweep angle of 38 degrees. The upper winglets were untwisted, cambered outward (upper surface inboard), inclined outward from vertical, and were positioned so that the trailing edge of the root section was located at the wing tip trailing edge. The lower surface winglets had a trapezoidal planform with an area 0.6% of the exposed basic wing area, a span 23% of the wing tip chord, a root chord 40% of the wing tip chord, and a leading edge sweep angle of 52 degrees. The lower winglets were cambered inward, inclined outward from the vertical, had an incidence of -7 degrees (toed in), were twisted about the leading edge with 4 degrees of washout at the tip, and were positioned so that the leading edge was located at the wing tip leading edge. Both upper and lower winglets had 9% thick GA(W)-2 airfoil sections.

The Boeing winglets had a trapezoidal planform with an area of 3.5% of the exposed basic wing area, a root chord 60% of the wing tip chord, a height 13.5% of the wing (not exposed) semispan, and a winglet leading edge sweep angle of 37 degrees. The Boeing winglets had a strake at the leading edge, were cambered outward, were inclined 6 degrees outward from vertical, and were positioned so that the trailing edge of the root chord was located at the wing trailing edge. The winglets had a 6% thick, Boeing developed, supercritical airfoil and incorporated twist in the winglet root.

Results of Boeing Investigations

In Reference 1, potential performance improvements from winglets were investigated analytically. Results of this investigation indicated an 8.4 percent improvement in cruise  $M(L/D)$ , a net improvement in range factor of 8.1 percent, and an increase in overall empty weight of 592 lb. Performance improvements from equal area tip extensions were also investigated.

The primary effect of winglets and tip extensions is to reduce induced drag, and, consequently, reduce total aircraft drag. However, in addition to performance gains from winglets or tip extensions, their effects on the aircraft structure must be considered. The weight of the winglets and their attachment structure will cancel some aerodynamic benefit and the local and wing root bending moments will be increased, possibly increasing wing weight.

Various winglet parameters were investigated analytically to determine the potential aerodynamic improvement on the KC-135 aircraft at cruise conditions. For all cases investigated, the winglets were located at the tip on the upper wing surface only. This investigation indicated that winglet chordwise location, sweep, taper ratio, and area do not significantly affect the overall aerodynamic characteristics of the KC-135 aircraft. Winglet length and cant angle appear to be the most significant parameters (Figures 8 and 9).

For the winglet length selected for the KC-135 aircraft ( $0.135 \frac{b}{2}$ ), a reduction in the induced drag of about 14 percent and an increase in the wing root bending moment of about 4 percent was indicated at cruise (Figure 8) for a winglet with no cant. As the winglet is canted outward (Figure 9), the induced drag is further reduced; however, the wing root bending moment is



increased. For the KC-135 winglets (cant 20 degrees), the induced drag reduction was about 17 percent and the wing root bending moment increase about 6 percent.

A number of different equal area tip extensions were also investigated (Figure 10). Comparison of the induced drag reduction and wing root bending moment increase for zero cant winglets and wing tip extensions is shown in Figure 11. When the winglet and tip extension produce the same induced drag improvement (14% for an C.135  $b/2$  winglet with no cant), the tip extension had 31 percent greater wing root bending moment than the winglet. When the root bending moment of the winglet and tip extension are equal, the induced drag was reduced about 22.9 percent more by the winglet than by the tip extension. The winglet gives greater aerodynamic improvement or a lighter structure.

Both winglets and wing tip extensions increase the aircraft nose-down pitching moment. Figure 12 shows that the nose-down pitching moment change of the KC-135 was considerably greater for a tip extension than for a corresponding zero cant winglet. When the winglet and tip extension produce the same induced drag improvement (14%), the pitching moment change from the tip extension was about 80 percent greater than that of the winglet. For equal wing root bending moment, the pitching moment change from the tip extension was about 35.7 percent. Both winglets and tip extensions increased the aircraft longitudinal stability.

#### Aerodynamic Data

Aerodynamic force and moment measurements obtained on the KC-135A models are presented in coefficient form in the stability axis system and are referenced to the wing area, span, and wing reference chord. The data

have been corrected for tunnel flow angularity, tunnel wall, and blockage effects. Moments are presented about orthogonal axes through the moment reference center. The wing root bending moment is the rolling moment of the projecting semispan wing about an axis parallel to the plans of symmetry at the wing fuselage juncture. The incremental aerodynamic characteristics of the different configurations have been obtained from large-scale plots. Data without winglets are for the wing tip clipped configuration.

At cruise conditions,  $M = 0.77$  at 30,000 feet, the overall KC-135A airplane cruise lift coefficient is about 0.426. At take off, flaps are deflected 30 degrees and the lift coefficient is about 1.22, and at landing, the flap deflection is 50 degrees and the lift coefficient about 1.0.

#### Winglet Configuration.

Results from the semispan wind tunnel tests at high subsonic speed (Figure 13) indicated the greatest drag reductions with the NASA upper plus lower winglet configuration; however, drag reductions of similar magnitude were found with the upper winglet configurations at cruise lift coefficients. For a cruise lift coefficient of 0.426, a total drag reduction of about 5.4 percent was indicated with the Boeing winglet configuration ( $\phi_U = 6$  degrees) and about 6.9 percent with the NASA upper ( $\phi_U = 15$  degrees) and the NASA upper plus lower ( $\phi_U = 15$  degrees,  $\phi_L = 36$  degrees) winglet configurations.

At low speed, contrary to the high-speed results, the greatest drag reduction was found with the NASA upper winglet configuration (Figure 14). Analytical results from the Nonplanar Lifting Systems Program (Reference 2) also indicated the single upper winglet configuration to be slightly superior in reducing induced drag. References 1 and 3 indicate that the effect of the

lower winglet is generally favorable, but that improvement in overall performance is only marginal. Because gains from the lower winglet are small and structural complexity increased, the lower winglet was eliminated from later NASA KC-135 winglet configurations. However, winglet effects are most likely configuration dependent, and the dual winglet configuration could prove advantageous for other aircraft.

Contrary to results from the semispan model tests, the full-span KC-135A model tests indicated the greatest drag reduction generally with the NASA upper winglet configuration (Figures 15 to 20); however, drag reductions of similar magnitude were achieved with the other winglet configurations investigated. In addition, it must be considered that the cant angle of the Boeing winglet configuration was six degrees, and that greater drag reduction could be achieved if the cant angle was increased. For cruise conditions,  $M = 0.78$  and  $C_L = 0.426$  (Figure 19), a total drag reduction of about 5.3 percent was obtained with the Boeing and NASA upper plus lower winglet configurations and about 6.5 percent with the NASA upper winglet configuration. At low speed (Figure 15), drag reduction of the KC-135A model with NASA upper winglets at  $C_L = 0.426$  was approximately 3.0 percent, about half of the drag reduction achieved at cruise.

For lift coefficients less than about 0.2, the incremental winglet drag was positive, indicating the profile drag increase to be greater than the induced drag decrease generated by the winglets. For lift coefficients greater than about 0.2, the incremental total drag becomes negative indicating the decrease induced drag from the winglets to be greater than the increase in profile drag, resulting in an overall drag reduction for the KC-135A

model. As the drag reduction from winglets is primarily induced drag, these devices can be expected to be more effective at higher lift coefficients, and, as shown by Figures 15 to 20, drag reduction was considerably greater at higher lift coefficients. At cruise Mach number (Figure 19), drag reduction varied from about one percent at  $C_L=0.2$  to about 13 per cent at  $C_L=0.8$  for the NASA upper winglet configuration. The drag reduction achieved with the different winglet configurations on the KC-135A model at  $C_L=0.426$  with Mach number is shown in Figure 21.

The effect of the different winglet configurations on the lift of the KC-135A model (Figures 22 to 27) was to generally increase the lift about one to three percent. At cruise lift conditions (Figure 26), the increase in lift of the KC-135A model was about 2.5 percent with all of the winglet configurations investigated. Variation of the incremental lift of the KC-135A model with the different winglet configurations with Mach number is shown in Figure 28 and variation of the incremental lift curve slope with Mach number is shown in Figure 29. The lift curve slope of the KC-135A model was generally increased about one to three percent by the different winglet configurations. At low Mach numbers, the increase in lift curve slope appears to be slightly greater with the NASA upper plus lower winglet configuration; however, at higher Mach numbers, the increase is about the same as with the upper winglet configurations. Because of the increased lift with the winglets, the aircraft can fly at a reduced angle of attack which will reduce the profile drag. At cruise conditions, the reduction in angle of attack of the KC-135A model with winglets was about -0.1 degree (Figure 30).

A measure of the aerodynamic efficiency is the lift-drag ratio. The increase in the ~~maximum~~ untrimmed lift-drag ratio of the KC-135A model with

the different winglet configurations is shown in Figure 31 for different Mach numbers. The increase in maximum untrimmed lift-drag ratio was about the same with all of the different winglet configurations investigated. At cruise conditions, the increase in the model maximum untrimmed lift-drag ratio because of winglets was about 8 percent.

The effect of the different winglet configurations on the pitching moment was to increase the nose down pitching moment and increase the longitudinal stability of the KC-135A model (Figures 32 to 37). At cruise lift conditions, the increase in nose-down pitching moment was about 13 percent for the model with the NASA upper and Boeing winglet configurations and about 16 percent for the NASA upper plus lower winglet configuration. Variation of the increase in nose-down pitching moment of the KC-135A model with the different winglet configurations with Mach number is shown in Figure 38 for  $C_L = 0.426$ .

The effect of winglet configuration on the model aerodynamic characteristics at low speed was also investigated at a flap deflection of 50 degrees and a horizontal tail incidence angle of -10 degrees (Figures 39 to 41). The greatest drag reduction was found with the upper winglet configurations (Figure 39), and, as shown, the drag reduction was essentially the same for both configurations investigated. At  $C_L = 1.0$  (landing condition), Figure 39 indicates a total drag reduction of about 2.5 percent for the upper winglet configurations and about 1.0 percent for the NASA upper plus lower winglet configuration. Because of the difference in cant angle, the model tests at  $\delta_F = 0$  (tail off) generally indicate a slightly greater drag reduction with the NASA upper winglet configuration than with the Boeing winglet configuration. No explanation is known for the different behavior at  $\delta_F = 50$  degrees. The effect of the different winglet configurations on the lift of the model at

$\delta_F = 50$  degrees,  $i_H = -10$  degrees (Figure 40) was to generally increase the lift about 1 to 2 percent, except at very high lift coefficients. The effect of the winglets on the pitching moment at  $\delta_F = 50$  degrees,  $i_H = -10$  degrees (Figure 41) was to increase the nose-down pitching moment and increase the longitudinal stability of the model.

#### Wing Root Bending Moment

Potential aerodynamic benefits from winglets appear to be significant; however, their total impact on the performance and structure of an aircraft has to be evaluated. The weight of the winglets and their attachment structure offset some of the aerodynamic benefit, and both the local and wing root bending moment will be increased. To accommodate the increased moments, wing weight may have to be increased, and an assessment between the benefits of improved aerodynamic performance and increased wing weight must be made.

To evaluate the effects of winglets on the KC-135 aircraft, all effects on the aircraft structure have been assumed to be proportional to measured model wing root bending moments. The wing root bending moments of the semi-span KC-135A model with and without winglets were measured by a strain gage built into the model wing. For this case, the wing root bending moment was the rolling moment of the exposed semispan wing. At cruise conditions ( $M = 0.78$ ,  $C_L = 0.426$ ) (Figure 42), the measured increase in the wing root bending moment of the semispan KC-135A model was about 2.5 percent with the Boeing winglet configuration and about 3 percent with both the NASA upper and the NASA upper plus lower winglet configurations. The Boeing analytical investigation indicated an increase of about 4.8 percent (Figure 9) in the wing root bending moment for a cant angle of 6 degrees at cruise conditions, a value

somewhat greater than the measured wing root bending moment. At low speed (Figure 43), the increase in the wing root bending moment of the KC-135A model with the NASA upper plus lower winglet configuration was approximately 6 percent for wing lift coefficients from about 0.6 to 0.95.

#### Winglet Incidence

As winglets are basically small, cambered, wings flying at an angle of attack determined by the wing tip cross flow, winglet incidence can affect the efficiency. To determine winglet incidence angle, the different winglet configurations were investigated at several incidence angles.

The effect of winglet incidence on the drag of the KC-135A model with the NASA upper and the Boeing winglet configurations at near cruise conditions is shown in Figures 44 to 46. Incidence angle, within the range investigated, influenced the drag reduction characteristics of the winglets only very slightly. An incidence angle of -4 degrees was selected for the KC-135A model with the NASA upper winglet configuration and an angle of -1 degree was selected for the model with the Boeing winglet configuration. The bulk of the data obtained from the KC-135A model with winglets was for these incidence angles. Results from the semispan KC-135A model tests with the NASA upper plus lower winglet configuration also indicated the greatest drag reductions for an upper winglet incidence angle of -4 degrees.

The effect of lower winglet incidence on the drag of the KC-135A model with the NASA upper plus lower winglet configuration at near cruise conditions is shown in Figures 47 and 48. The upper winglet incidence angle was fixed at -4 degrees. The drag reduction of the NASA upper plus lower winglet configuration was improved slightly as the lower winglet incidence angle was reduced. At  $M = 0.78$ , the drag of the model was reduced about 4.7 percent

at a lower winglet incidence angle of -8 degrees and about 5.1 percent for incidence angles from about -7 to -5 degrees. A lower winglet incidence angle of -7 degrees was selected for the NASA upper plus lower winglet configuration and most data are for this incidence angle.

#### Winglet Cant

As indicated by the Boeing analytical investigations, winglet length and cant angle appear to be the most significant geometric parameters affecting the overall aircraft aerodynamic characteristics. All of the (upper) winglets investigated were essentially the same length, and winglet cant angle, per se, was not investigated. However, as the cant angles of the different winglet configurations varied somewhat, some deductions concerning cant angle can be made. Because the basic purpose of winglets is to reduce drag, drag reduction at cruise has been selected as the primary criterion for winglets.

The effect of cant angle on the drag of the KC-135A model with the different upper winglet configurations at cruise lift conditions (Figures 49 and 50) was to reduce the drag as the winglet was canted. The drag of the model was reduced about 5.3 percent with a cant angle of 6 degrees, and about 6.5 percent with a cant angle of 12 degrees (Figure 50). Linear extrapolation of the curve to zero cant (vertical winglets) indicated a drag reduction of about 4.1 percent.

The effect of lower winglet cant angle on the drag of the KC-135A model with the NASA upper plus lower winglet configuration at cruise lift conditions (Figures 51 and 52) shows only a very slight change in the drag of the model as the lower winglet is canted. Figure 52 indicates a drag reduction of about 5.3 percent with a lower winglet cant angle of 12 degrees and about 5.9 percent



with a cant angle of 36 degrees. Linear extrapolation to zero cant angle indicates a drag reduction of about 5 percent with the lower winglet vertical.

#### Wing Tip Extensions

The effect of wing tip extensions on the KC-135 aircraft was investigated analytically in Reference 1. Results of this investigation indicate that an equal area wing tip extension can reduce the induced drag about 10 percent more than an  $0.135^{b/2}$  zero cant winglet (Figure 9), but that the wing root bending moment is more than doubled.

A wing tip extension was investigated with the semispan KC-135A model. The configuration investigated (Figure 2) was designed to produce wing root bending moments similar to those of winglets and was not optimized for maximum drag reduction.

Comparison of the drag reduction of the semispan model with the tip extension and with the different winglet configurations (Figure 53) shows that the drag reduction from the tip extension was considerably less than from the winglets. At cruise conditions, the total drag reduction with the tip extension was about 3 percent, while that from the winglets varied from about 5.4 percent with the Boeing configuration to about 7 percent with the NASA upper and upper plus lower winglet configurations.

Comparison of the measured wing root bending moments of the semispan model with the tip extension and with the different winglet configurations (Figure 54) shows that the bending moment from the tip extension is greater than those from the winglet configurations. At cruise conditions, the measured increase in the model wing root bending moment was about 3.5 percent

for the tip extension, about 3.0 percent for the NASA upper and upper plus lower winglet configurations, and about 2.5 percent for the Boeing winglet configuration.

Comparison of the increase in lift and nose-down pitching moment of the semispan model with winglets and tip extension is shown in Figures 55 and 56, respectively. The increase in lift was approximately the same with both the tip extension and the winglet configurations. At cruise conditions, the increase in lift was about 2-3 percent. However, as shown by Figure 56, the change in nose down pitching moment was considerably greater with the tip extension. Both the tip extension and the winglets increase the nose down pitching moment and increase the longitudinal stability of the model.

#### Flaps and Horizontal Tail Deflection

Comparison of the drag reduction achieved with the NASA upper winglet configuration at low speed and  $C_L = 1.0$  (Figure 57) for different horizontal tail incidence angles indicated horizontal tail incidence angle to have only small influence on the drag reduction, and that the drag reduction was proportional to flap deflection, varying from about 12 percent at zero deflection to about 2.5 percent at 50 degrees deflection. The increase in lift from the winglets ( $C_L = 1.0$ ) (Figure 58), was basically not affected by horizontal tail incidence, but becomes greater with increased flap deflection, varying from about 0.5 percent at  $\delta_F = 0$  to about 2 percent at  $\delta_F = 50$  degrees. The increase in lift curve slope (Figure 59) varied from about 1 to 3 percent with the greatest increase occurring at 30 degrees flap deflection. The increase in untrimmed maximum lift-drag ratio of the model (Figure 60) was essentially not influenced by tail incidence, but was decreased by flap

deflection. The increase in lift-drag ratio ranged from about 7.5 percent at zero flap deflection to about 3.5 percent at 50 degrees flap deflection. The effect of horizontal tail incidence and flap deflection on the model incremental pitching moment is shown in Figure 61. The model incremental pitching moment was not greatly affected by flap deflection, but was somewhat more negative at a tail incidence angle of -4 degrees than at zero and -10 degrees.

#### Lateral-Directional Stability

An important consideration of winglets is their effect on the lateral and directional stability characteristics. The effect of the different winglet configurations on the lateral and directional characteristics of the KC-135A model is shown in Figures 62 and 63 for  $\delta_p = 50$  degrees. All of the winglet configurations affected the lateral-directional characteristics about the same and always increased the lateral and directional stability of the model.

#### Aileron Deflection

The effect of aileron deflection on the lateral-directional characteristics of the KC-135A model with winglets is shown in Figures 64 to 69.

The effect of aileron deflection on the rolling moment of the model with and without winglets is shown in Figures 64 and 65 for flap deflections of 30 and 50 degrees, respectively. The winglets increased the outboard aileron effectiveness and the increase in effectiveness is essentially constant across most of the lift range. At  $C_L = 1.0$  to 30 degrees flap deflection (Figure 64), the increase in the rolling moment was about 3 and 6 percent for aileron deflections of 10 and 20 degrees, respectively. At  $C_L = 1.0$  and 50 degrees flap deflection (Figure 65), the increase in the rolling moment was about 10 and 7 percent for 10 and 20 degrees aileron deflection, respectively.

The effect of aileron deflection on the yawing moment of the model with and without winglets is shown in Figures 66 to 69 for flap deflections of 30 to 50 degrees. There is essentially no change in yawing moment with aileron deflection.

#### Winglet Loss

The loss of one winglet, e.g., structural failure or combat, could quite possibly be detrimental to the aircraft safety or performance.

To investigate the effect of winglet loss, the KC-135A model was tested with a NASA upper winglet on the left wing tip only. This investigation was made for a flap deflection of 50 degrees and a horizontal tail incidence angle of -10 degrees.

The most obvious effect of the loss of a winglet is on the aircraft lateral and directional characteristics. Consider, for example, a KC-135 aircraft with winglets flying in equilibrium, and suddenly the right winglet is lost. The change in yawing moment and rolling moment with the loss of the right winglet is shown in Figures 70 and 71, respectively. The change in yawing moment of the KC-135A model was always negative over the lift coefficient range investigated, while the change in rolling moment was always positive, requiring right rudder and left ailerons to maintain aircraft equilibrium. As shown by Figure 72, there was essentially no change in the yawing moment slope parameter,  $C_{n\delta}$  of the KC-135A model when one winglet was lost; however, as shown by Figure 73, there was a slight positive shift of the rolling moment parameter,  $C_{l\delta}$ . At  $C_L = 1.0$ , the change in  $C_{l\delta}$  was about 25 percent.

The effect of the loss of a winglet on the longitudinal aerodynamic characteristics is shown in Figures 74 to 76. The lift of the KC-135A model

was decreased up to about 1 percent (Figure 74) and the drag increased up to about 2 percent with the loss of a winglet (Figure 75). The effect of the pitching moment (Figure 76) was to increase the nose-down pitching moment even more than the original two winglet configuration. At  $C_L = 1.0$ , the change in nose-down pitching moment was about 50 percent greater than for the model with two winglets. In view of the large nose-down pitching moment introduced by winglets on the KC-135A model, it is surprising that removal of one of the winglets further increased the nose-down pitching moment. It would be expected that removal of one winglet would relieve the nose-down pitching moment somewhat, but the data do not indicate this.

#### Full-Scale Winglet Performance

At full-scale flight conditions, the total drag reduction from winglets should be somewhat greater than that measured at test conditions because of decreased skin friction drag and the increased lift from winglets which permits the aircraft to fly at a lower angle of attack decreasing the profile drag. Additional effects which influence the full-scale aircraft drag include trim drag changes and excrescence drag. The effect of winglets on the full-scale aircraft can therefore be assumed to be expressed by the following equation,

$$C_{D \text{ WITH WINGLETS}} = C_{D \text{ WITHOUT WINGLETS}} + \Delta C_{D \text{ WINGLETS}} + \Delta C_{D \text{ SCALE}} + \Delta C_{D \text{ EXCRES}} + \Delta C_{D \text{ PROFILE}} + \Delta C_{D \text{ TRIM}}$$

Full-scale drag polars for the KC-135 aircraft with winglets have been derived from wind tunnel and flight test data using the above equation (Figure 77). The aircraft has been assumed to be equipped with winglets having the NASA upper winglet configuration. The winglet incremental drag

as been taken from the data shown in Figure 19.  $\Delta C_{D\text{TRIM}}$  and  $\Delta C_{D\text{EXCES}}$  have been shown to be close to zero and estimates of  $\Delta C_{D\text{SCALE}}$  and  $\Delta C_{D\text{PROFILE}}$  have indicated values of -0.00022 and -0.00015 for these coefficients. As shown by Figure 77, the full-scale drag improvement with winglets has been estimated to be about  $\Delta C_D = -0.0020$  or about 8.2 percent of the aircraft cruise drag. The improvement in the aircraft maximum lift-drag ratio because of the winglets (Figure 78) was about 1.68 or about 9.5 percent.

### CONCLUSIONS

The aerodynamic characteristics of semispan and full-span KC-135A models with winglets and a tip extension have been investigated in the NASA/LRC 8-Foot Transonic Pressure Tunnel. Some basic results from these investigations have been presented in this Report. The following conclusions have been derived.

1. Results from semispan wind tunnel tests at high subsonic speeds indicated the greatest drag reductions from the NASA upper plus lower winglet configuration; however, drag reductions of similar magnitude were found with the upper winglet configurations at cruise lift coefficients.
2. Contrary to the semispan model tests, full-span model tests indicated the greatest drag reductions at high subsonic speeds with the NASA upper winglet configuration. At cruise conditions, a total drag reduction of about 5.3 percent was found for the model with the Boeing and NASA upper plus lower winglet configurations and a reduction of about 6.5 percent for the model with the NASA upper winglet configuration.
3. At low speeds, a total drag reduction of about 3.0 percent was found for the full-span model with the NASA upper winglet configuration.

4. Drag was decreased with upper winglet cant. The drag of the full-span model was decreased about 5.3 percent with an upper winglet cant angle of 6 degrees and about 6.5 percent with a cant angle of 12 degrees.
5. Drag was decreased with lower winglet cant. The drag of the full-span model was decreased about 5.3 percent with a lower winglet cant angle of 12 degrees and about 5.9 percent with a cant angle of 36 degrees.
6. Results from semispan model tests at high subsonic speeds indicate the drag reduction from winglets to be greater than from a wing tip extension configuration. At cruise conditions, the total drag reduction of the semispan model with the tip extension was about 3 percent while reduction from the winglets varied from about 5.4 to 7 percent.
7. At high subsonic speeds, the increase in wing root bending moment of the semispan KC-135A model was greatest with a wing tip extension and least with the upper winglet configurations. At cruise conditions, the increase in wing root bending moment varied from about 2.5 percent with the Boeing winglet configuration to about 3.5 percent with the tip extension.
8. At cruise conditions, winglets generally increased the lift of the model about 1 to 3 percent.
9. At cruise conditions, winglets increased the model untrimmed maximum lift-drag ratio about 8 percent.
10. Both winglets and tip extensions increase the nose-down pitching moment and increase the longitudinal stability; however, the increase in pitching moment was considerably greater for the tip extension. At cruise conditions, the increase in nose-down pitching moment was about 13 percent for the full-span model with NASA upper and Boeing winglets and about 16 percent with the NASA upper plus lower winglet configuration.

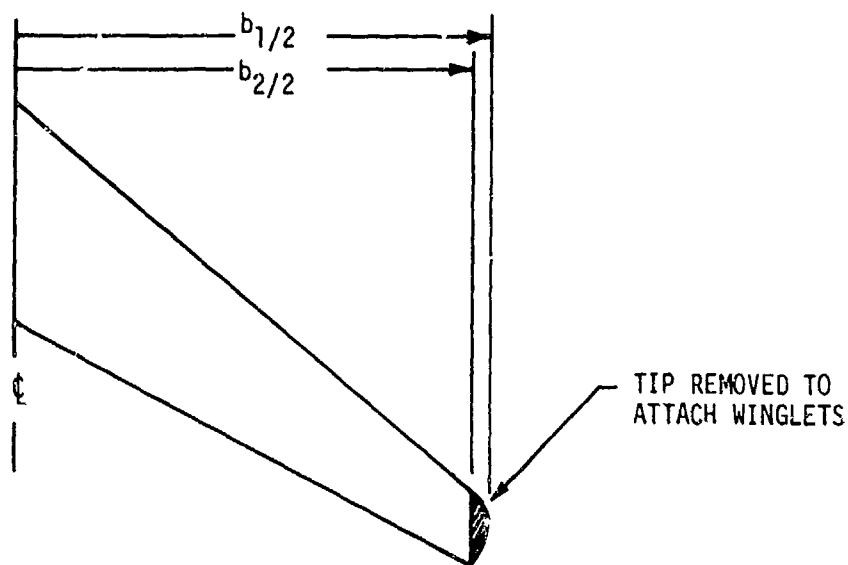
11. At  $M = 0.30$  and  $C_L = 1.0$ , total drag reduction of the full-span model varied from about 12 percent at zero flap deflection to about 2.5 percent at 50 degrees flap deflection.
12. At  $M = 0.30$ , the untrimmed maximum lift-drag ratio of the full-span KC-135A model with winglets was increased about 7.5 percent at zero flap deflection and about 4 percent at 50 degrees flap deflection.
13. Winglets increased the directional and lateral stability of the full-span KC-135A model.
14. Winglets increased the aileron effectiveness of the full span model. At  $M = 0.30$  and  $C_L = 1.0$ , the increase in rolling moment was about 10 and 7 percent for 10 and 20 degrees aileron deflection, respectively.
15. The change in the aerodynamic characteristics of the KC-135A with the loss of one winglet appears to be sufficiently small so as not to impair aircraft capability or safety.
16. Estimated winglet effects at cruise flight conditions indicated a reduction in drag of 8.2 percent and an increase in  $(L/D)_{MAX}$  of 9.5 percent.



## APPENDIX A

EFFECT OF WING TIP REMOVAL  
ON BASIC KC-135A WING

To accommodate mounting the winglets, a small portion of the model wing was removed, changing the wing span, area, and aspect ratio. Consider the following sketch, where subscript 1 denotes the original wing and 2 denotes the wing shortened to accommodate the attachment of winglets.



Lift can be expressed as

$$C_{L_1} = \frac{L_1}{qS_1}, \quad C_{L_2} = \frac{L_2}{qS_2} \quad (1)$$

where, at cruise,  $L_1 = L_2 = W$ , and

$$C_{L_2} = C_{L_1} \frac{S_1}{S_2} \quad (2)$$

Drag for the corresponding conditions can be expressed as,

$$C_{D_1} = C_{D_{0_1}} + \frac{C_{L_1}^2}{\pi AR_1 e_1}, \quad C_{D_2} = C_{D_{0_2}} + \frac{C_{L_2}^2}{\pi AR_2 e_2} \quad (3)$$

$$\text{where, } C_{D_{0_2}} = C_{D_{0_1}} \frac{S_1}{S_2} \quad (4)$$

$$\text{and, } C_{D_2} = C_{D_{0_1}} \frac{S_1}{S_2} + \frac{C_{L_1}^2 S_1^2}{\pi S_2^2 AR_2 e_2} \quad (5)$$

From flight data for the KC-135 aircraft at a cruise  $C_L$  of 0.426,  $M = 0.78$ , and a Reynolds number based on the mean aerodynamic chord of  $42 \times 10^6$ ,

$$C_{L_1} = 0.4260, \quad C_{D_1} = 0.0241, \quad e_1 = 0.7491$$

which gives

$$C_{D_1} = C_{D_{P_1}} + \frac{C_{L_1}^2}{\pi AR_1 e_1} = 0.0241$$

$$\text{or, } C_{D_{P_1}} = 0.0241 - \frac{(0.4260)^2}{\pi(7.035)(0.7491)} = 0.0241 - 0.0110 = 0.0131$$

From equation (2) the corresponding lift coefficient for the aircraft with the tip removed is

$$C_{L_2} = 0.4260 \left( \frac{2433}{2422} \right) = 0.4279$$

and the corresponding drag coefficient from equation (3) for the same wing efficiency factor

$$\begin{aligned} C_{D_2} &= 0.0131 \left( \frac{2433}{2422} \right) + \frac{(0.4279)^2}{\pi(6.98)(0.7491)} \\ &= 0.0132 + 0.0111 = 0.0243 \end{aligned}$$

Consequently,

AFFDL-TR-78-124

$$(L/D)_2 = \frac{0.4279}{0.0243} = 17.809$$

and,  $(L/D)_1 = \frac{0.4260}{0.0241} = 17.676$

a loss in aircraft lift-drag ratio of -0.067 or a loss of 0.4 percent.

## APPENDIX B

## CHARACTERISTICS OF THE BASIC KC-135A MODEL

To investigate the aerodynamic effects of different winglet configurations on the KC-135A model, it was necessary to determine the aerodynamic characteristics of the basic KC-135A model. To accommodate mounting the winglets a small portion of the model wing tips were cut off, reducing the aspect ratio of the basic wing from 7.035 to 6.98. An analysis (Appendix A) indicated a loss in aircraft lift-drag ratio of about -0.067, or about 0.4 percent, with the wing tips removed.

The variation of the lift of the basic model with angle of attack is shown in Figures 79, 80, and 81 for flap deflection of zero, 30 and 50 degrees. Extrapolation of Figure 79 ( $M = 0.30$ ) to zero lift indicates the angle of zero lift of the model at zero flap deflection and zero horizontal tail incidence angle to be about -3 degrees. The lift curve slope varied from about 0.0796 at  $M = 0.30$  to about 0.1008 at  $M = 0.80$  for the model with the tail off. Variation of the drag with lift is shown in Figures 82, 83, and 84. At zero flap deflection and zero horizontal tail incidence, Figure 82 indicates the zero lift drag coefficient at  $M = 0.30$  to be about 0.0218, the minimum drag coefficient to be about 0.0210, and the lift coefficient corresponding to the minimum drag coefficient to be about 0.075. For cruise conditions, Figure 84 indicates the drag coefficient of the model without tail to be about 0.0260. Variation of the model pitching moment with lift is shown in Figures 85, 86, and 87. At low speed (Figures 85 and 86), the slope of the pitching moment curves in the linear region was essentially unaffected by horizontal tail incidence or flap deflection.

For zero flap deflection (Figure 85), the zero-lift pitching moment coefficient was about -0.047 and the slope,  $dC_m/dC_L$ , about -0.220. As shown by Figures 88 to 91, horizontal tail incidence and flap deflection had only small effect on the yawing and rolling moment of the basic KC-135A model except at high lift coefficients. Figures 92 and 93 show that the slope of the yawing and rolling moment curves was also little affected by horizontal tail incidence except for high lift coefficients.

## APPENDIX C

## COMPARISON OF FULL-SPAN AND SEMISPAN MODEL DATA

Aerodynamic coefficients are normally referenced to the theoretical wing area, although other areas may be used, and careful definition is required. The aerodynamic coefficients of wall-mounted semispan wing (or panel) models are generally referenced to the exposed wing area, and the results are normally comparable with full-span wind tunnel or flight data.

The KC-135A semispan model wing was directly attached to the wall mounted balance system; however, that portion next to the tunnel wall was shielded by the model body. The body pitched as the wing angle of attack was changed; however, the fuselage was completely isolated and no body loads were recorded. The body had a slot through which the wing passed. The wing was designed so that the tip deflected approximately the same as the tip of the full-scale airplane at cruise conditions. The aerodynamic coefficients of the KC-135A semispan model are referenced to the area of that portion of the wing outboard of the body, i.e., the exposed wing area. Data obtained are, therefore, for the exposed wing (plus winglets) in the presence of, but not attached to, the model body.

The full-span KC-135A model was mounted in the center of the tunnel test section on a sting-supported six-component balance system. The model wings were rigid and did not deflect aeroelastically. The aerodynamic coefficients are referenced to the theoretical wing area.

Comparison of the incremental lift and drag obtained with the 0.035-scale full-span model and the 0.07-scale semispan model with different

AFFDL-TR-78-124

winglet configurations is shown in Figures 94 to 97 for Mach numbers of 0.70 and 0.78. Agreement of the data from the two different models is generally very good, however, some differences exist in the lift at  $M = 0.78$ .



Figure 1. Semispan KC-135A Model in the NASA/LaRC 8-Foot  
Transonic Pressure Tunnel



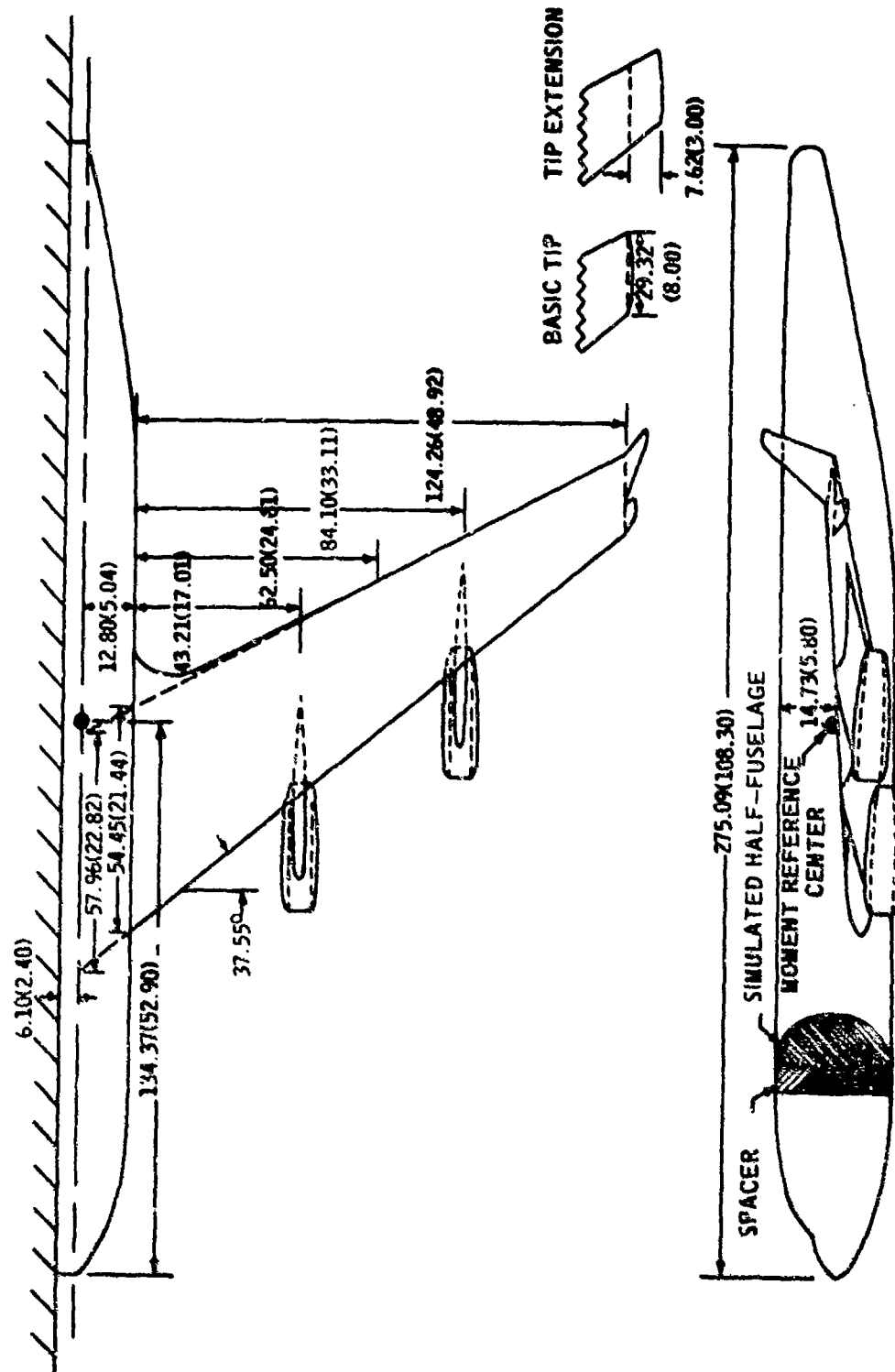


Figure 2. Basic Dimensions of KC-135A Semispan Model  
(Dimensions in centimeters (inches))

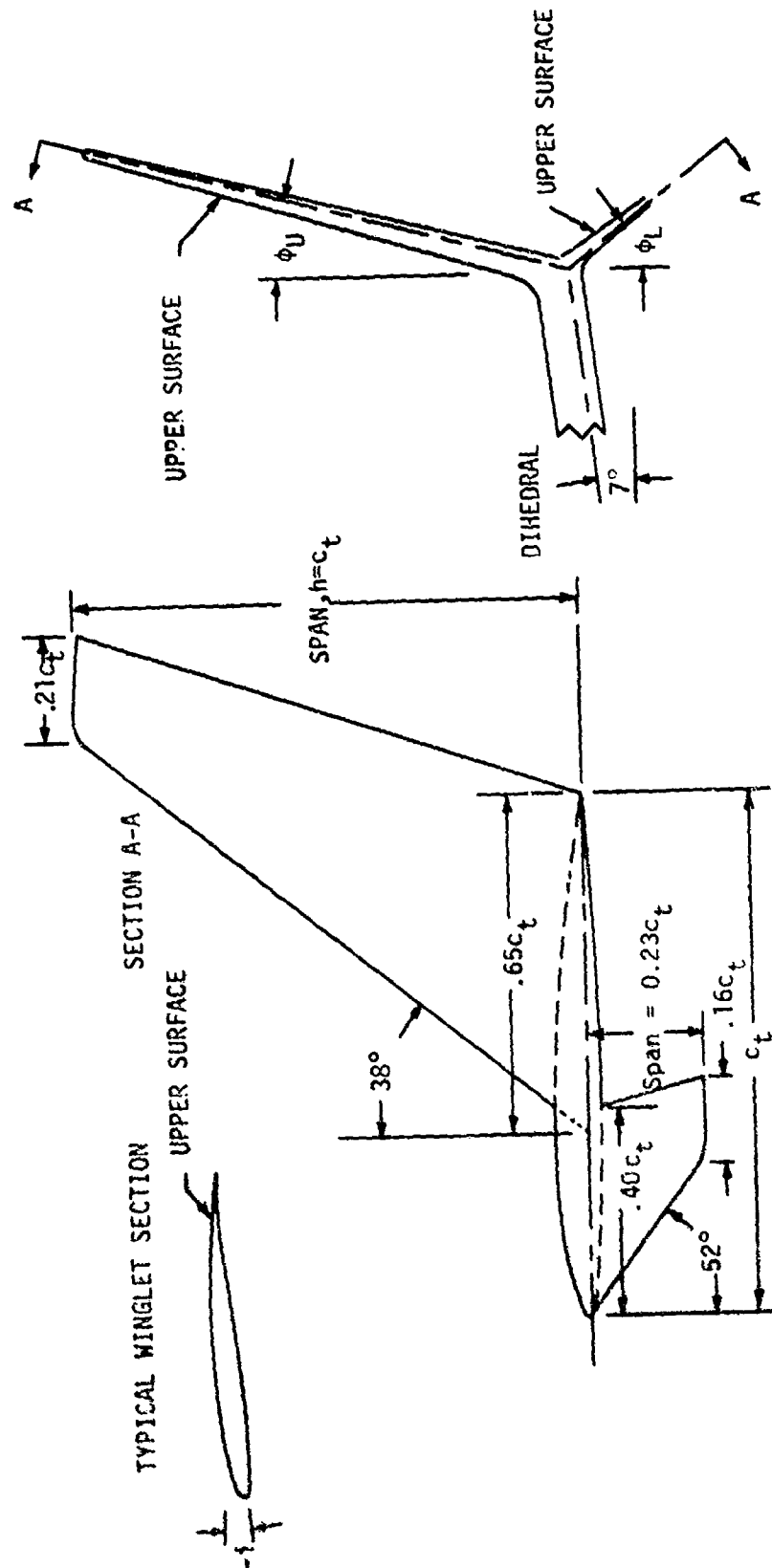


Figure 3. NASA Winglet Configurations

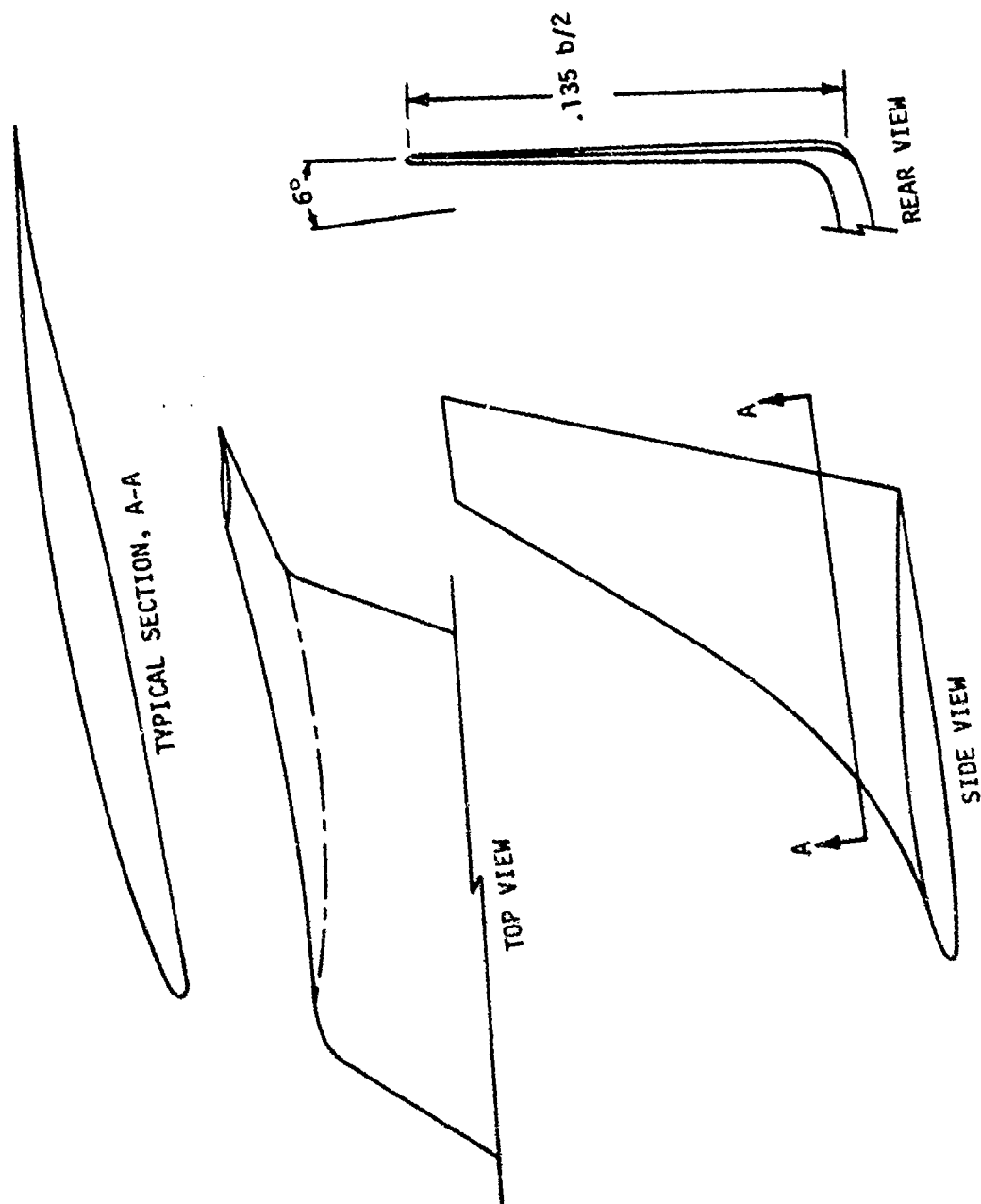


Figure 4. Boeing Winglet Configuration

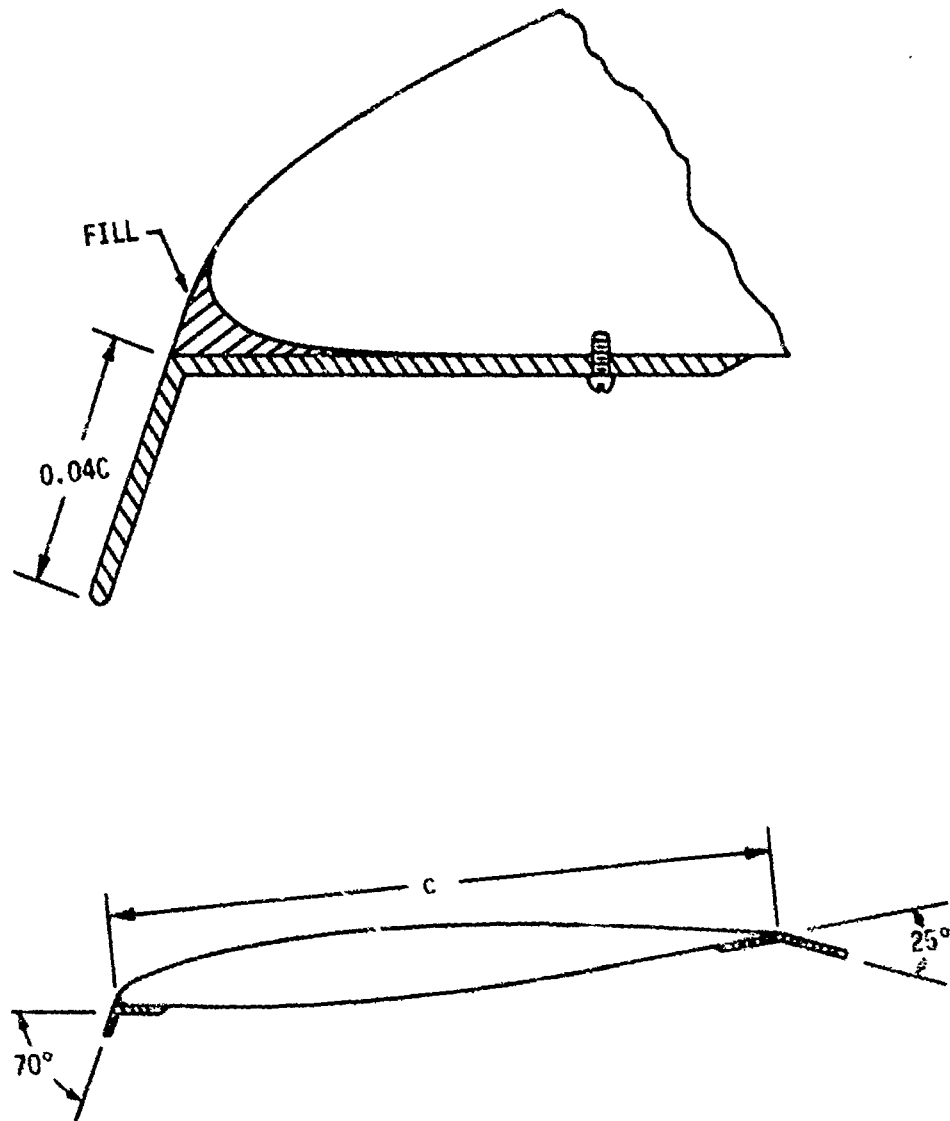


Figure 5. Leading and Trailing Edge Flaps for Semispan KC-135A Model



Figure 6. Full Span 0.035 Scale KC-135A Model With Low Speed Wing and Winglets

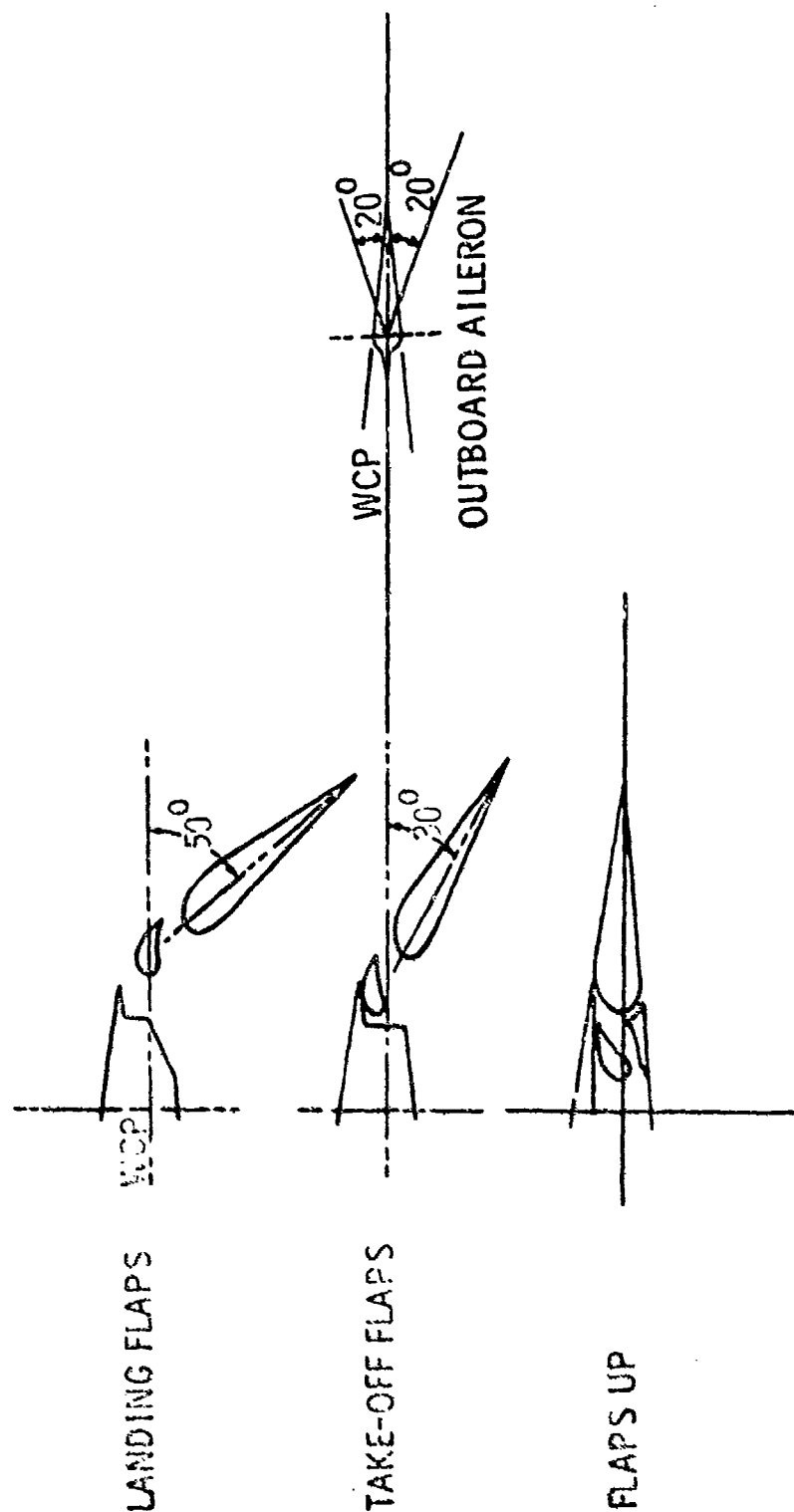


Figure 7. Wing Flap and Aileron Geometry of Full-Span KC-135A Model

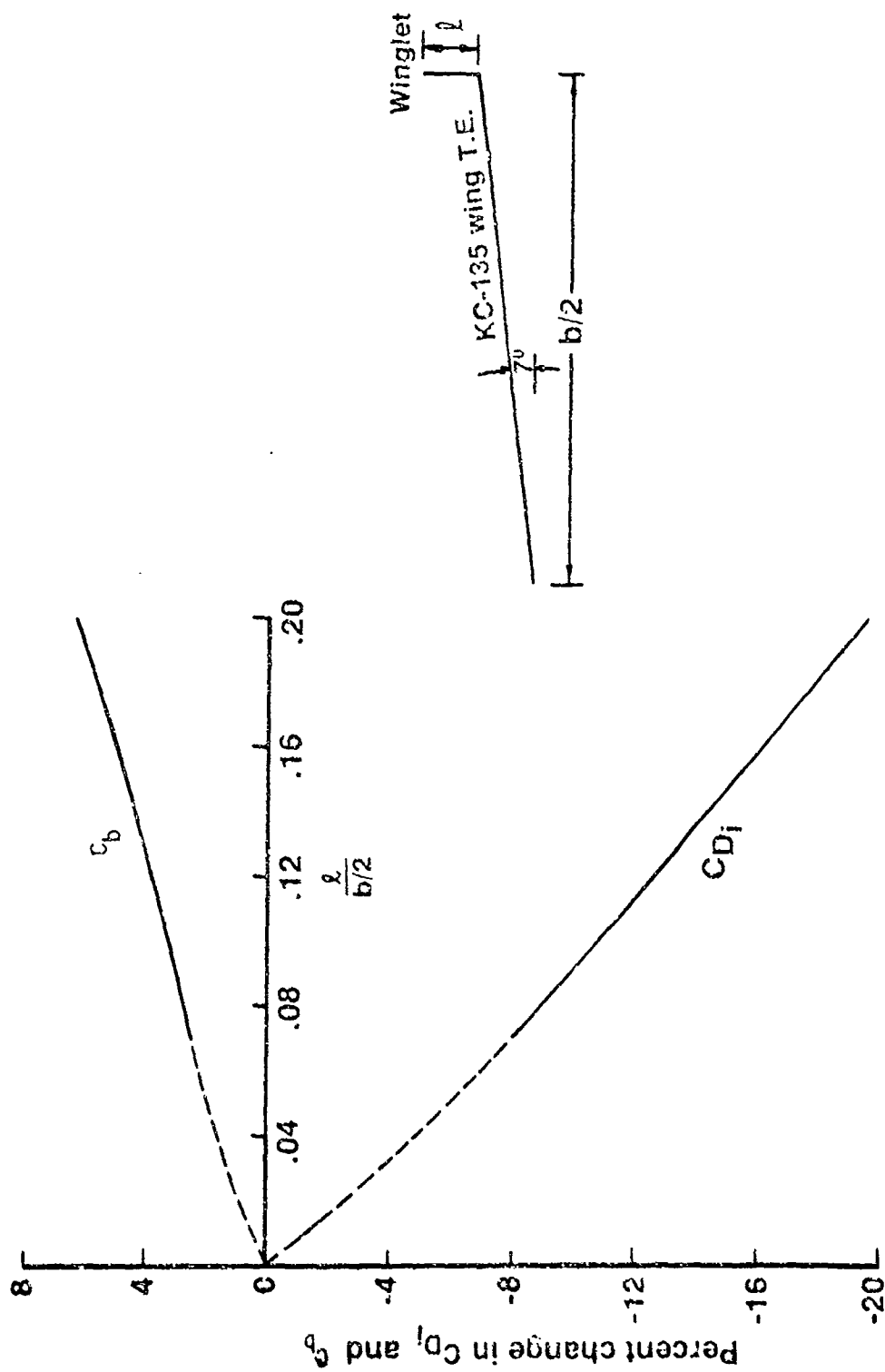


Figure 8. Effect of Winglet Length at Zero Cant  
 $C_{L\_CONFIG} = 0.426$  (Reference 1)

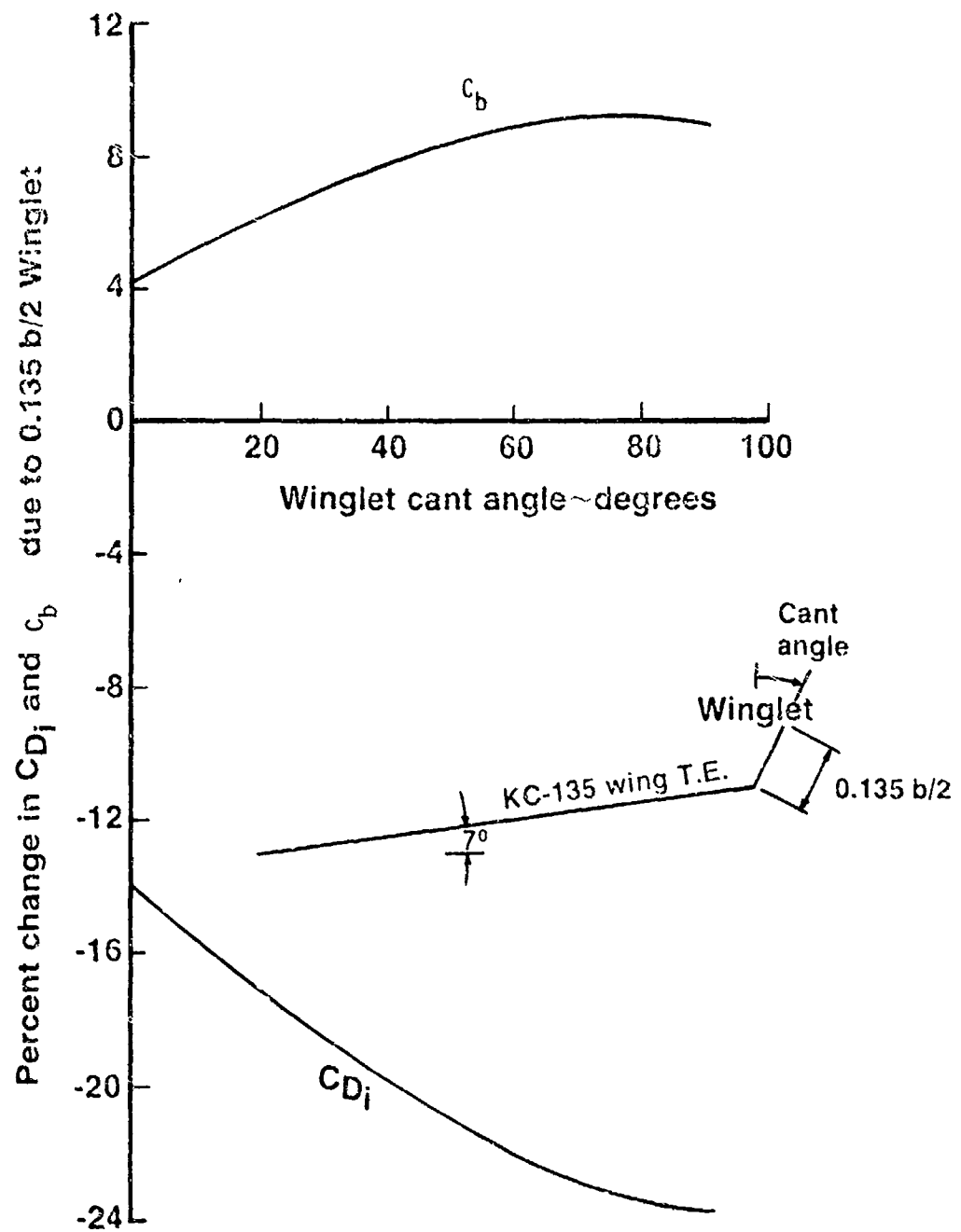


Figure 9. Effect of Winglet Cant Angle - Variable Span  
 $C_{L_{CONFIG}} = 0.426$  (Reference 1)



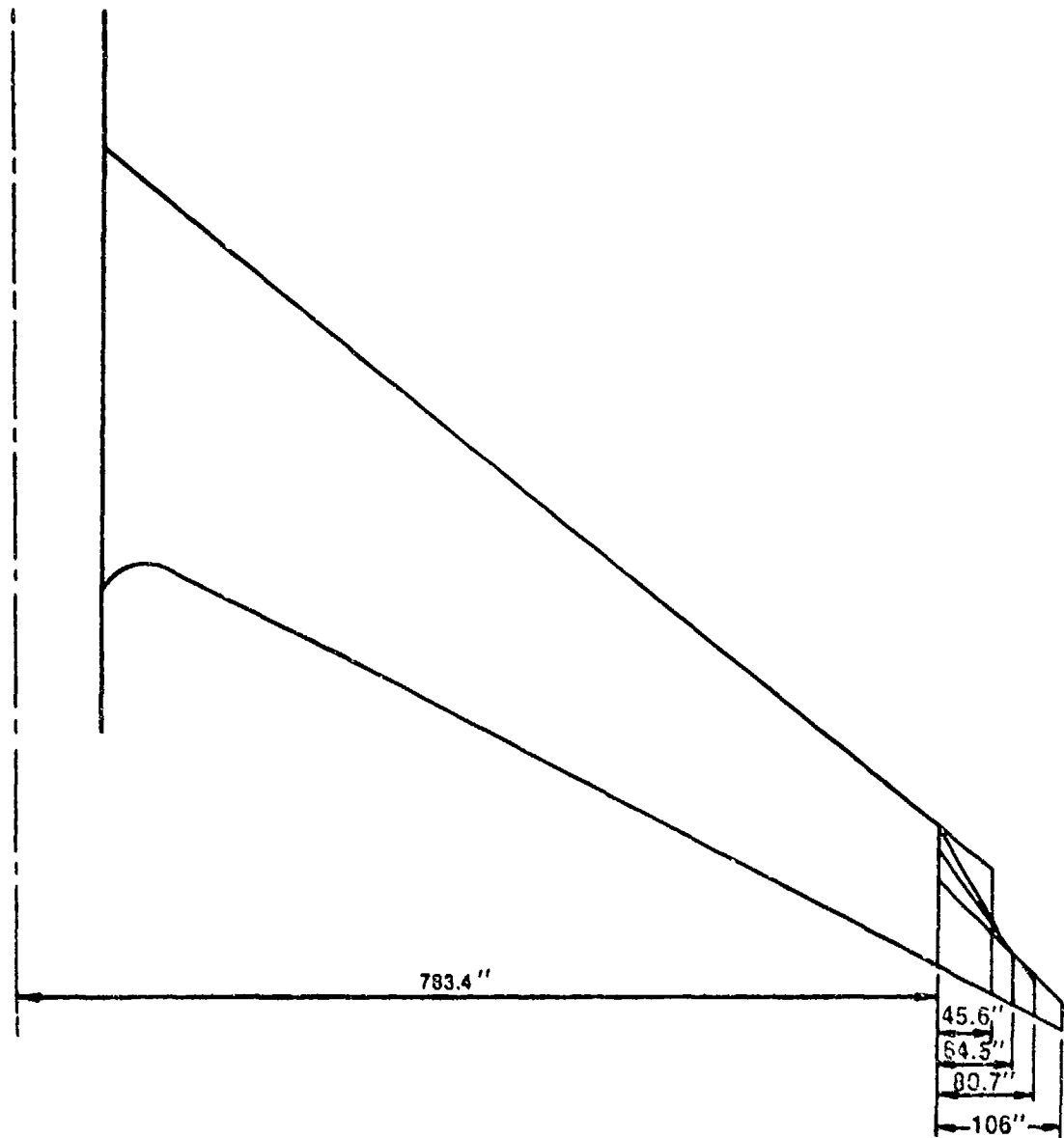


Figure 10. Equal Area Tip Extension Geometry Investigated  
in Reference 1

$$C_L = .426$$

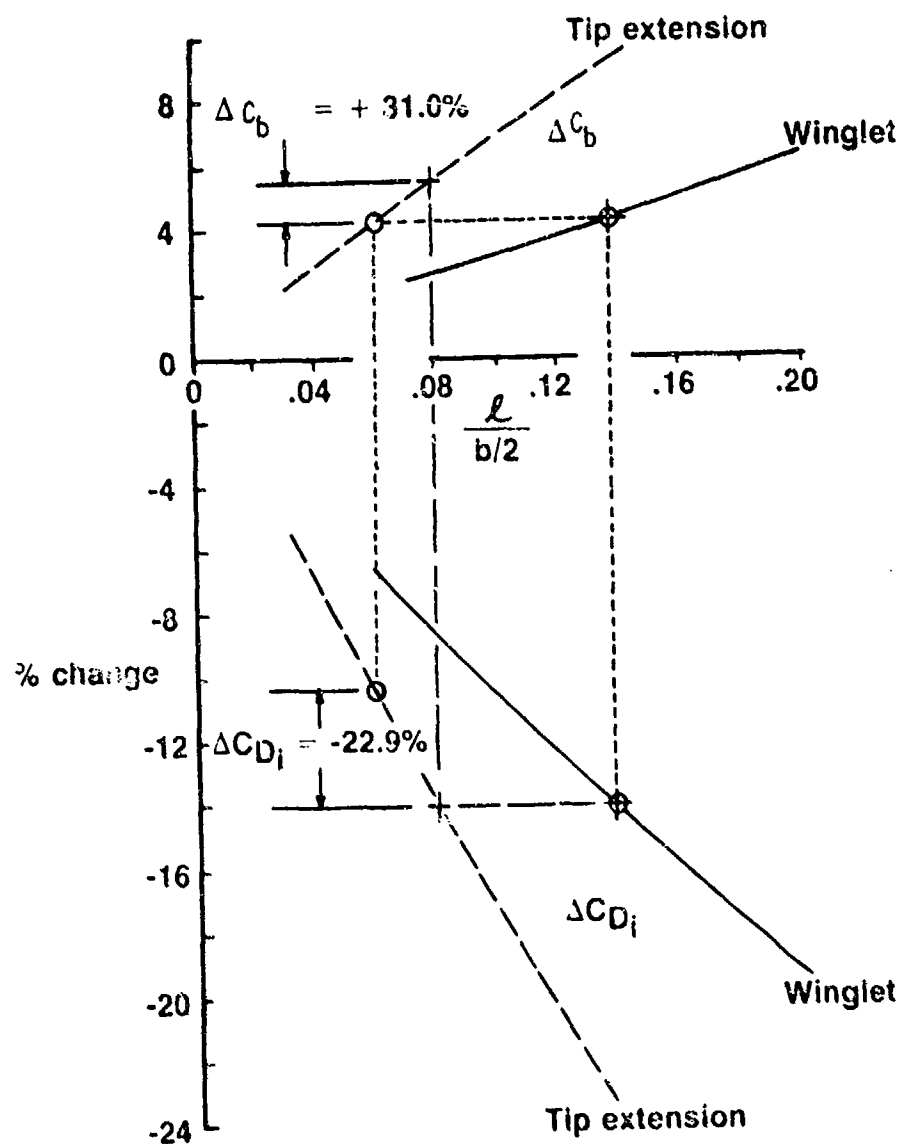


Figure 11. Comparison of Induced Drag and Wing Root Bending Moment Increments Between Zero Cant Winglets and Tip Extensions (Reference 1)

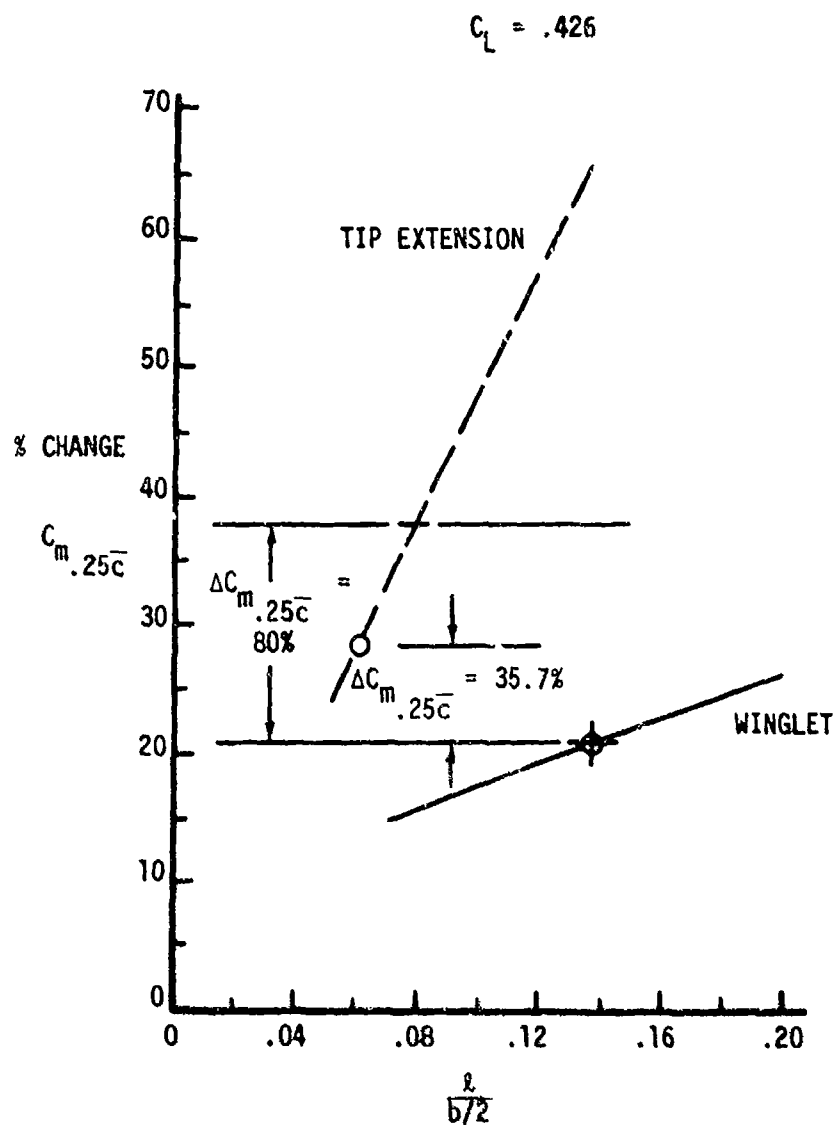


Figure 12. Comparison of Pitching Moment Increment Between Zero Cant Winglets and Tip Extensions (Reference 1)

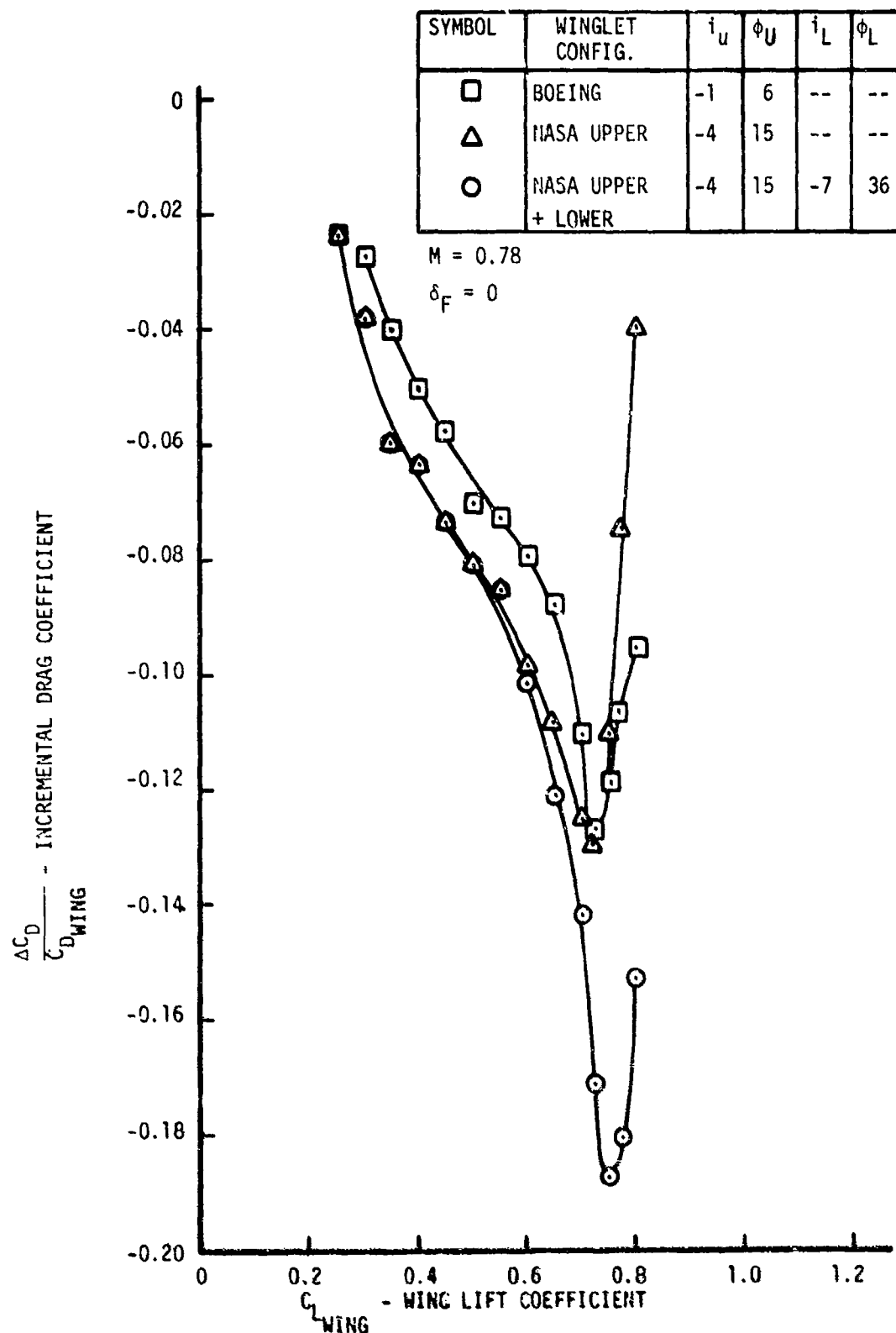


Figure 13. Effect of Winglet Configuration on Semispan KC-135A Model Drag.  $M = 0.78$ .  $\delta_F = 0$

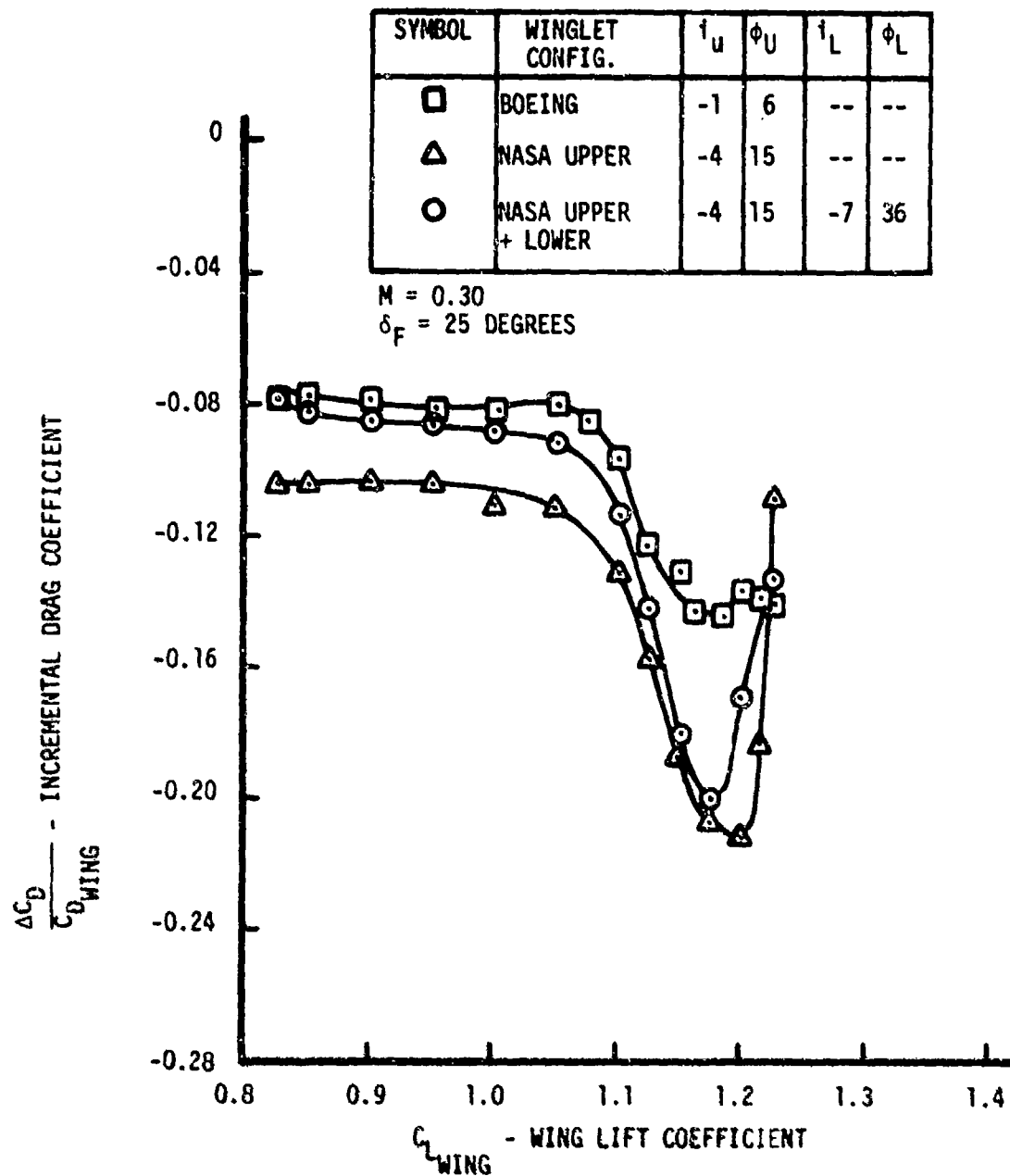


Figure 14. Effect of Winglet Configuration on Semispan KC-135A Model Drag.  $M = 0.30$ .  $\delta_F = 25$  Degrees

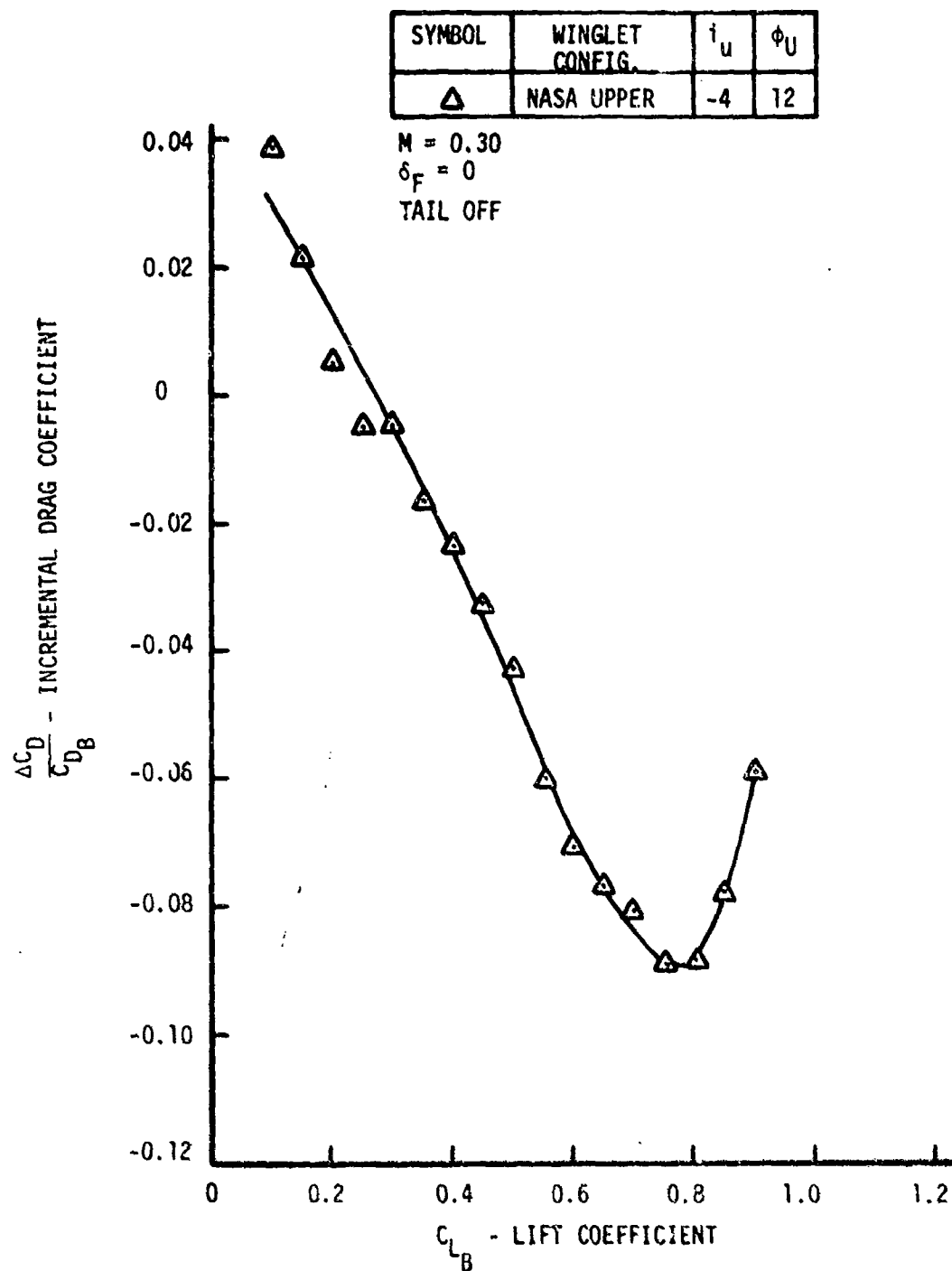


Figure 15. Effect of Winglet Configuration on Full-Span KC-135A Model Drag.  $M = 0.30$ .  $\delta_F = 0$

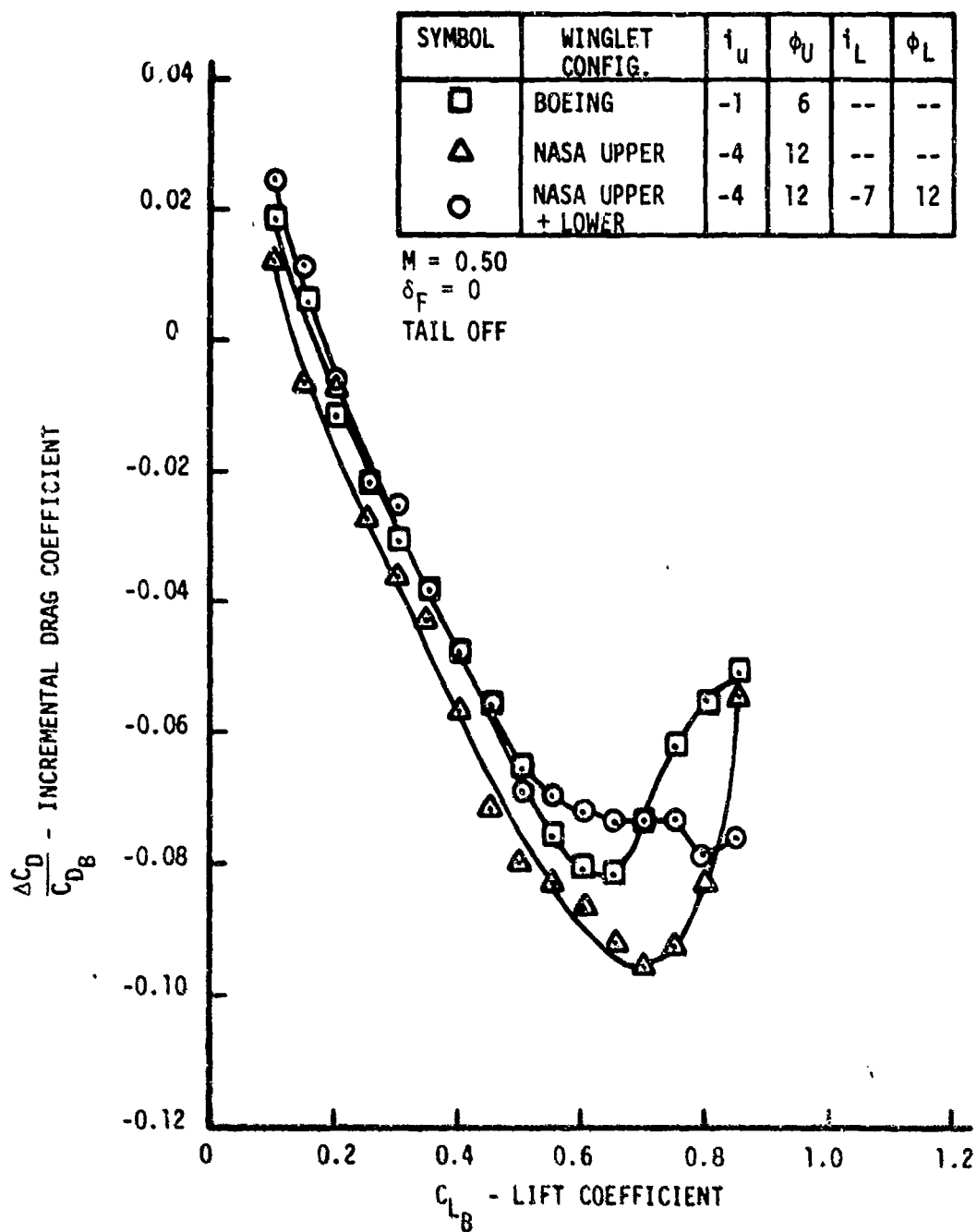


Figure 16. Effect of Winglet Configuration on Full-Span KC-135A Model Drag.  $M = 0.50$ .  $\delta_F = 0$

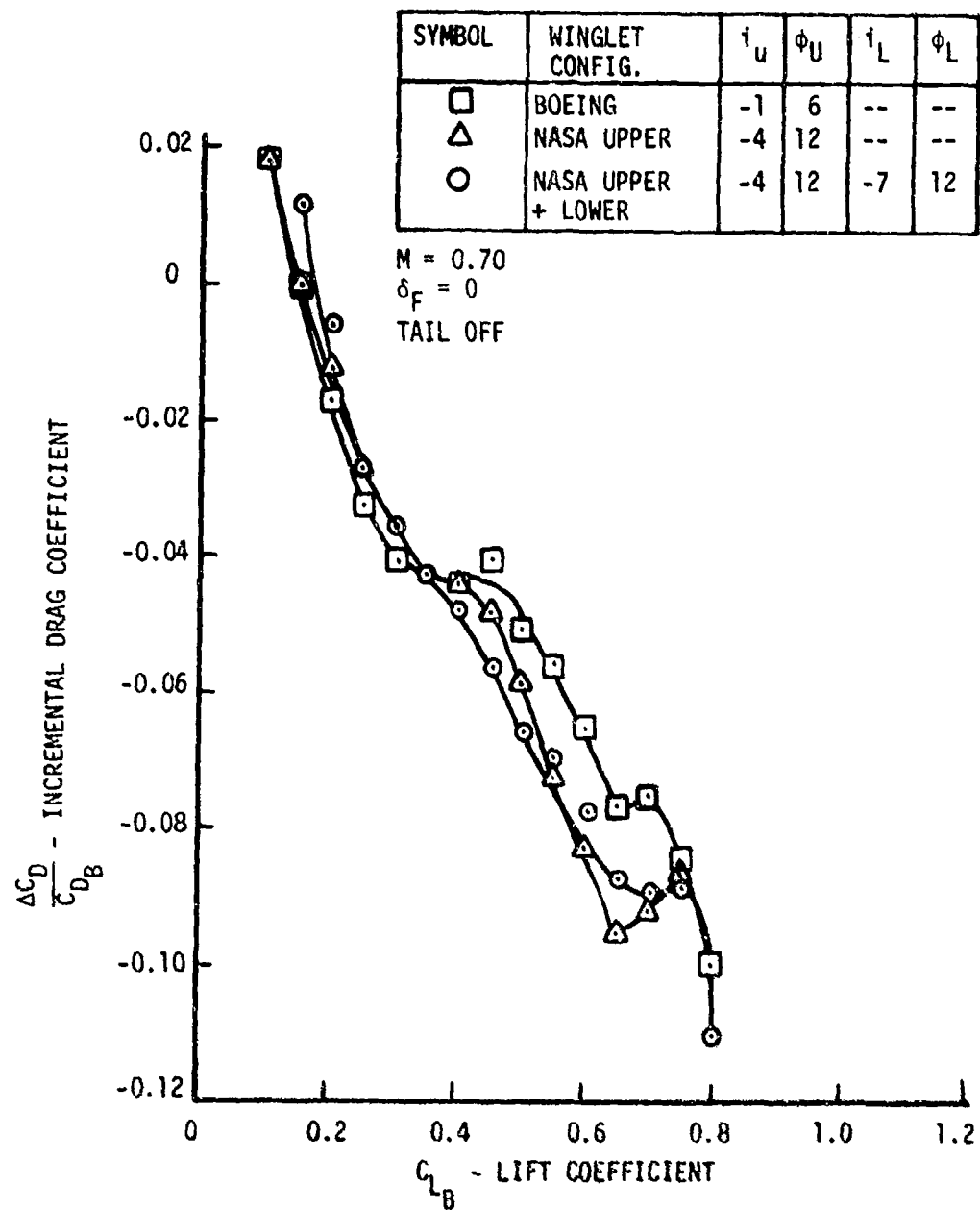


Figure 17. Effect of Winglet Configuration on Full-Span KC-135A Model Drag.  $M = 0.70$ .  $\delta_F = 0$



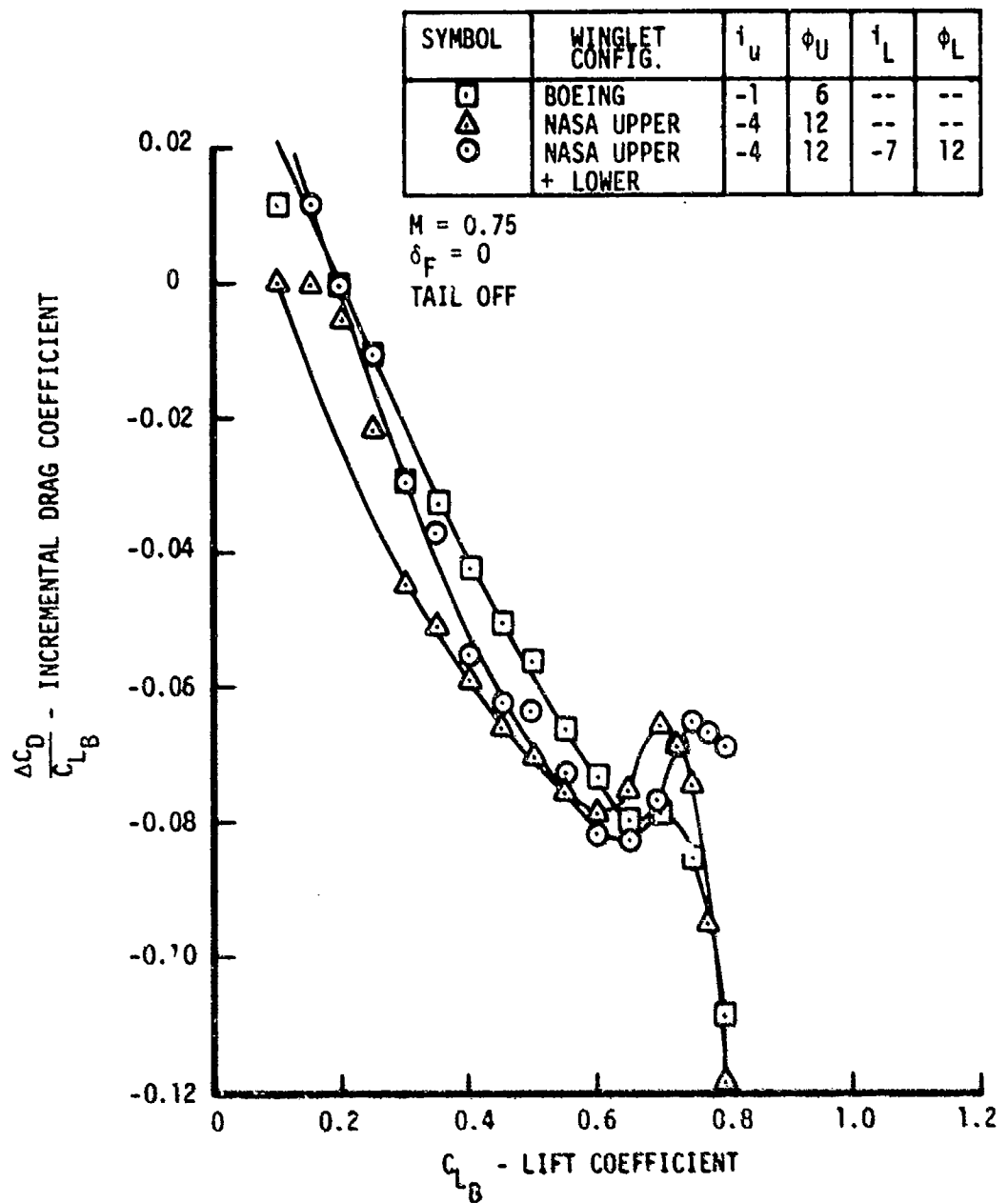


Figure 18. Effect of Winglet Configuration on Full-Span KC-135A Model Drag.  $M = 0.75$ .  $\delta_F = 0$

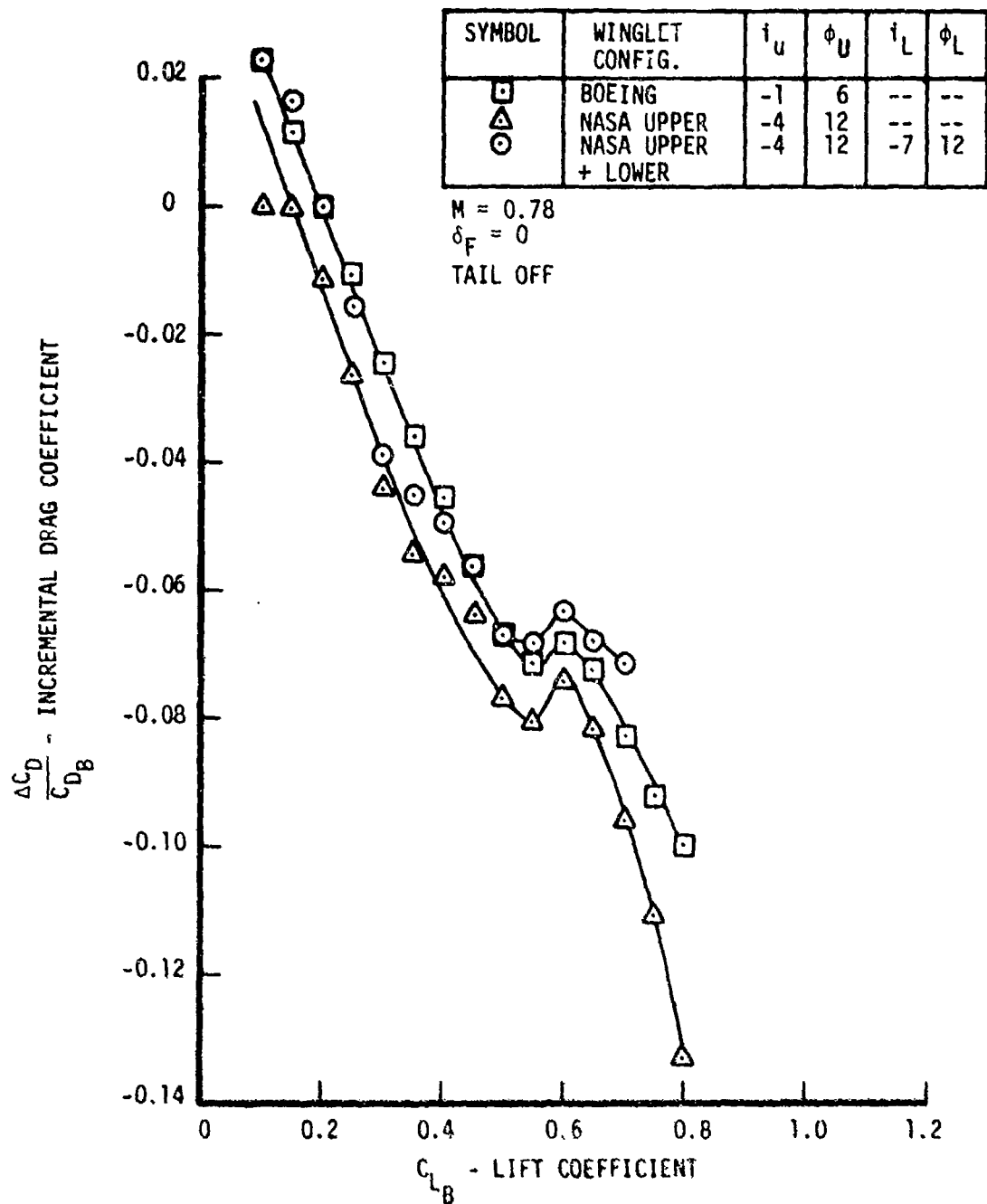


Figure 19. Effect of Winglet Configuration on Full-Span KC-135A Model Drag.  $M = 0.78$ .  $\delta_F = 0$

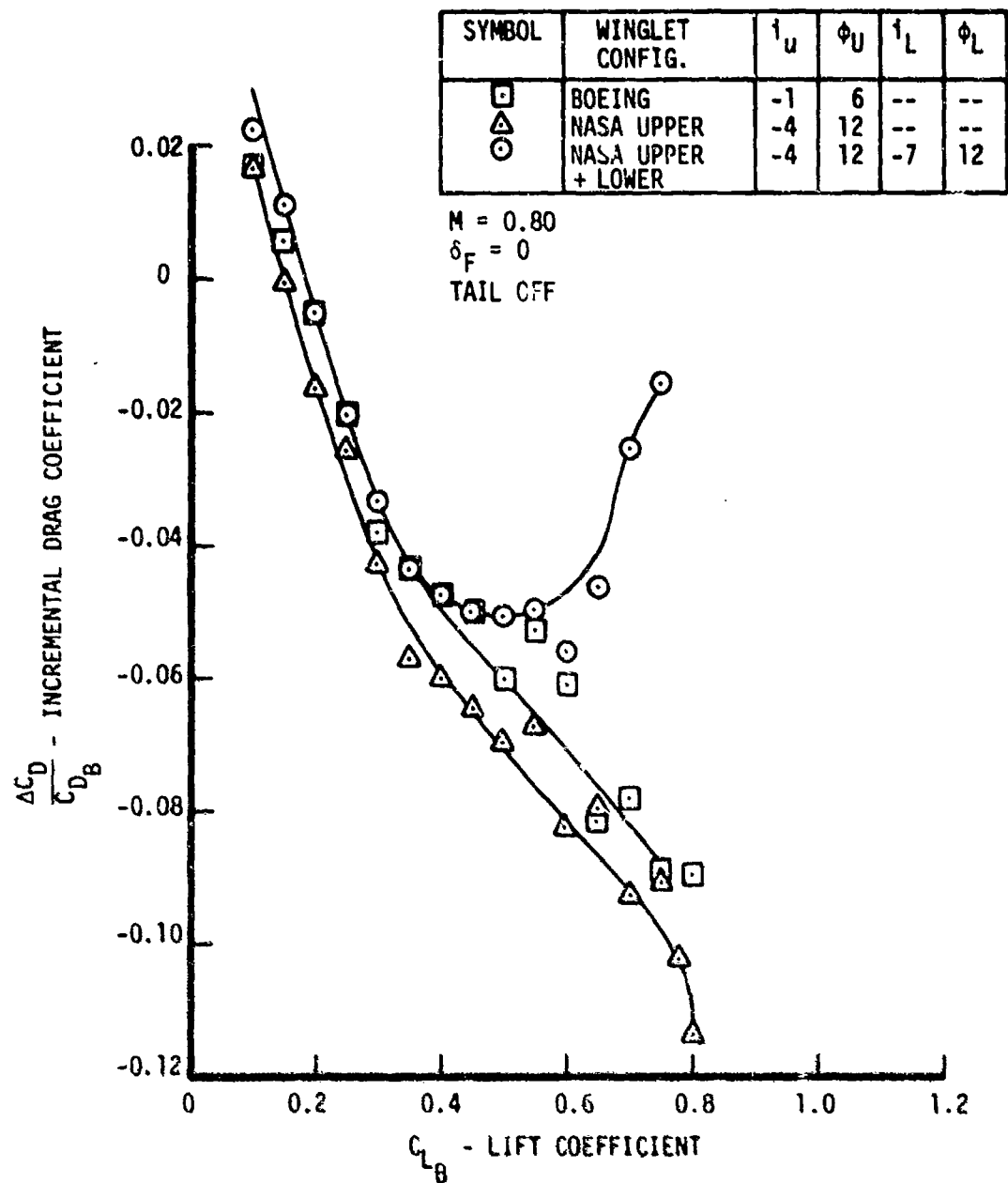


Figure 20. Effect of Winglet Configuration on Full-Span KC-135A Model Drag.  $M = 0.80$ .  $\delta_p = 0$

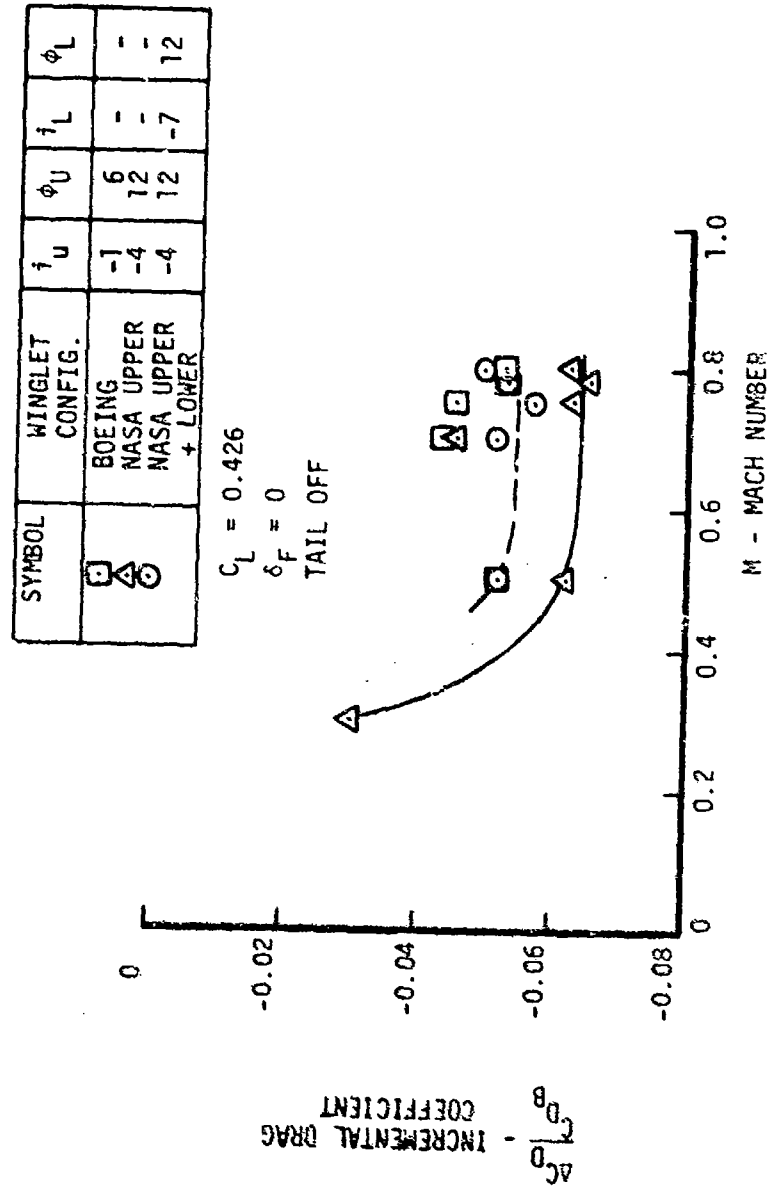


Figure 21. Effect of Winglet Configuration on Full-Span KC-135A Model Drag for Different Mach Numbers.  
 $C_L = 0.426$

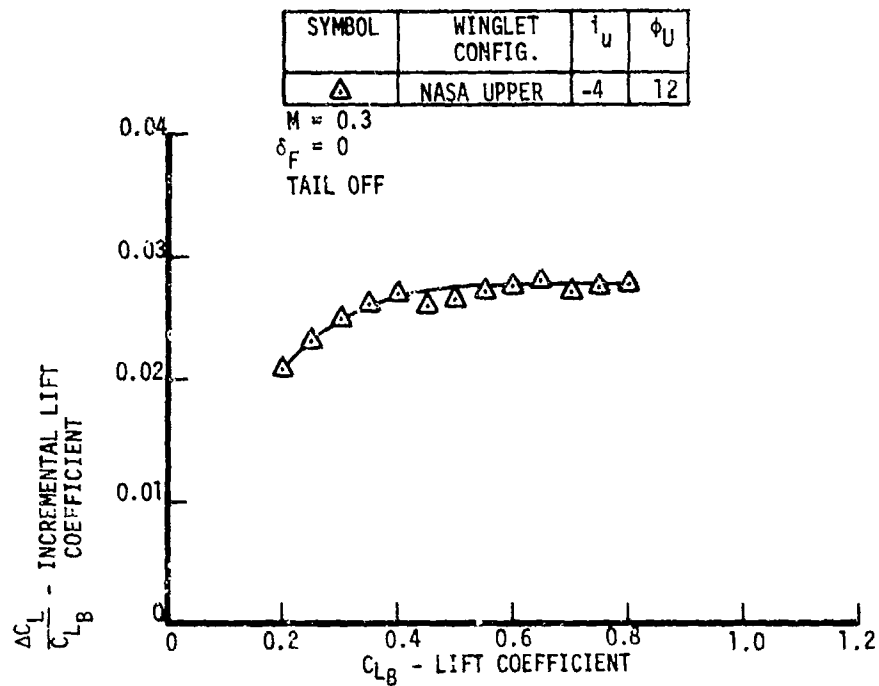


Figure 22. Effect of Winglet Configuration on Full-Span KC-135A Model Lift.  $M = 0.30$ .  $\delta_F = 0$

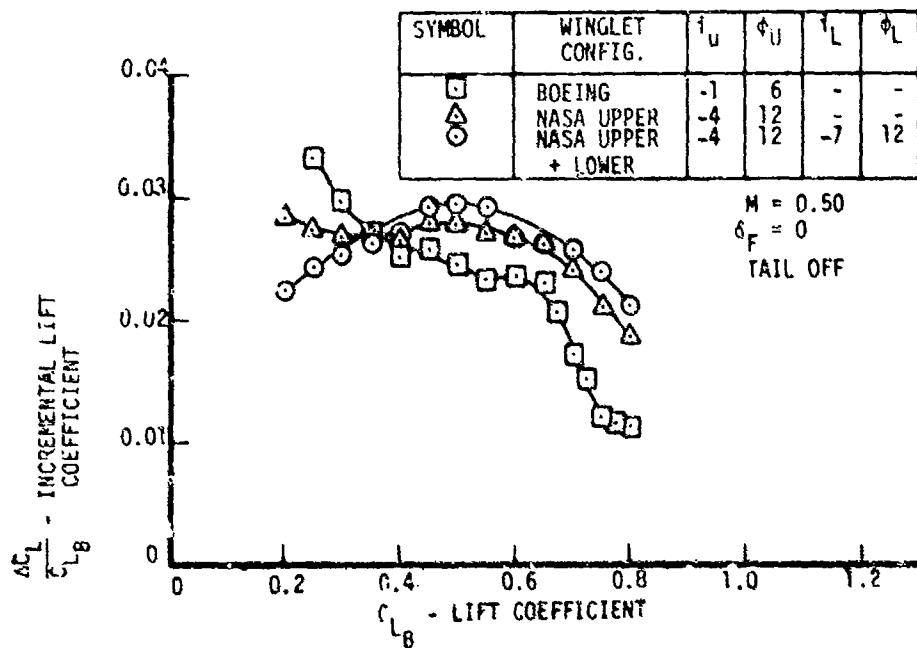


Figure 23. Effect of Winglet Configuration on Full-Span KC-135A Model Lift.  $M = 0.50$ .  $\delta_F = 0$

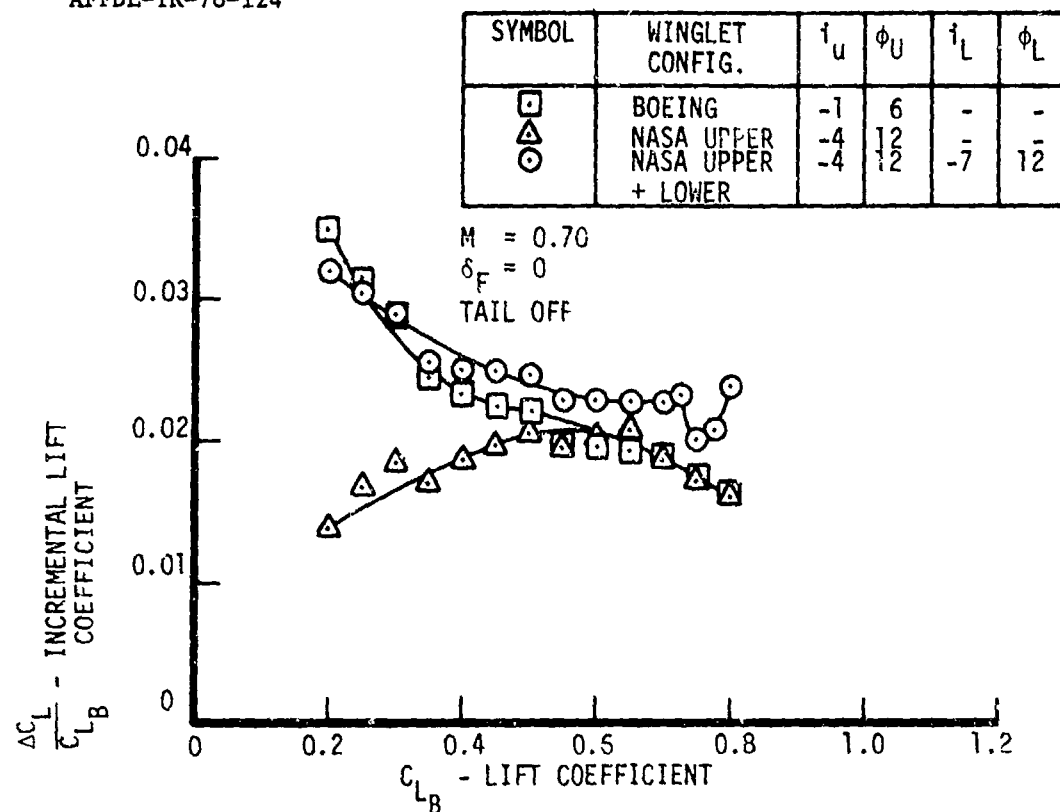


Figure 24. Effect of Winglet Configuration on Full-Span KC-135A Model Lift.  $M = 0.70$ .  $\delta_F = 0$

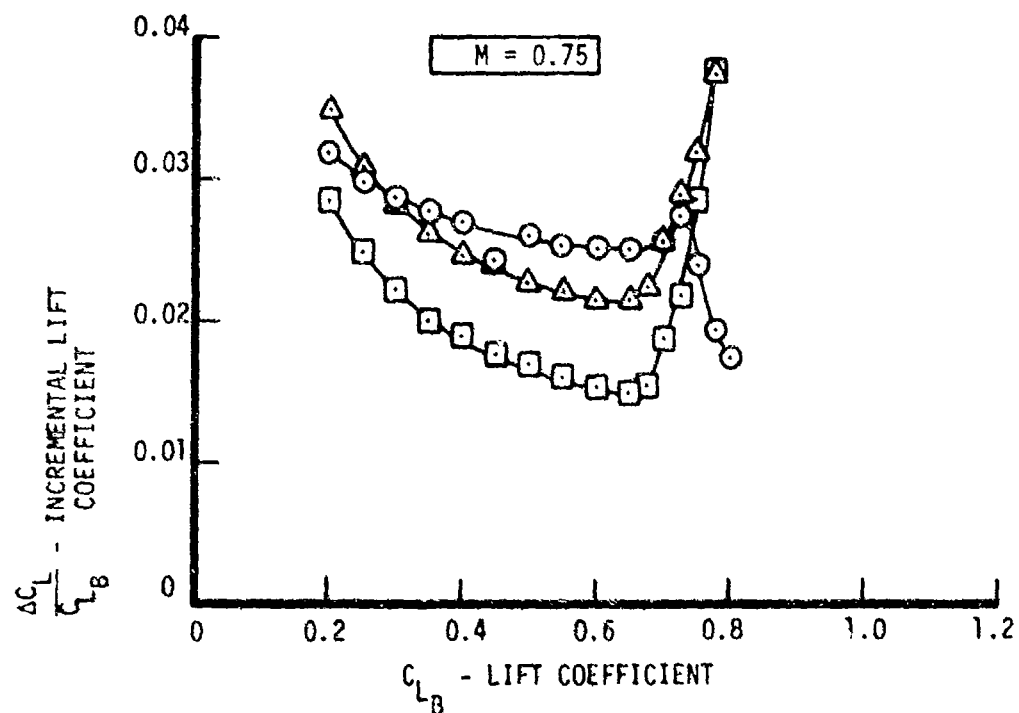


Figure 25. Effect of Winglet Configuration on Full-Span KC-135A Model Lift.  $M = 0.75$ .  $\delta_F = 0$

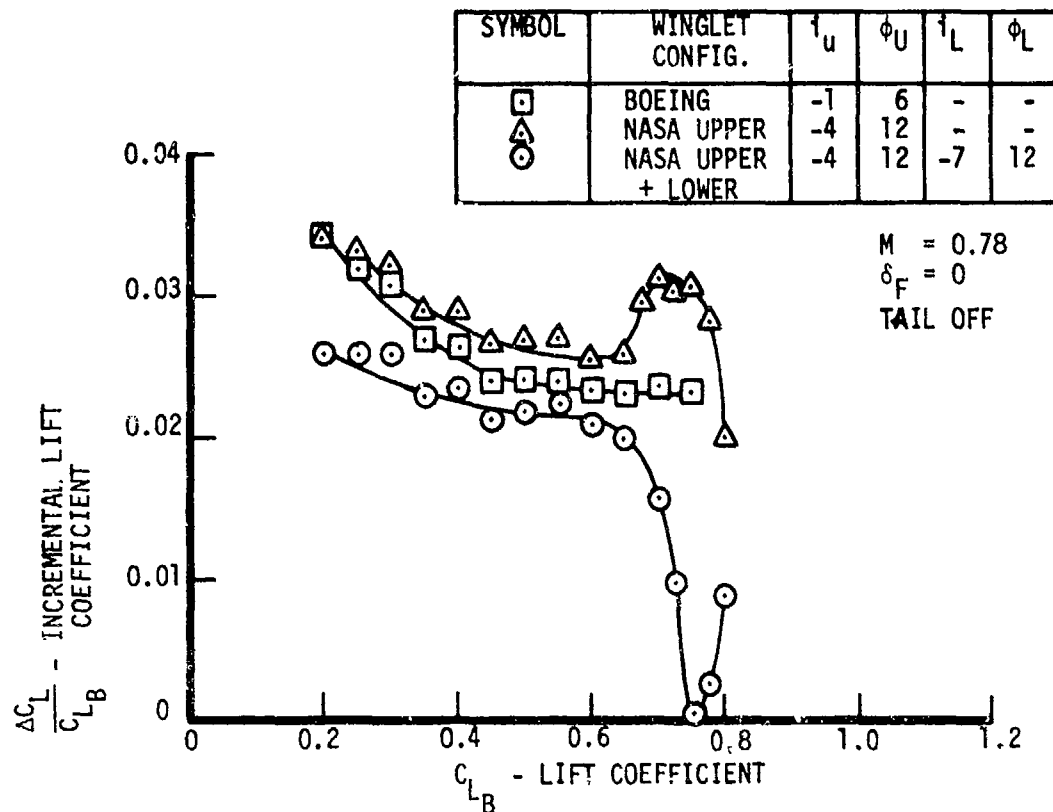


Figure 26. Effect of Winglet Configuration on Full-Span KC-135A Model Lift.  $M = 0.78$ .  $\delta_F = 0$

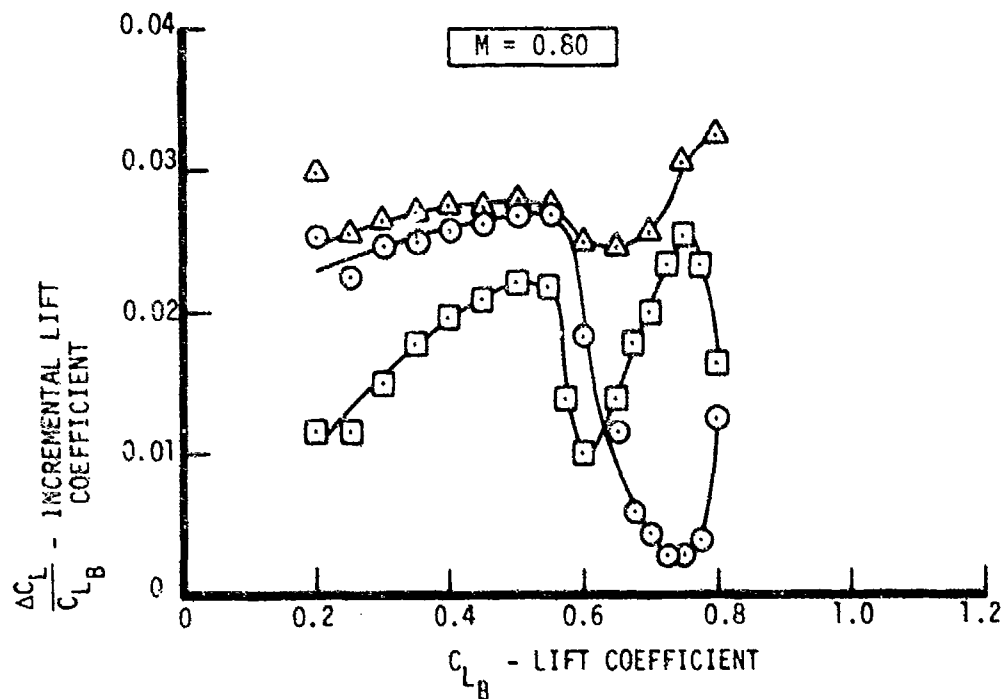


Figure 27. Effect of Winglet Configuration on Full-Span KC-135A Model Lift.  $M = 0.80$ .  $\delta_F = 0$

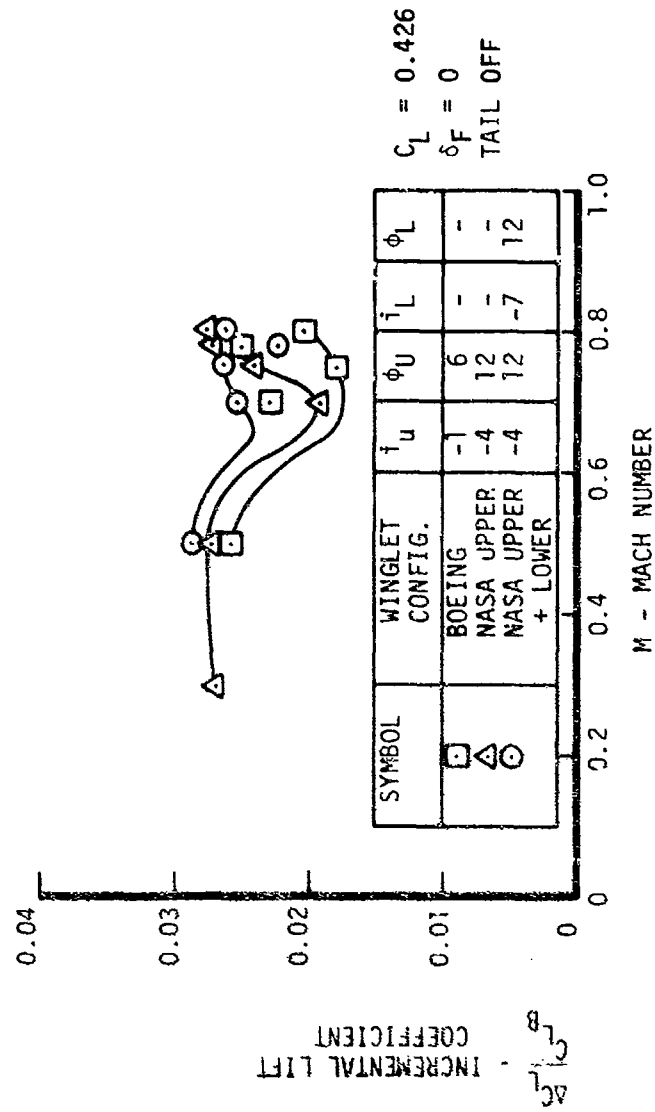


Figure 28. Effect of Winglet Configuration on Full-Span KC-135A Model Lift for Different Mach Numbers.  
 $C_L = 0.426$



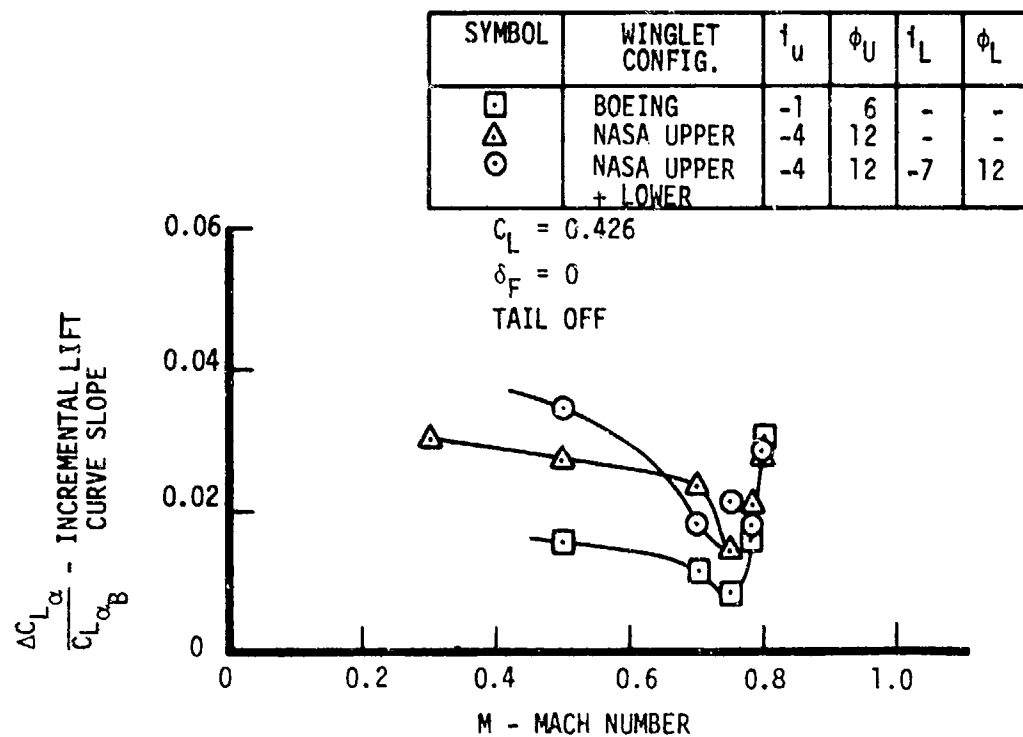


Figure 29. Effect of Winglet Configuration on Full-Span KC-135A Model Lift Curve Slope for Different Mach Numbers

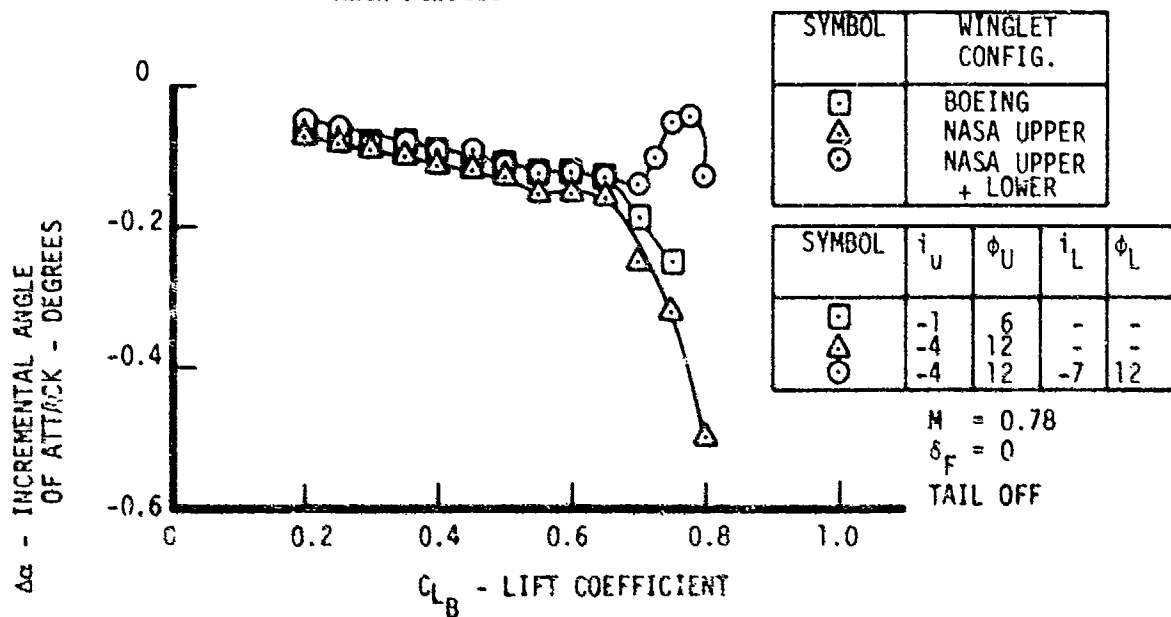


Figure 30. Effect of Winglet Configuration on Full-Span KC-135A Model Angle of Attack Near Cruise Conditions

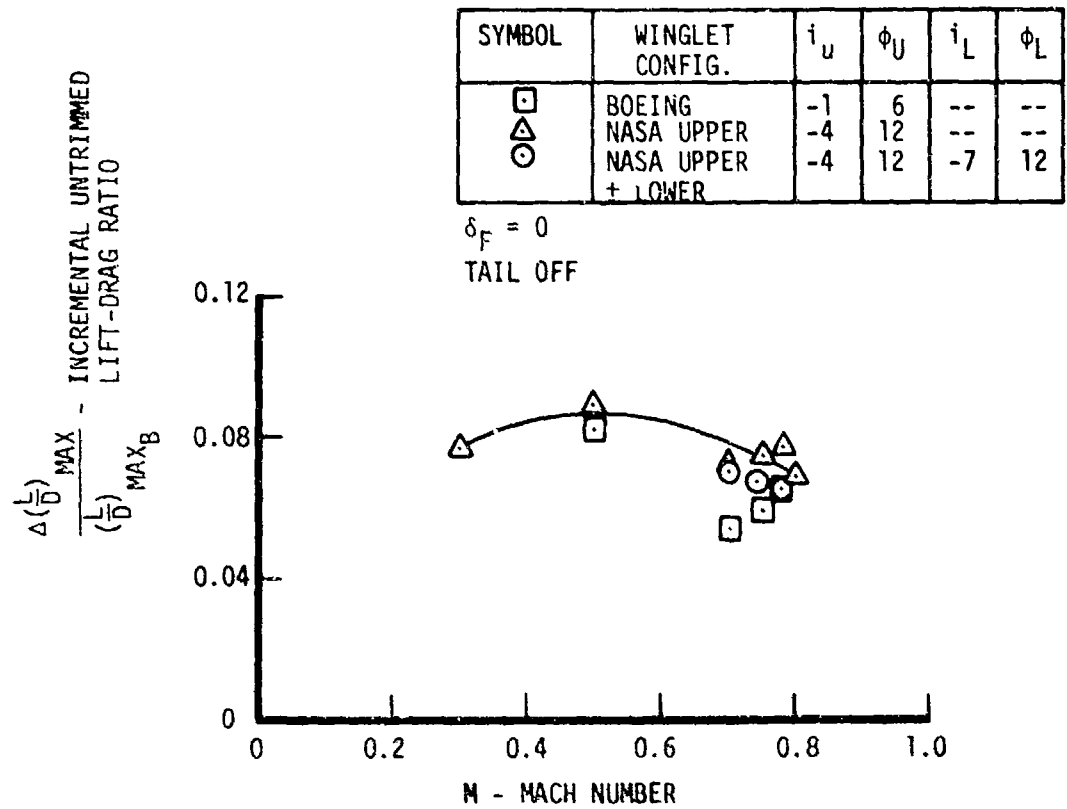


Figure 31. Effect of Winglet Configuration on Full-Span KC-135A Model Untrimmed Maximum Lift-Drag Ratio for Different Mach Numbers

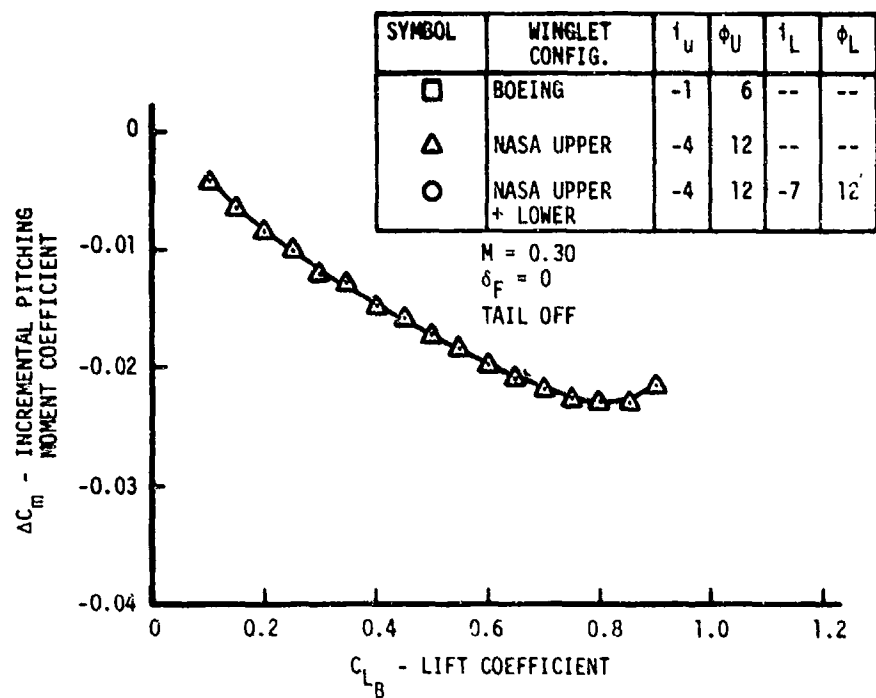


Figure 32. Effect of Winglet Configuration on Full-Span KC-135A Model Pitching Moment.  $M = 0.30$ .  
 $\delta_F = 0$

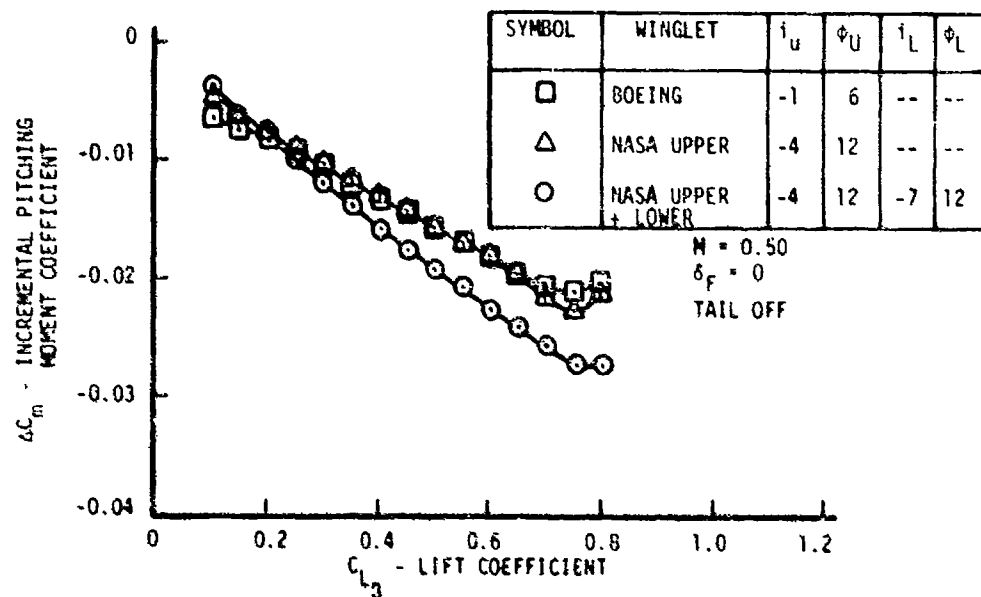


Figure 33. Effect of Winglet Configuration on Full-Span KC-135A Model Pitching Moment.  $M = 0.50$ .  
 $\delta_F = 0$

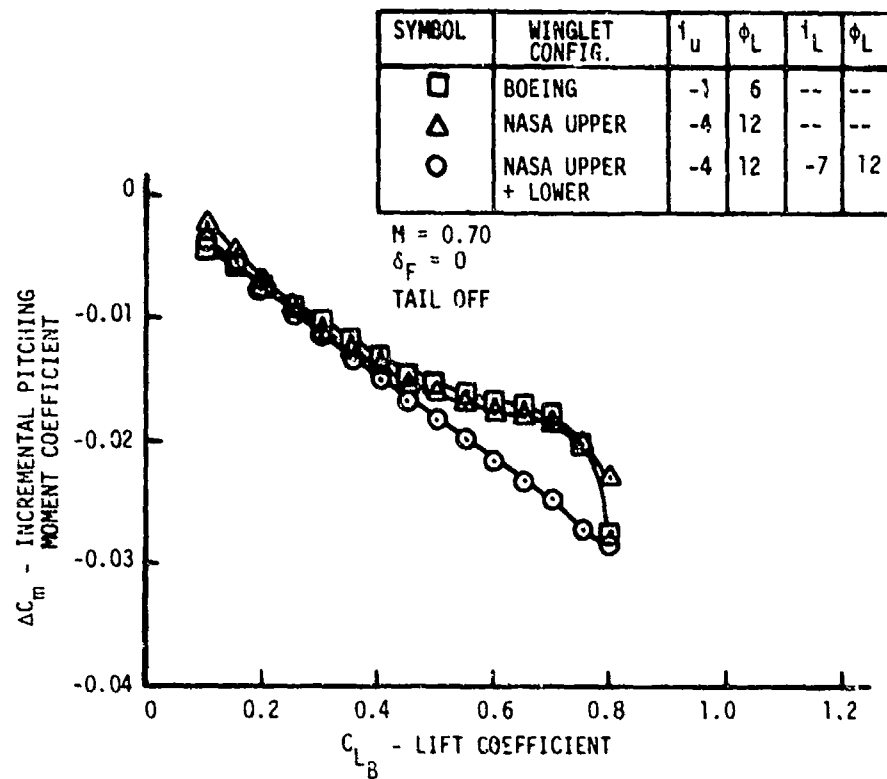


Figure 34. Effect of Winglet Configuration on Full-Span KC-135A Model Pitching Moment.  $M = 0.70$ .  
 $\delta_F = 0$

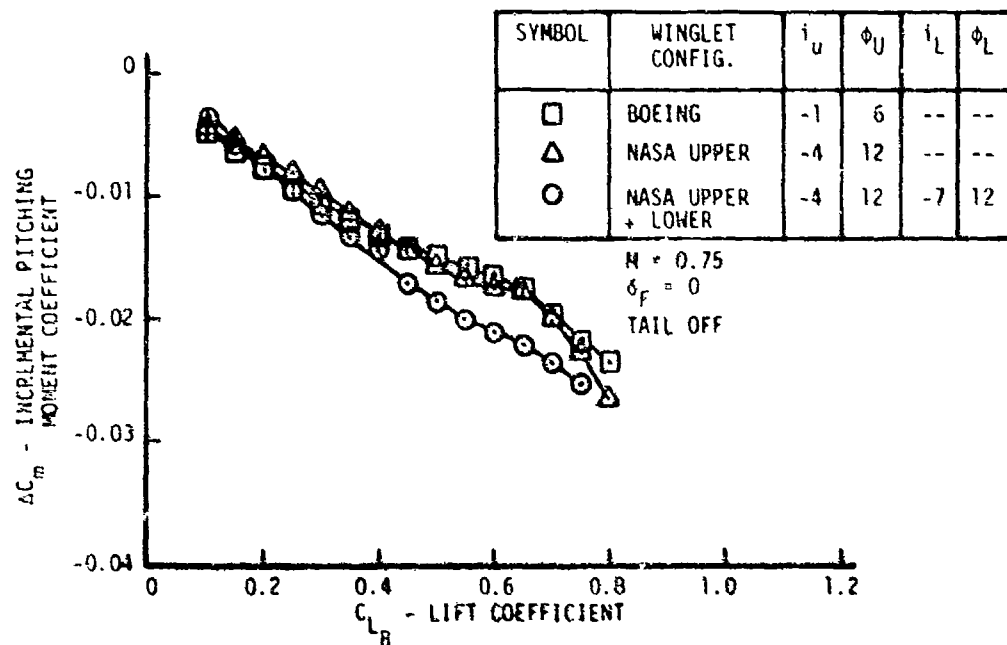


Figure 35. Effect of Winglet Configuration on Full-Span KC-135A Model Pitching Moment.  $M = 0.75$ .  
 $\delta_F = 0$

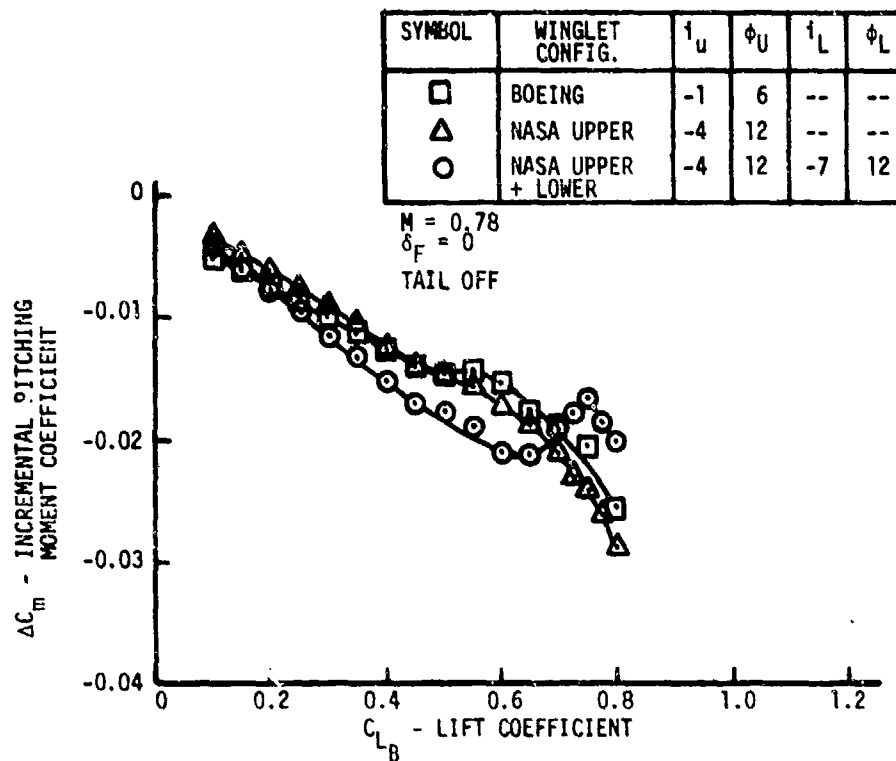


Figure 36. Effect of Winglet Configuration on Full-Span KC-135A Model Pitching Moment.  $M = 0.78$ .  
 $\delta_F = 0$

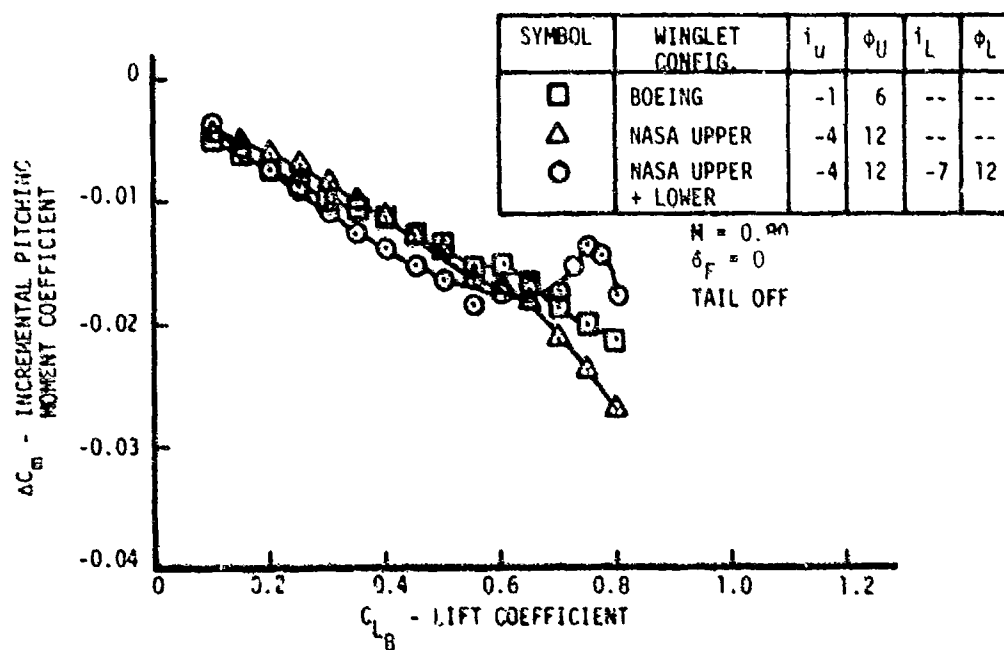


Figure 37. Effect of Winglet Configuration on Full-Span KC-135A Model Pitching Moment.  $M = 0.80$ .  
 $\delta_F = 0$

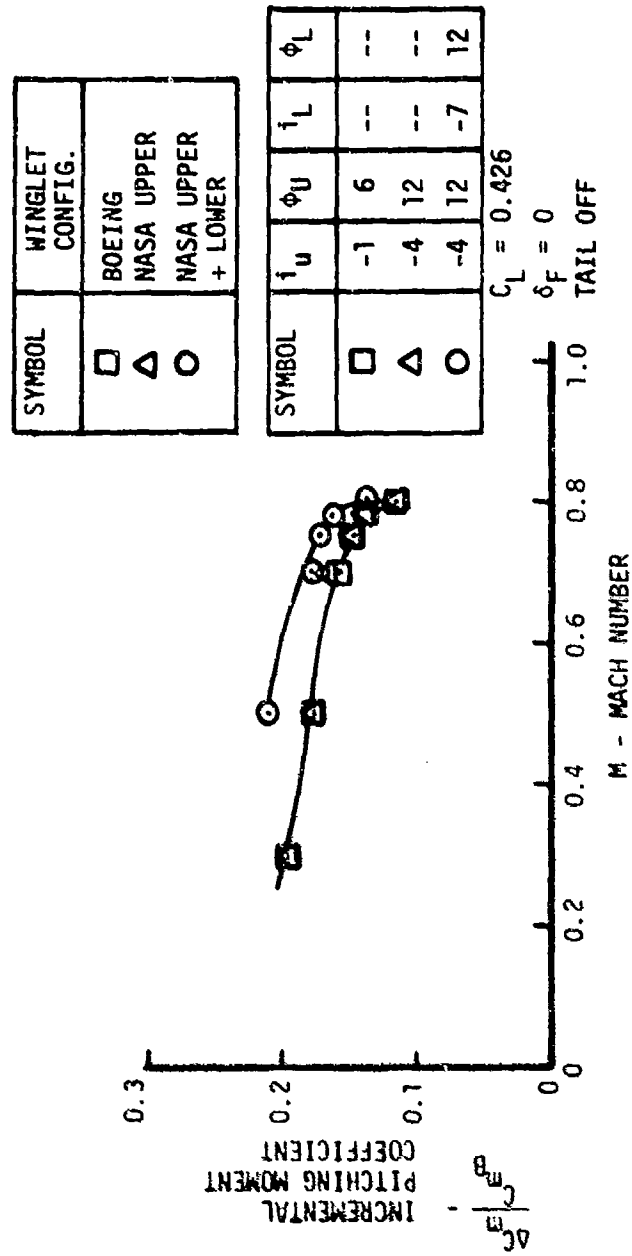


Figure 38. Effect of Winglet Configuration on Full-Span KC-135A Model Pitching Moment for Different Mach Numbers.  $C_L = 0.426$

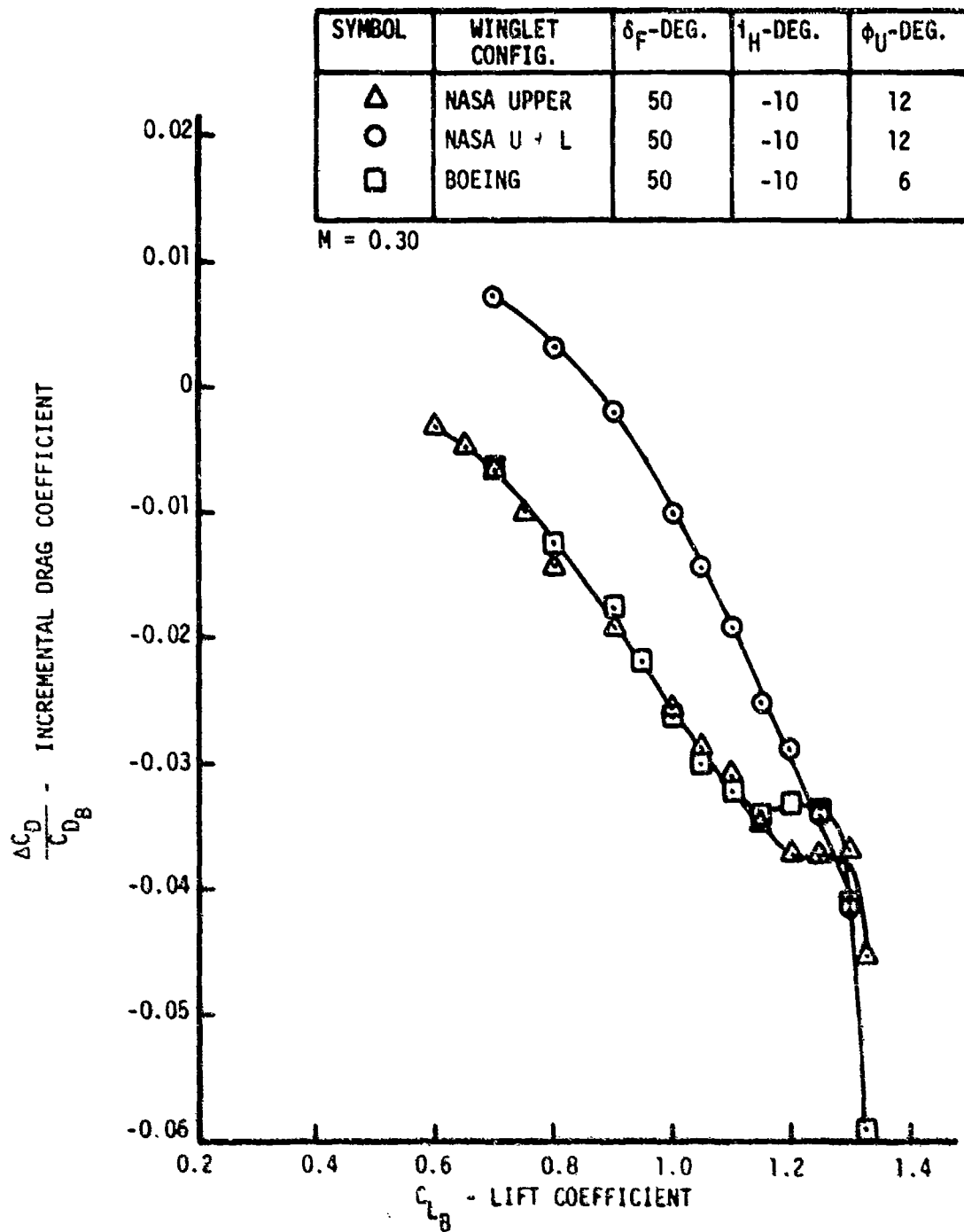


Figure 39. Effect of Winglet Configuration on Full-Span KC-135A Model Drag.  $M = 0.30$ .  $\delta_F = 50$  Degrees.  $i_H = -10$  Degrees

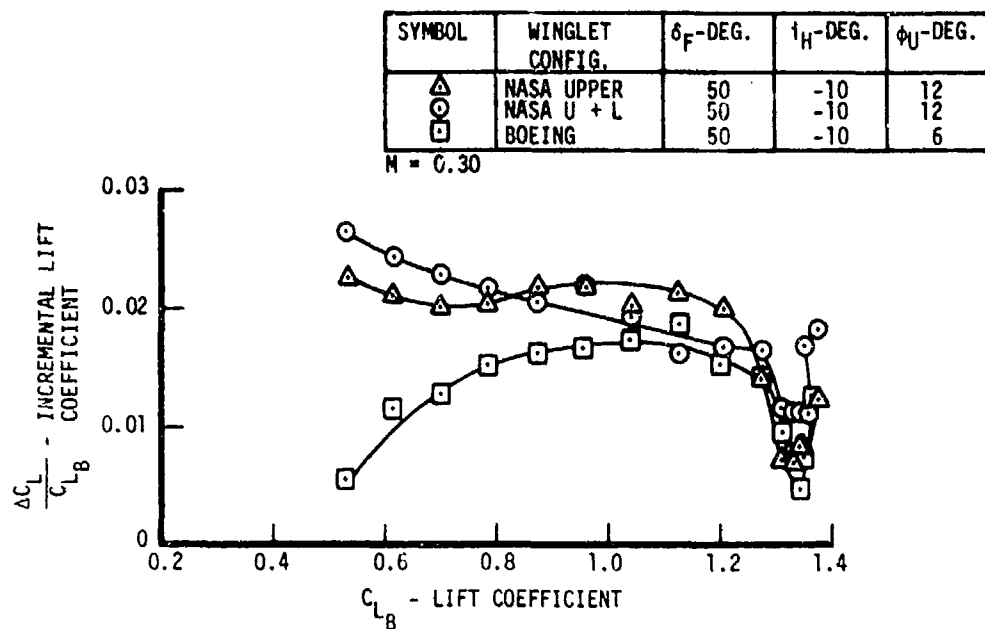


Figure 40. Effect of Winglet Configuration on Full-Span KC-135A Model Lift.  $M = 0.30$ .  $\delta_F = 50$  Degrees  $i_H = -10$  Degrees

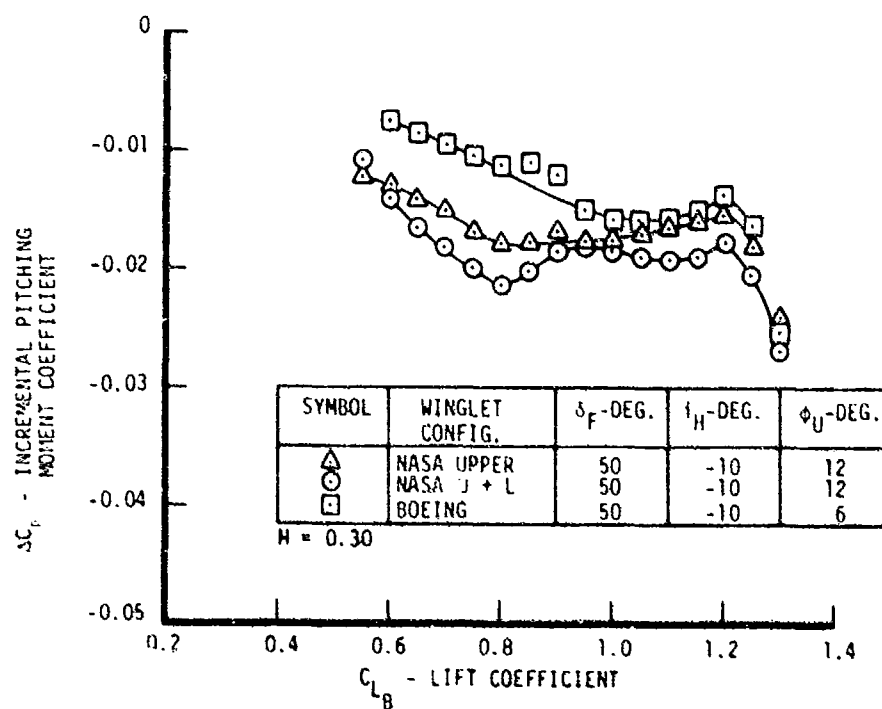


Figure 41. Effect of Winglet Configuration on Full-Span KC-135A Model Pitching Moment.  $M = 0.30$ .  $\delta_F = 50$  Degrees.  $i_H = -10$  Degrees



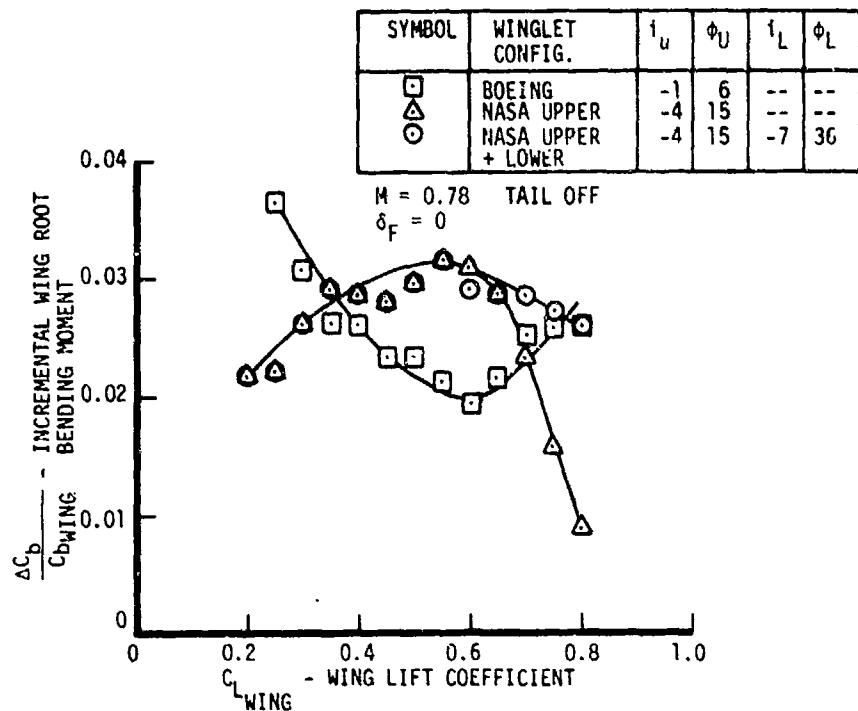


Figure 42. Effect of Winglet Configuration on Semispan KC-135A Model Wing Root Bending Moment.  
 $M = 0.78$ .  $\delta_F = 0$

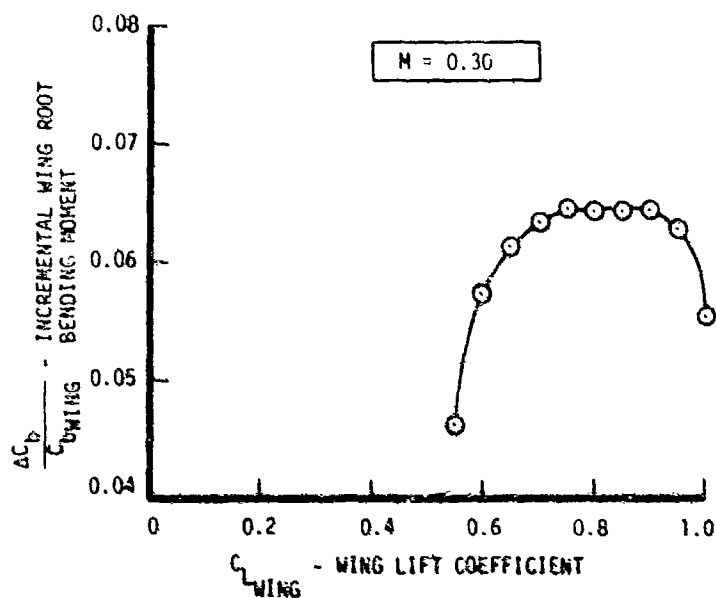


Figure 43. Effect of NASA Upper Plus Lower Winglet Configuration on Semispan KC-135A Model Wing Root Bending Moment.  $M = 0.30$ .  $\delta_F = 0$

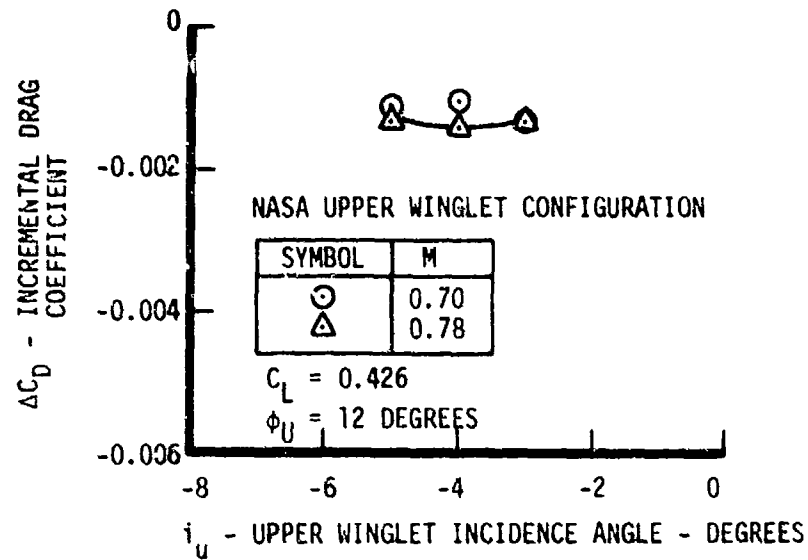


Figure 44. Effect of Upper Winglet Incidence on KC-135A Model Drag Near Cruise Conditions. NASA Upper Winglet Configuration.  $C_L = 0.426$

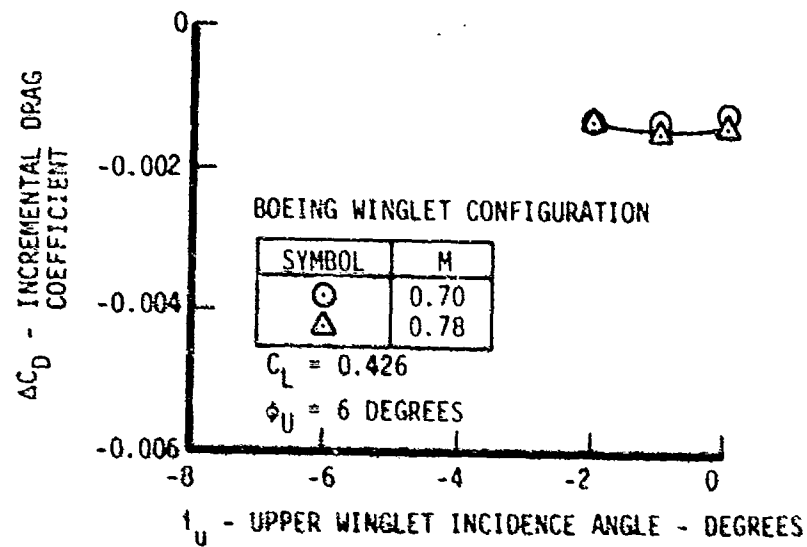


Figure 45. Effect of Upper Winglet Incidence on KC-135A Model Drag Near Cruise Conditions. Boeing Winglet Configuration.  $C_L = 0.426$

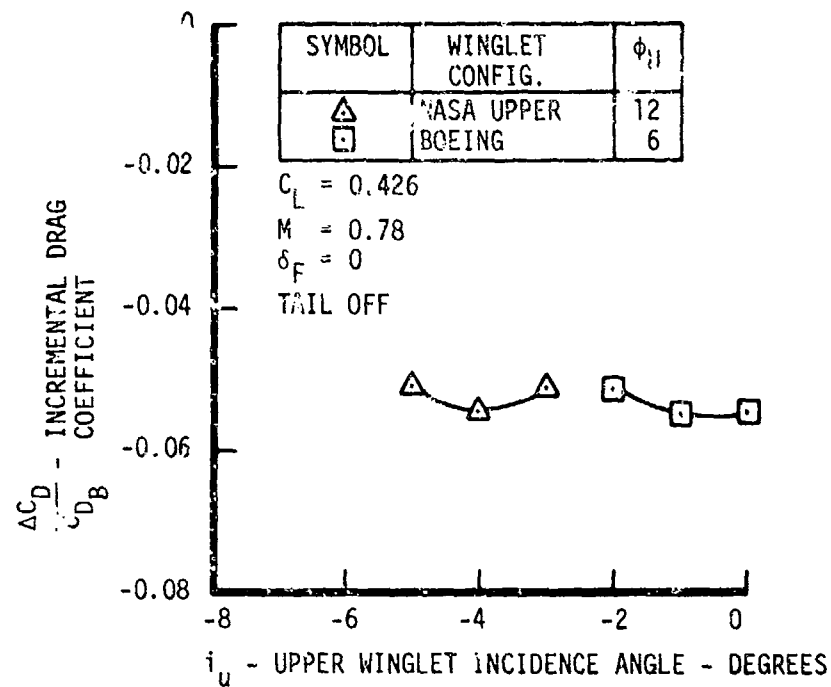


Figure 46. Effect of Upper Winglet Incidence on KC-135A Model Drag Near Cruise Conditions.  $C_L = 0.426$

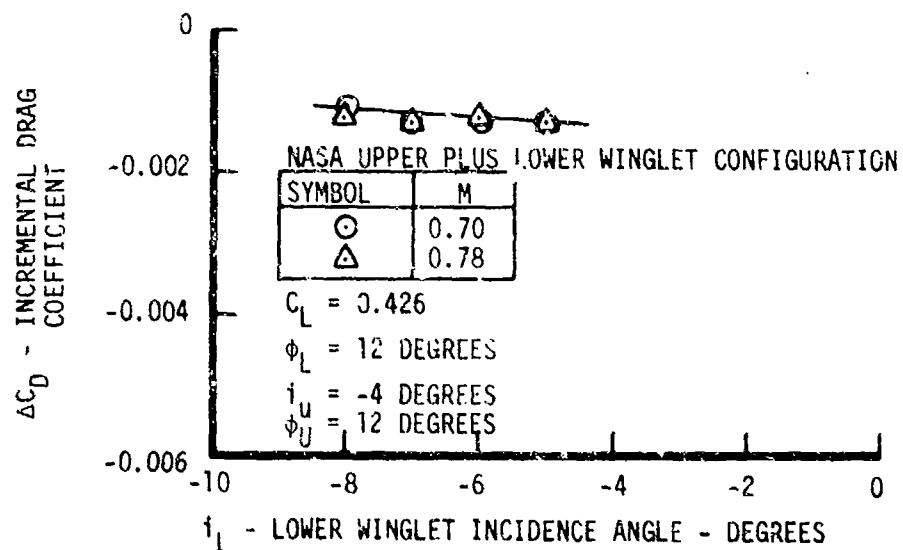


Figure 47. Effect of Lower Winglet Incidence on KC-135A Model Drag Near Cruise Conditions. NASA Upper Plus Lower Winglet Configuration.  $C_L = 0.426$

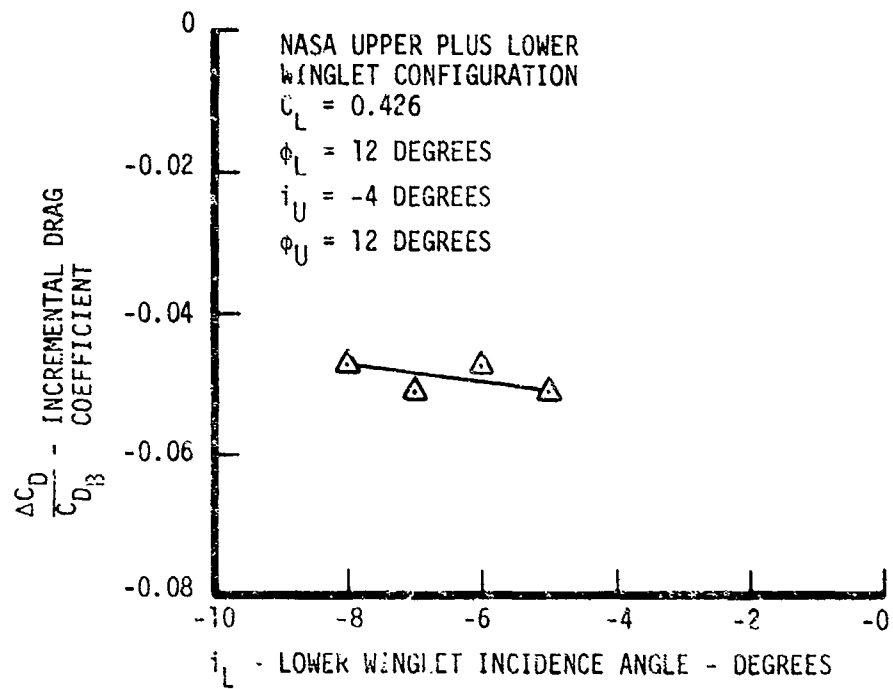


Figure 48. Effect of Lower Winglet Incidence on KC-135A Model Drag Near Cruise Conditions.  $C_L = 0.426$

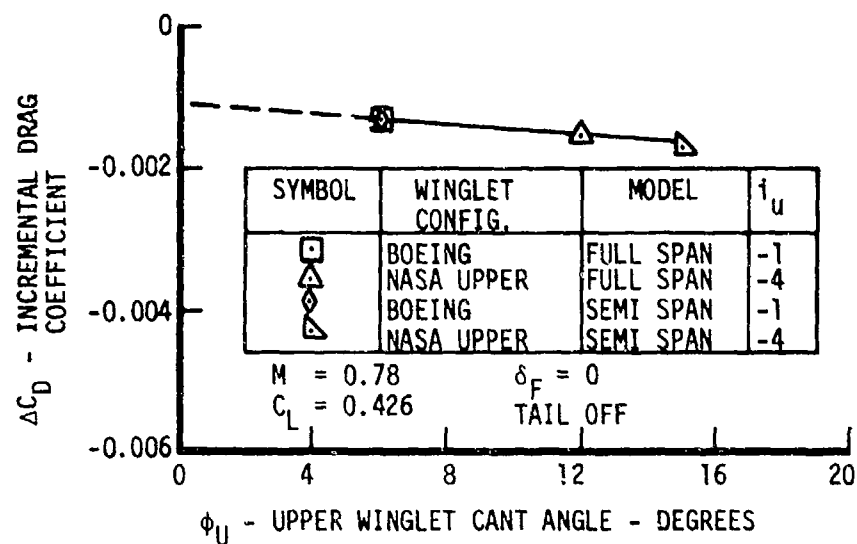


Figure 49. Effect of Upper Winglet Cant on KC-135A Model Drag.  $M = 0.78$ .  $C_L = 0.426$ .  $\delta_F = 0$

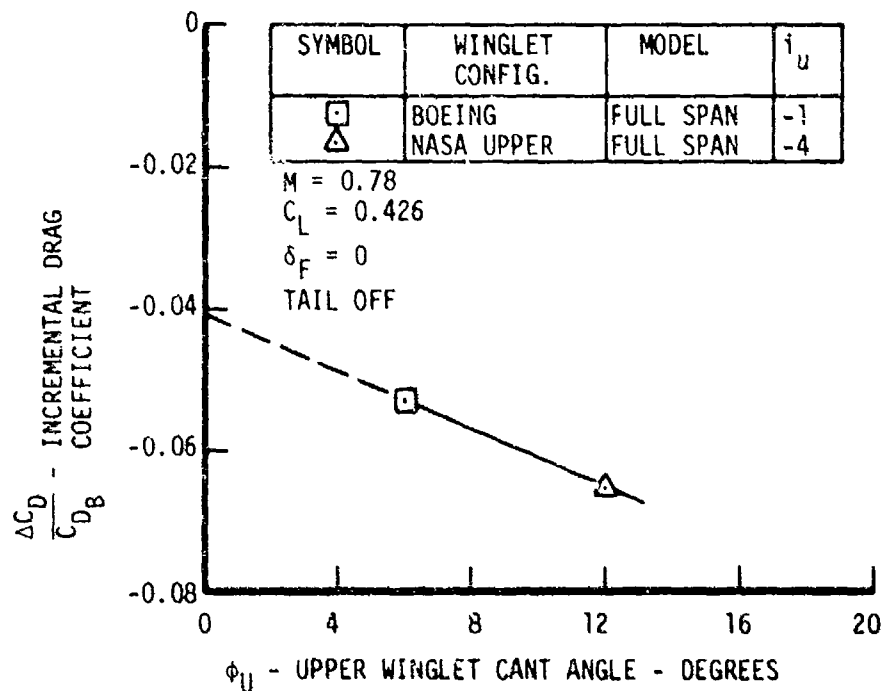


Figure 50. Effect of Upper Winglet Cant on KC-135A Model Drag.  $M = 0.78$ .  $C_L = 0.426$ .  $\delta_F = 0$

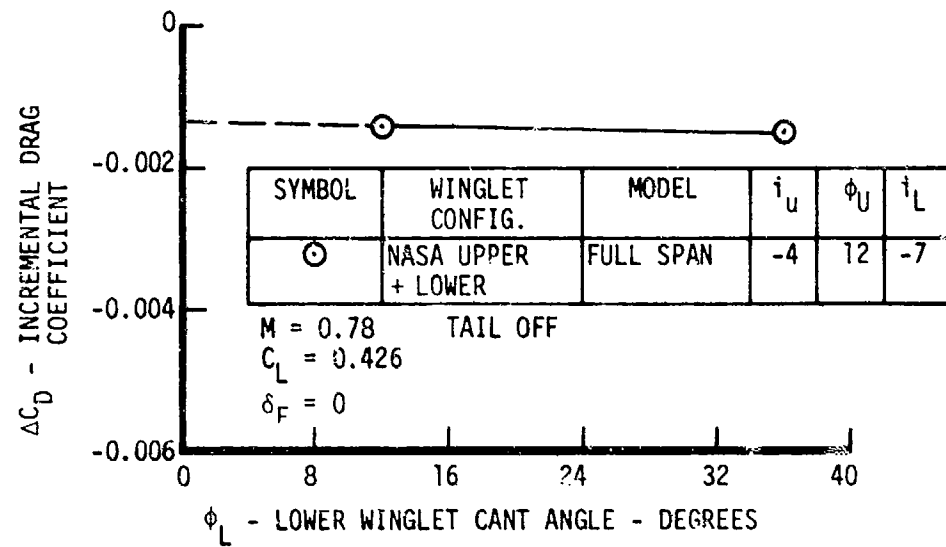


Figure 51. Effect of Lower Winglet Cant on KC-135A Model Drag.  $M = 0.78$ .  $C_L = 0.426$ .  $\delta_F = 0$

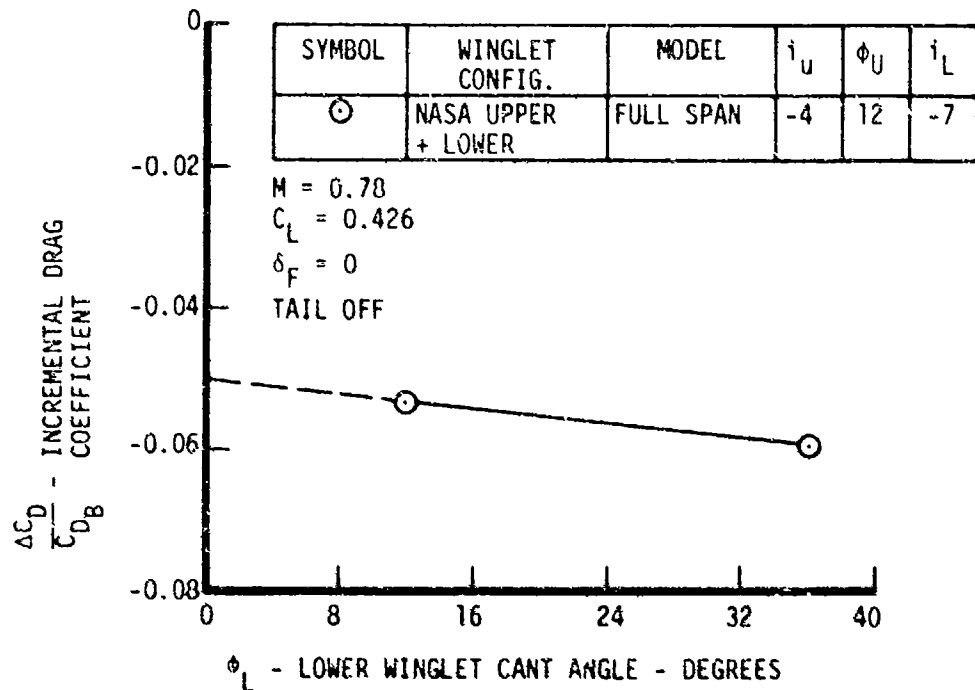


Figure 52. Effect of Lower Winglet Cant on KC-135A Model Drag.  $M = 0.78$ .  $C_L = 0.426$ .  $\delta_F = 0$

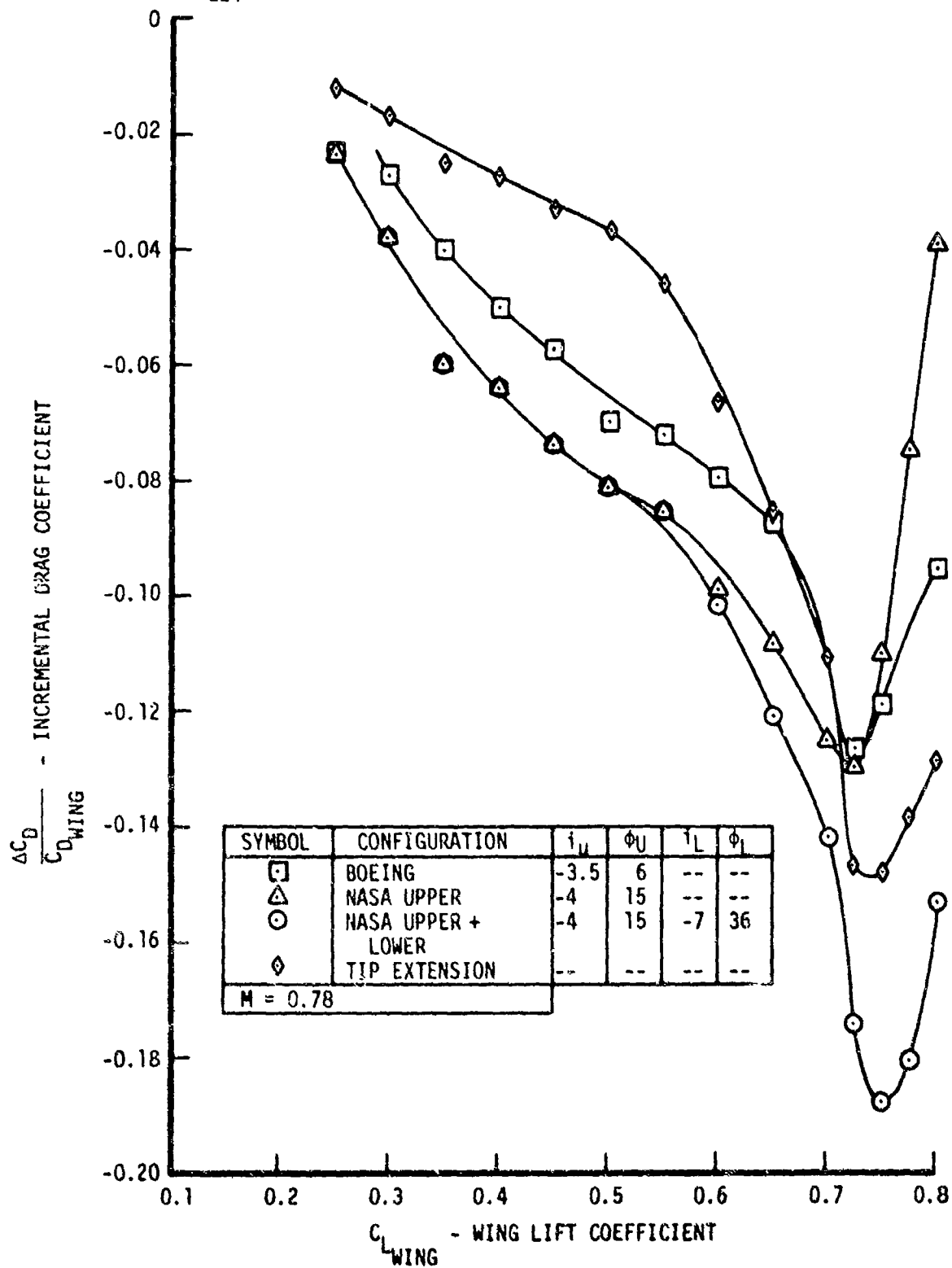


Figure 53. Comparison of Semispan KC-135A Model Drag with Winglets and Tip Extension.  $M = 0.78$ .  $\delta_F = 0$

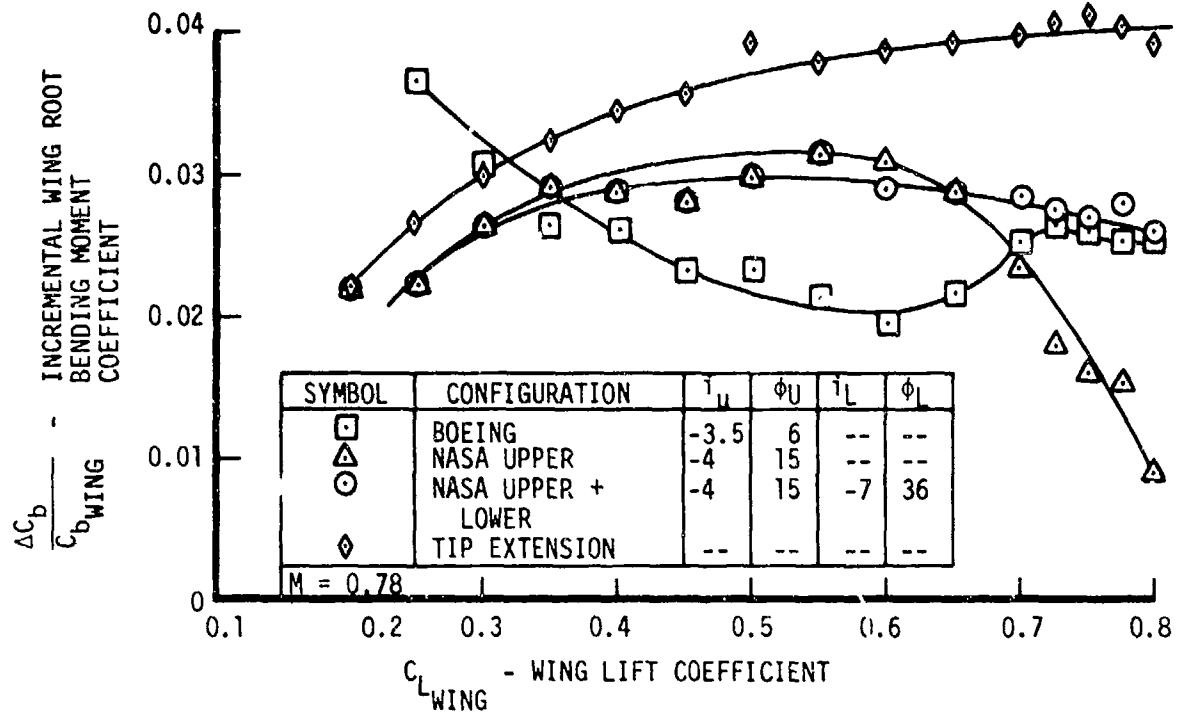


Figure 54. Comparison of Semispan KC-135A Model Wing Root Bending Moment with Winglets and Tip Extension  
 $M = 0.78$ .  $\delta_F = 0$

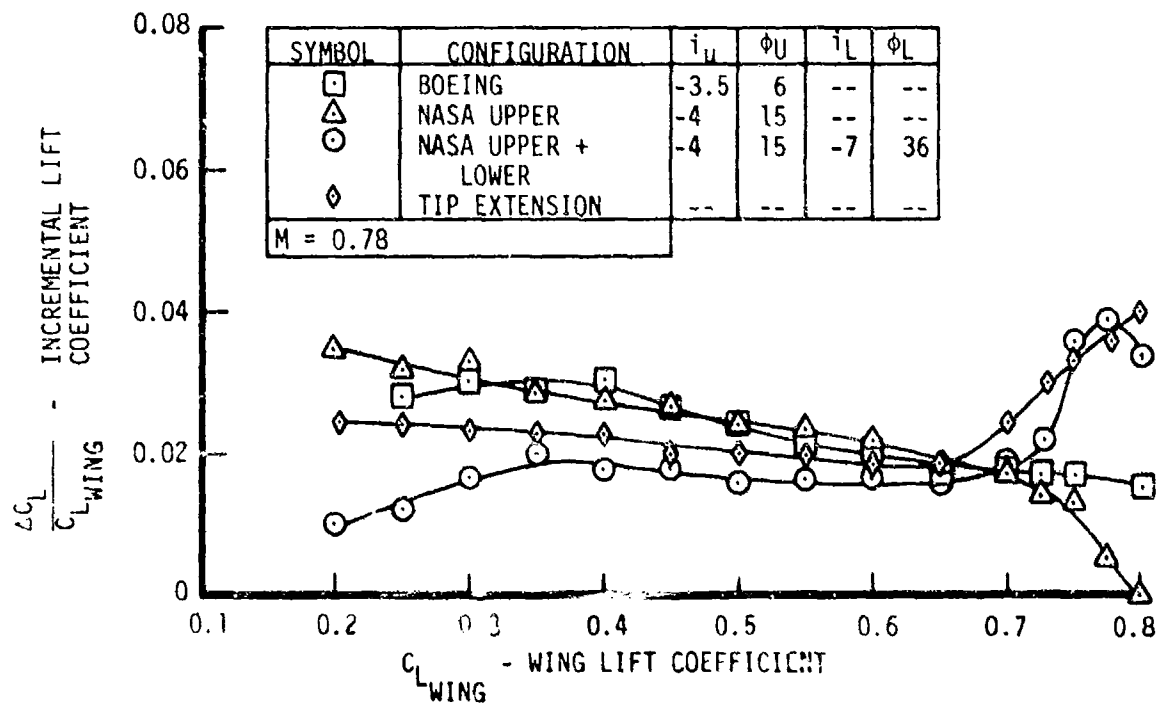


Figure 55. Comparison of Semispan KC-135A Model Lift with Winglets and Tip Extension.  $M = 0.78$ .  
 $\delta_F = 0$



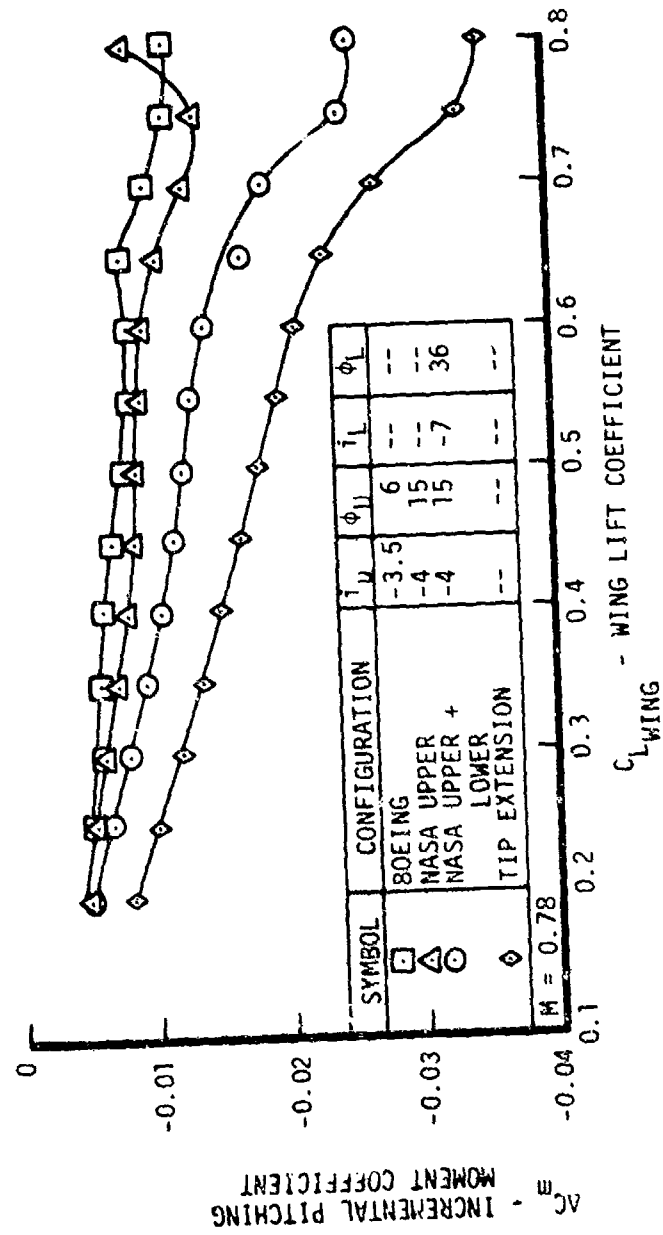


Figure 56. Comparison of Semispan KC-135A Model Pitching Moment with Winglets and Tip Extension.  $M = 0.78$ .  $\delta_F = 0$

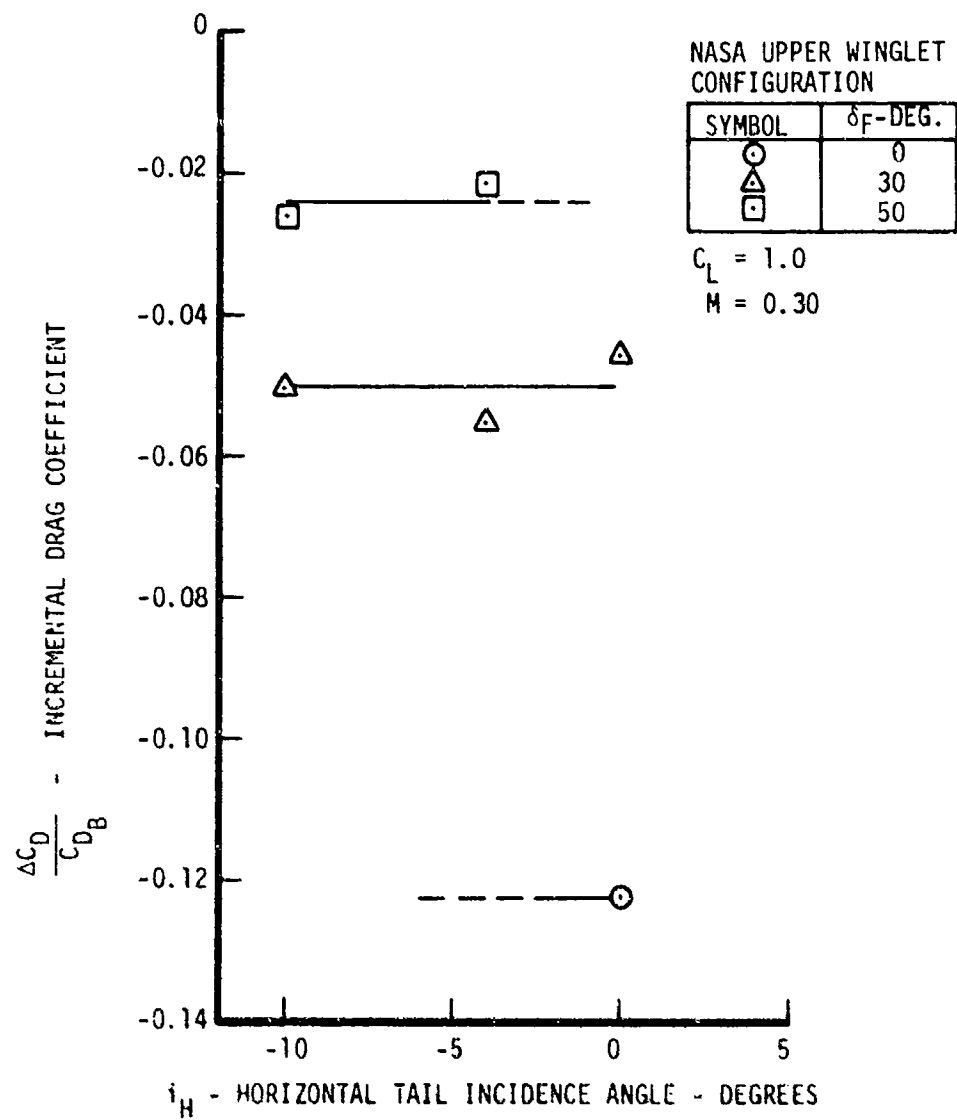


Figure 57. Effect of Flap and Horizontal Tail Deflection on KC-135A Model Drag.  $M = 0.30$ .  $C_L = 1.0$

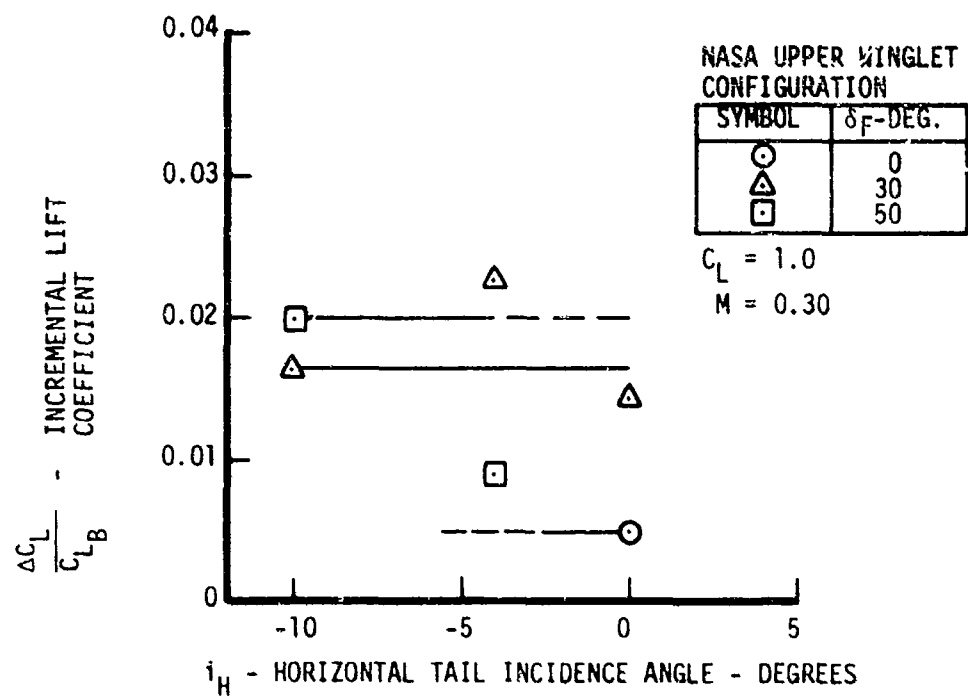


Figure 58. Effect of Flap and Horizontal Tail Deflection on KC-135A Model Lift.  $M = 0.30$ .  $C_L = 1.0$

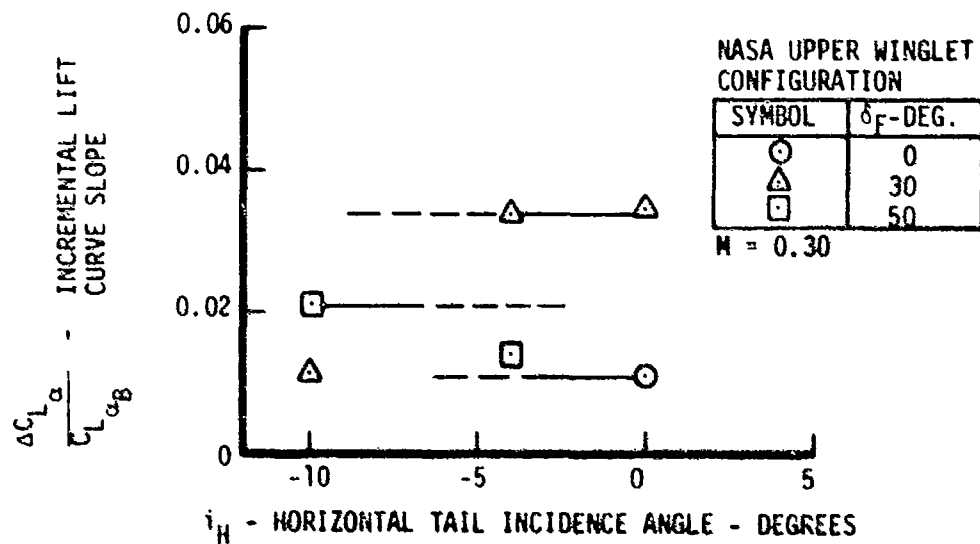


Figure 59. Effect of Flap and Horizontal Tail Deflection on KC-135A Model Lift Curve Slope.  $M = 0.30$

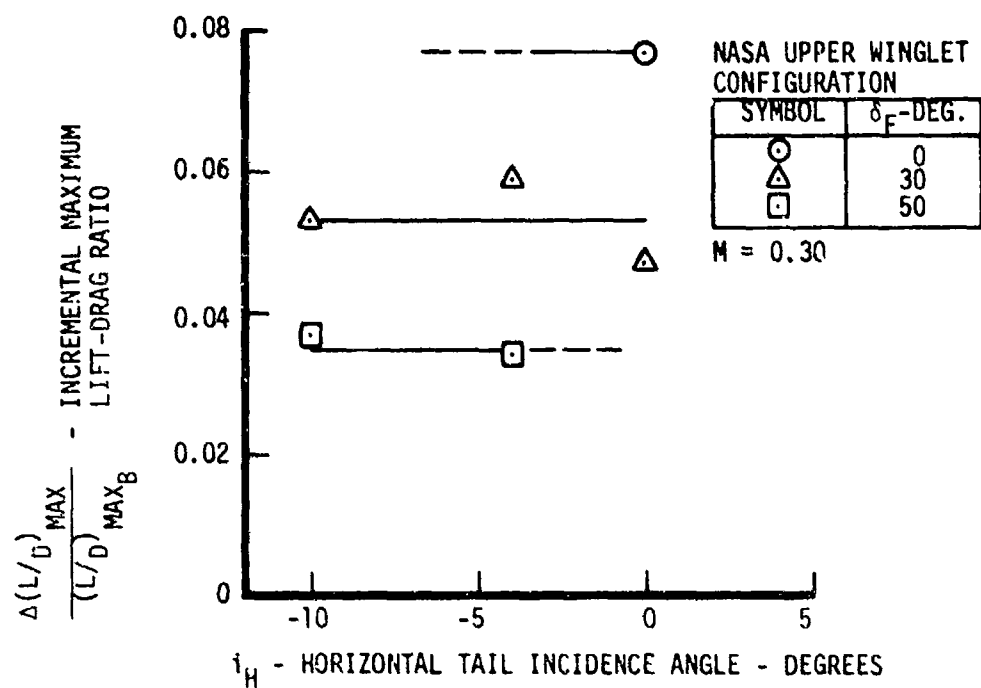


Figure 60. Effect of Flap and Horizontal Tail Deflection on KC-135A Model Lift-Drag Ratio.  $M = 0.30$

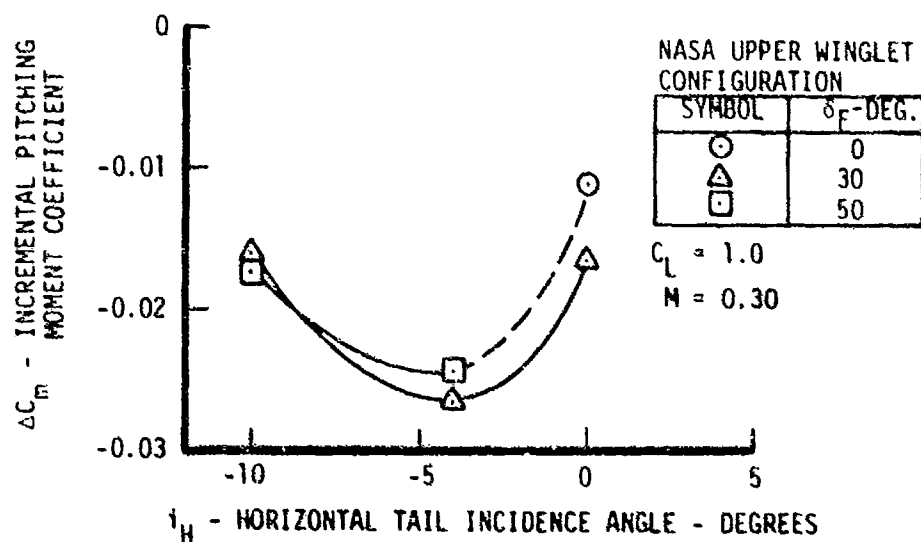


Figure 61. Effect of Flap and Horizontal Tail Deflection on KC-135A Model Pitching Moment.  $M = 0.30$ .  
 $C_L = 1.0$

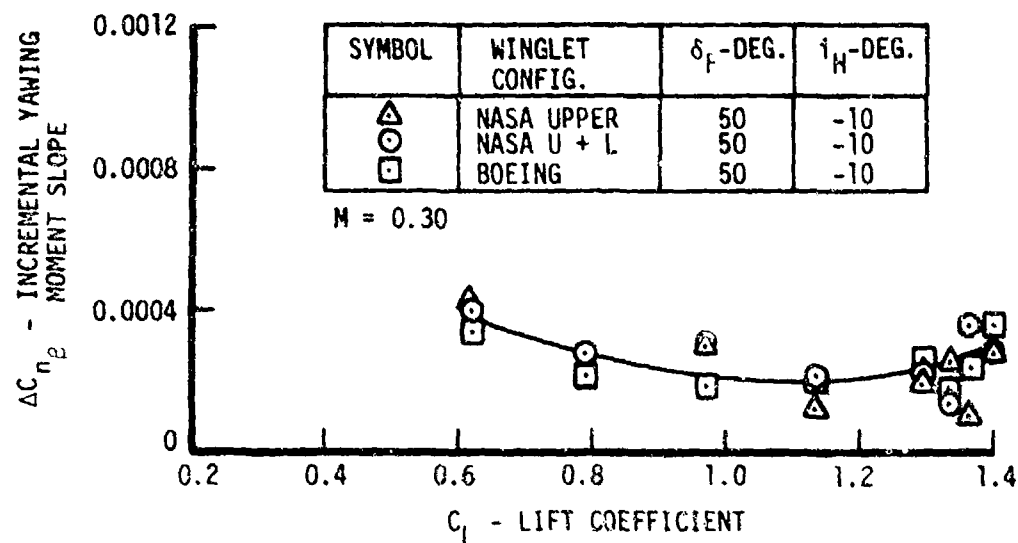


Figure 62. Effect of Winglet Configuration on Full-Span KC-135A Model Yawing Moment.  $M = 0.30$ .  
 $\delta_F = 50$  Degrees.  $i_H = -10$  Degrees

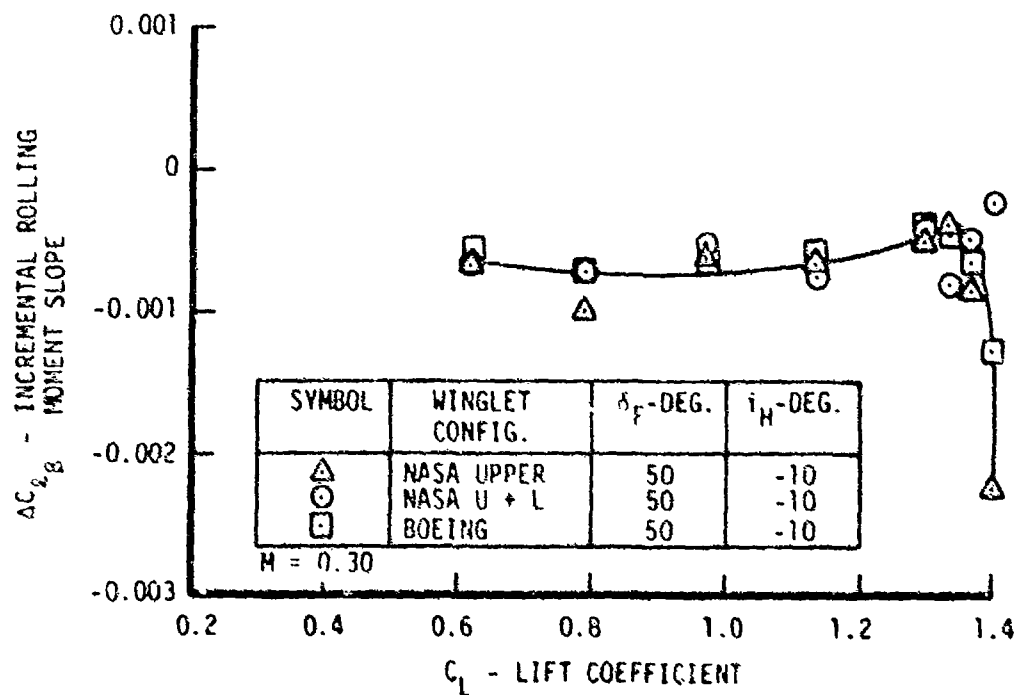


Figure 63. Effect of Winglet Configuration on Full-Span KC-135A Model Rolling Moment.  $M = 0.30$ .  
 $\delta_F = 50$  Degrees.  $i_H = -10$  Degrees

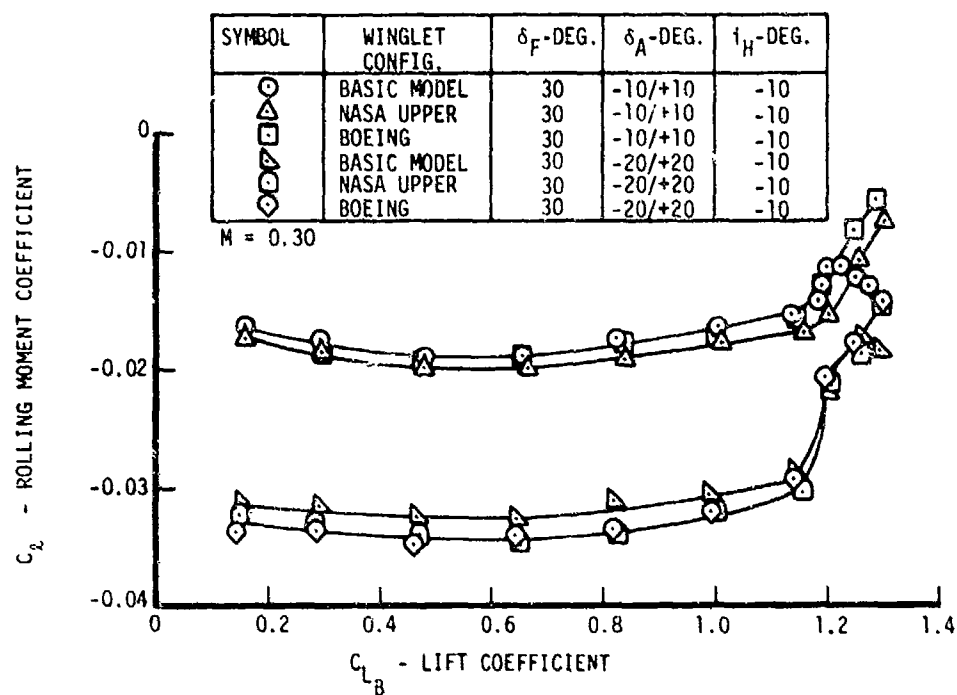


Figure 64. Effect of Aileron Deflection on Rolling Moment  
 $M = 0.30$ .  $\delta_F = 30$  Degrees.  $i_H = -10$  Degrees

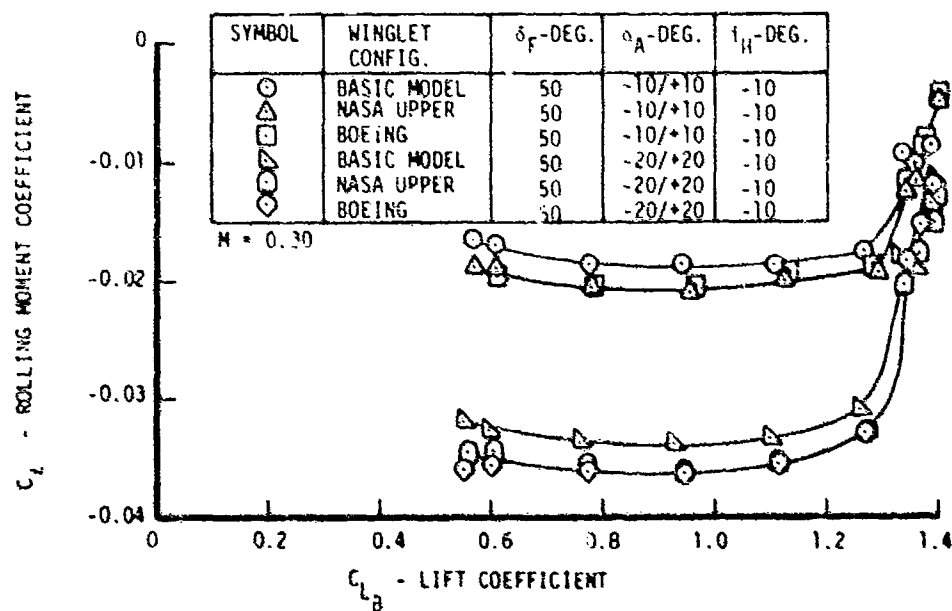


Figure 65. Effect of Aileron Deflection on Rolling Moment  
 $M = 0.30$ .  $\delta_F = 50$  Degrees.  $i_H = -10$  Degrees

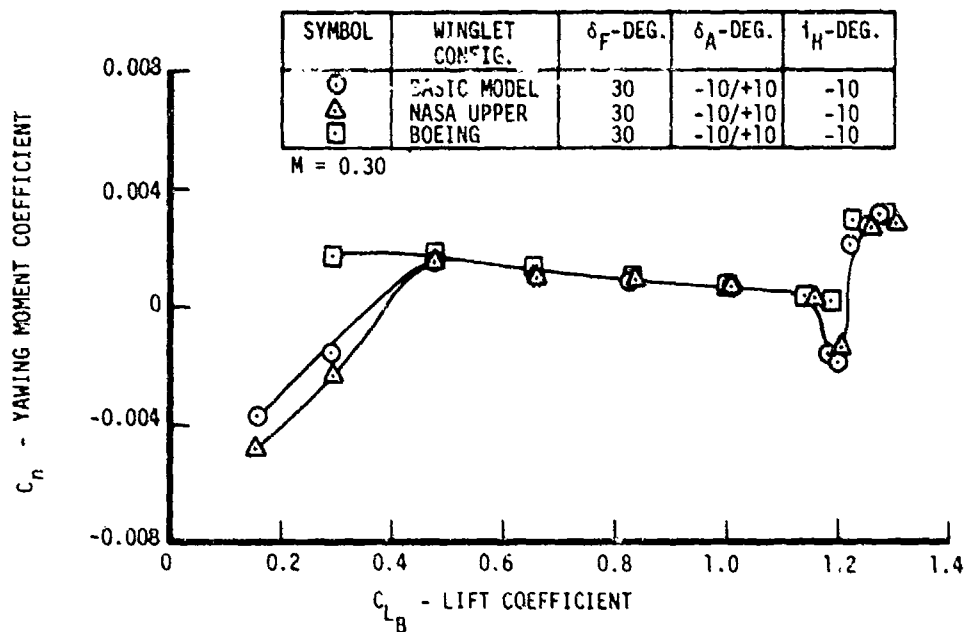


Figure 66. Effect of Aileron Deflection on Yawing Moment  
 $M = 0.30$ ,  $\delta_F = 30$  Degrees,  $i_H = -10$  Degrees  
 $\delta_A = -10/+10$  Degrees

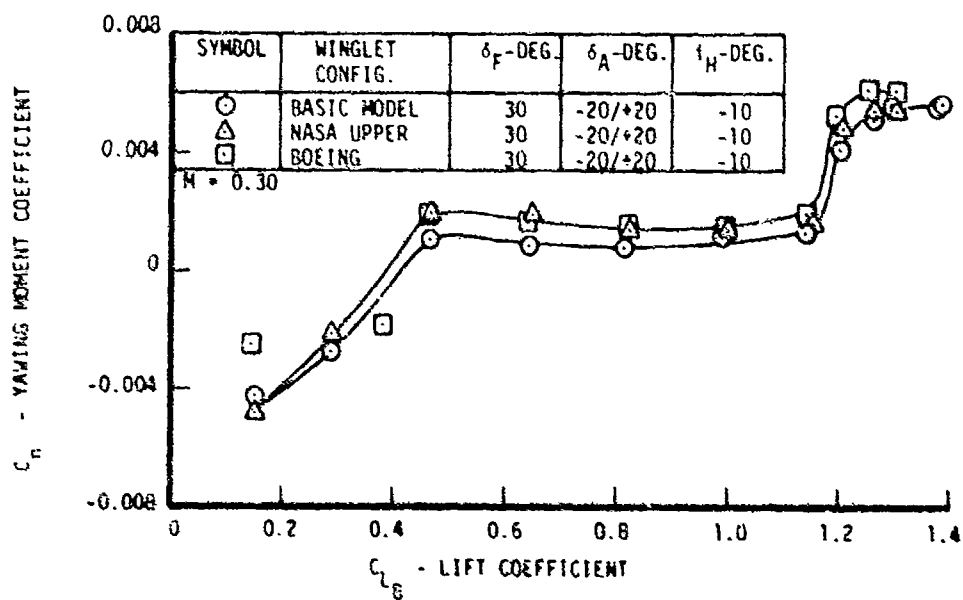


Figure 67. Effect of Aileron Deflection on Yawing Moment.  
 $M = 0.30$ ,  $\delta_F = 30$  Degrees,  $i_H = -10$  Degrees.  
 $\delta_A = -20/20$  Degrees

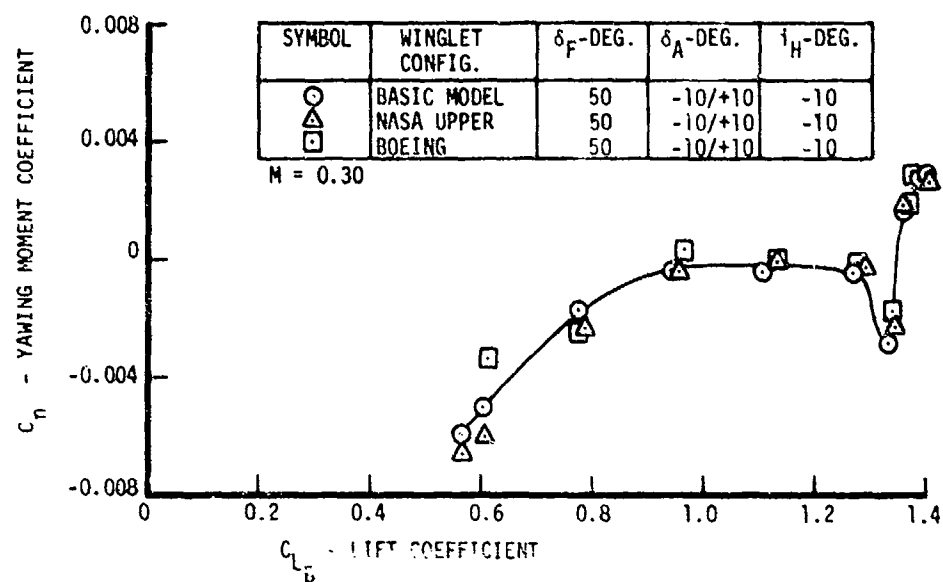


Figure 68. Effect of Aileron Deflection on Yawing Moment.  
 $M = 0.30$ .  $\delta_F = 50$  Degrees.  $i_H = -10$  Degrees.  
 $\delta_A = -10/10$  Degrees

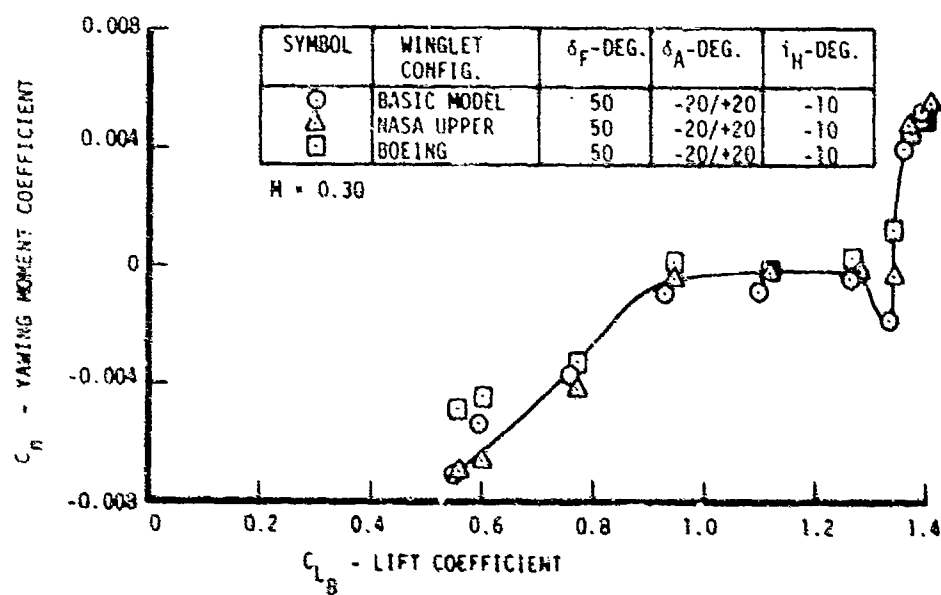


Figure 69. Effect of Aileron Deflection on Yawing Moment.  
 $M = 0.30$ .  $\delta_F = 50$  Degrees.  $i_H = -10$  Degrees.  
 $\delta_A = -20/+20$  Degrees



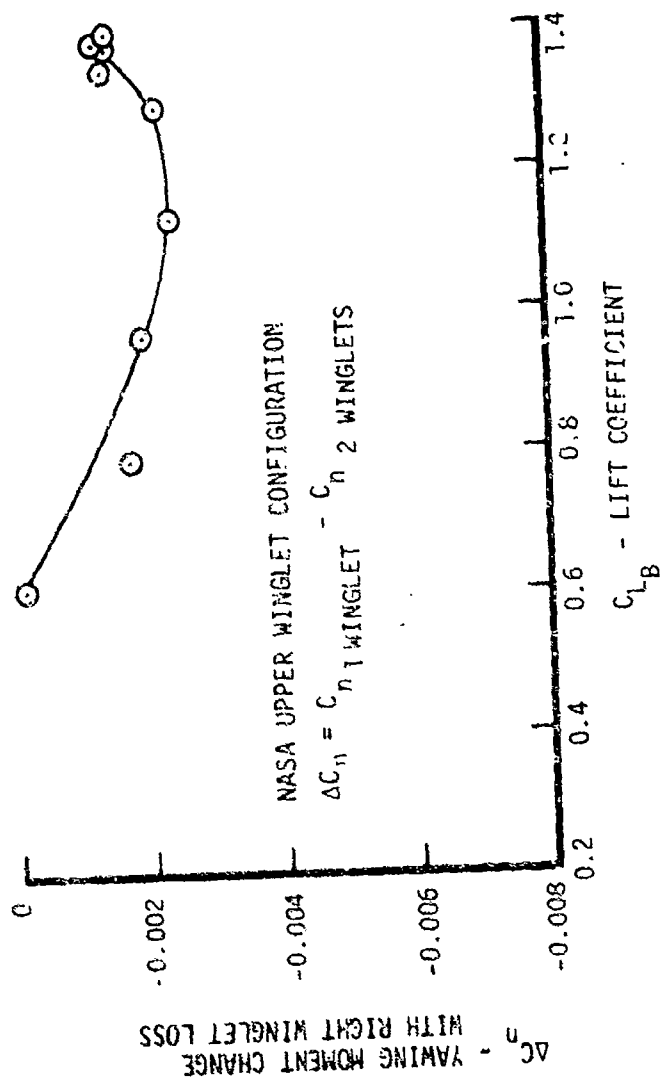


Figure 70. Effect of Winglet Loss on KC-135A Model yawing Moment.  $M = 0.30$ .  $\delta_F = 50$  Degrees.  $i_H = -10$  Degrees

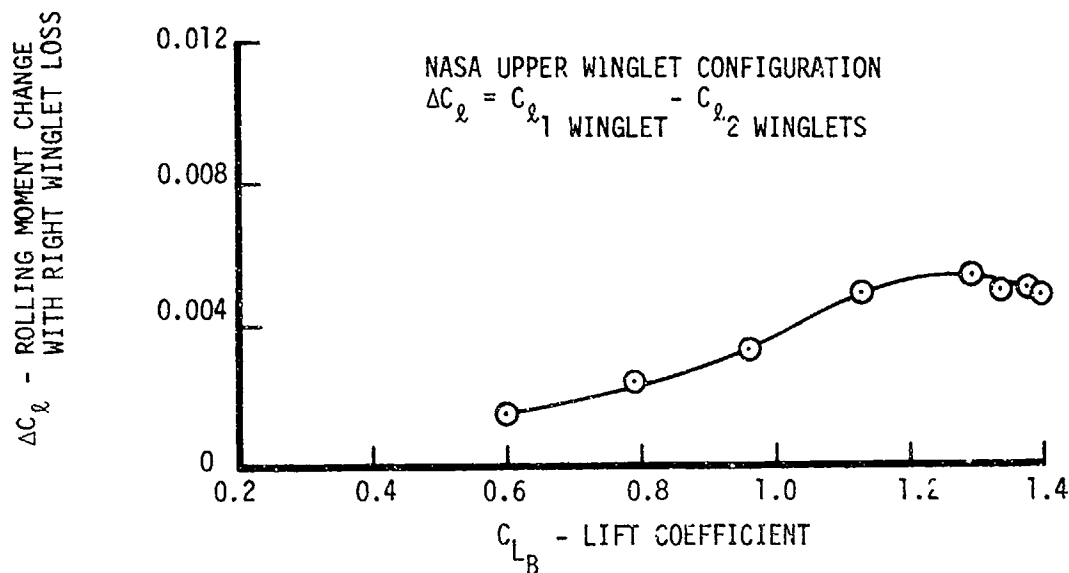


Figure 71. Effect of Winglet Loss on KC-135A Model Rolling Moment.  $M = 0.30$ .  $\delta_F = 50$  Degrees.  $i_H = -10$  Degrees

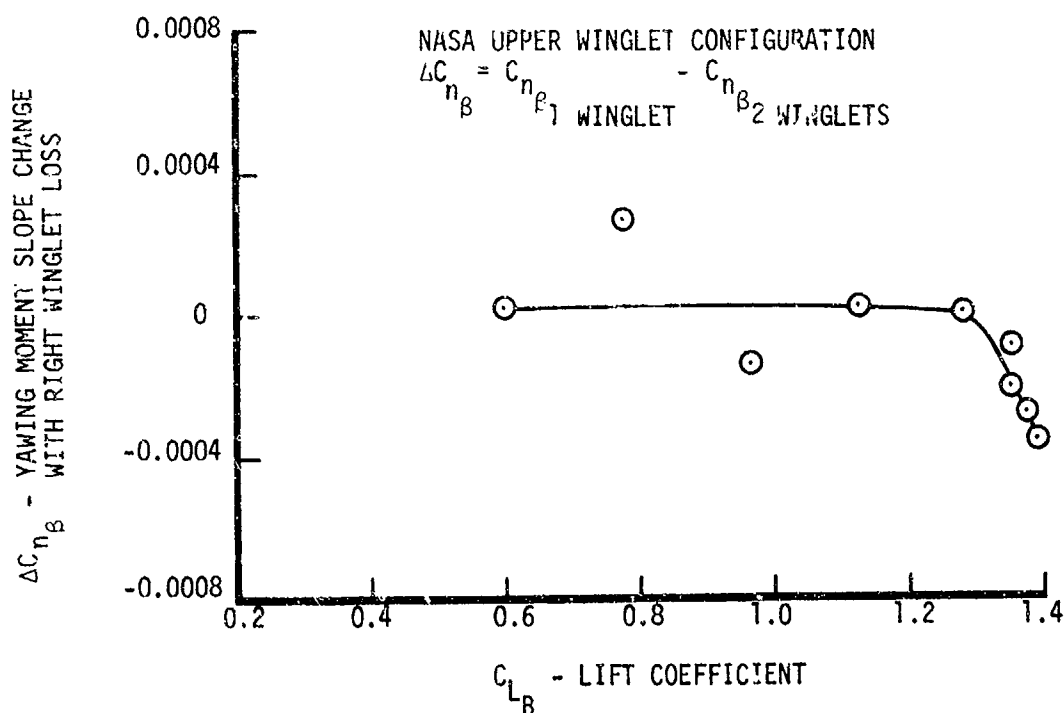


Figure 72. Effect of Winglet Loss on KC-135A Model Yawing Moment Slope.  $M = 0.30$ .  $\delta_F = 50$  Degrees.  $i_H = -10$  Degrees

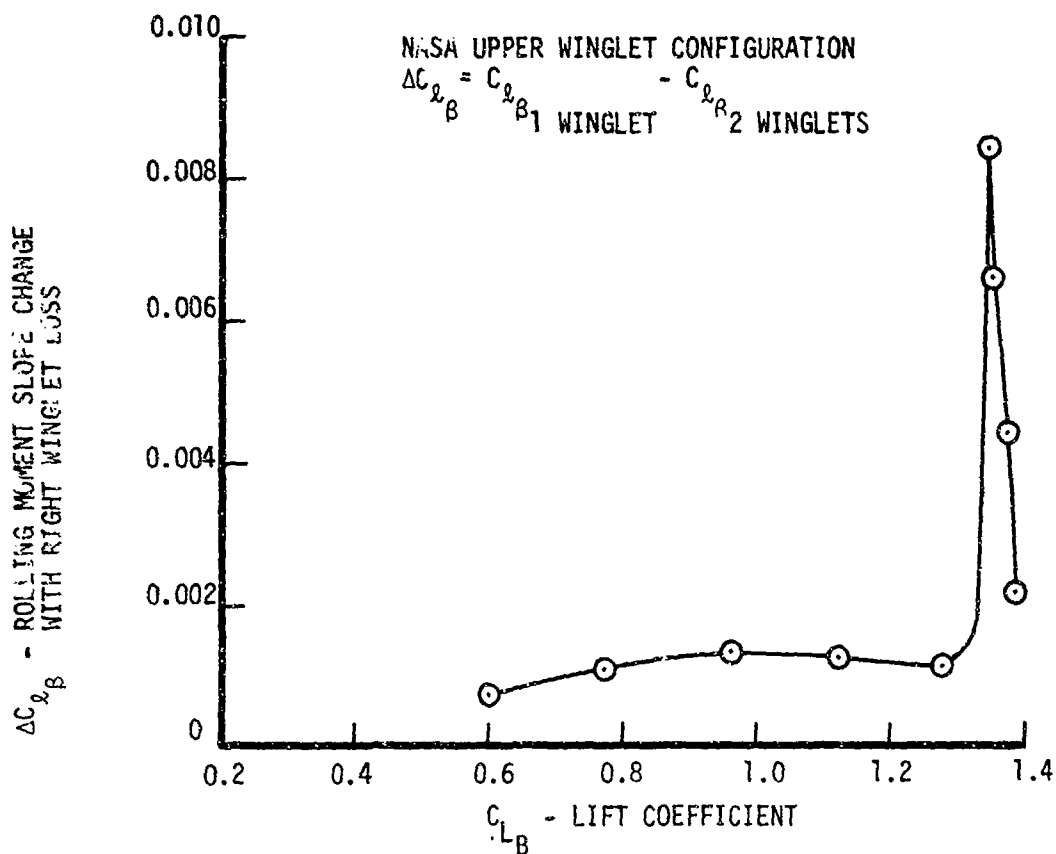


Figure 73. Effect of Winglet Loss on KC-135A Model Rolling Moment Slope.  $M = 0.30$ .  $\delta_F = 50$  Degrees.  $i_H = -10$  Degrees

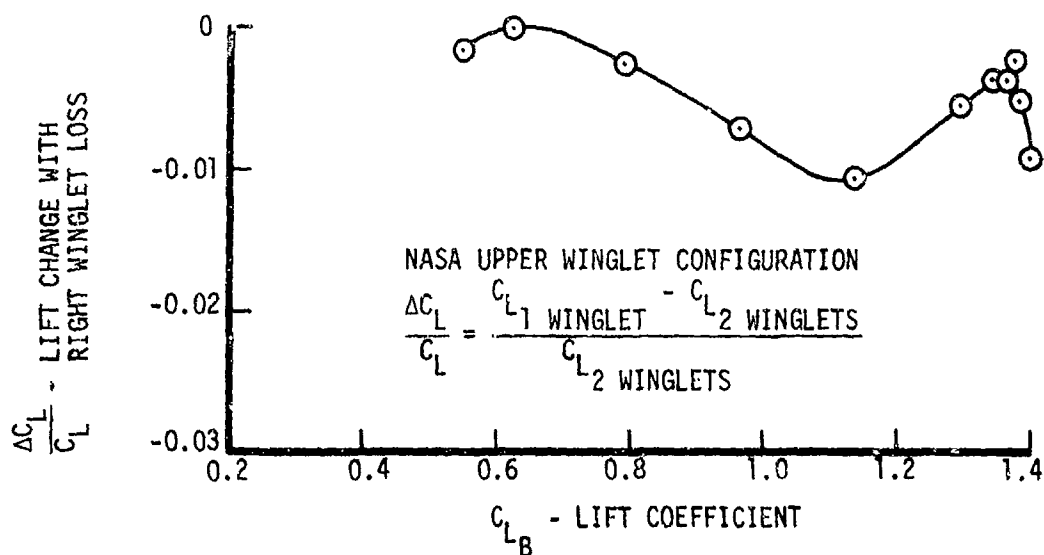


Figure 74. Effect of Winglet Loss on KC-135A Model Lift  $M = 0.30$ .  $\delta_F = 50$  Degrees.  $i_H = -10$  Degrees

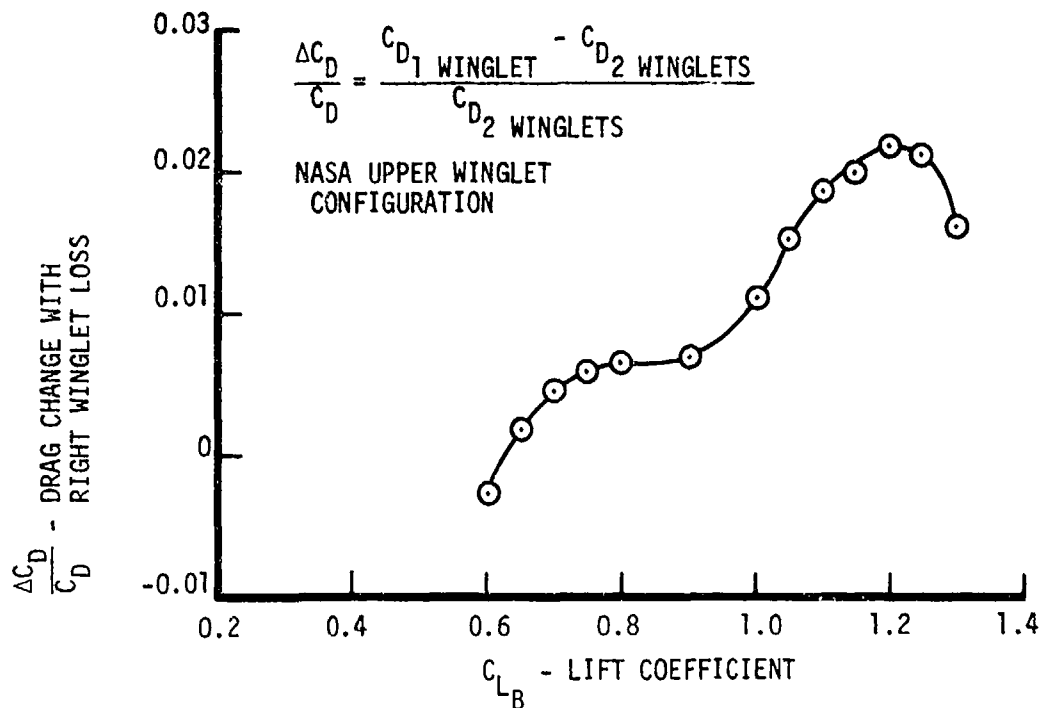


Figure 75. Effect of Winglet Loss on KC-135A Model Drag  
 $M = 0.30$ .  $\delta_F = 50$  Degrees.  $i_H = -10$  Degrees

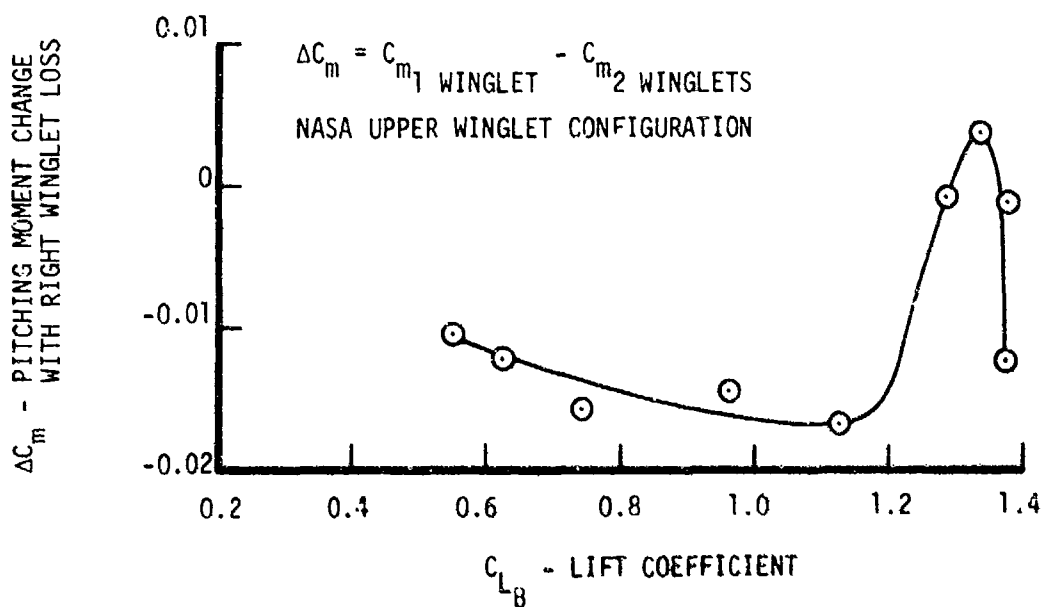


Figure 76. Effect of Winglet Loss on KC-135A Model Pitching Moment.  $M = 0.30$ .  $\delta_F = 50$  Degrees.  $i_H = -10$  Degrees

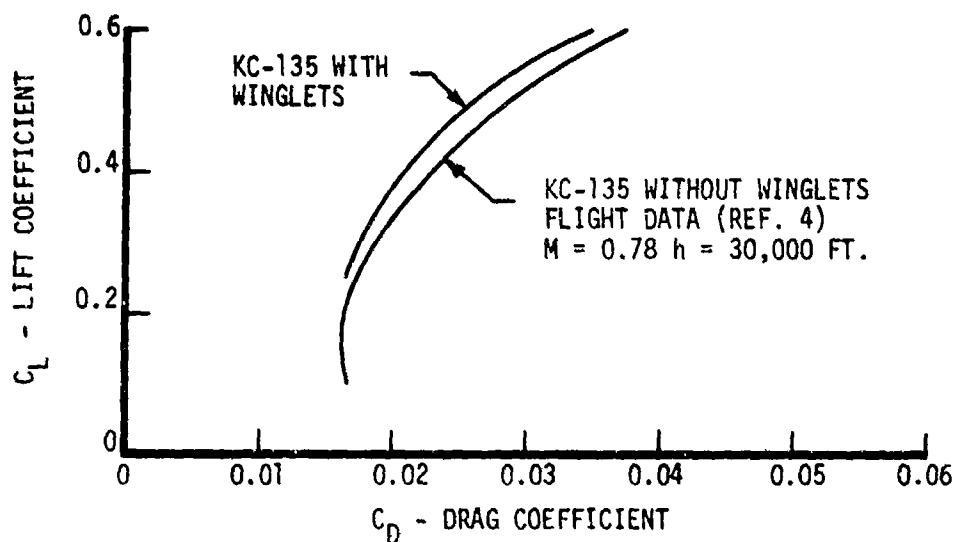


Figure 77. Effect of Winglets on KC-135A Aircraft Drag at Cruise Flight Conditions

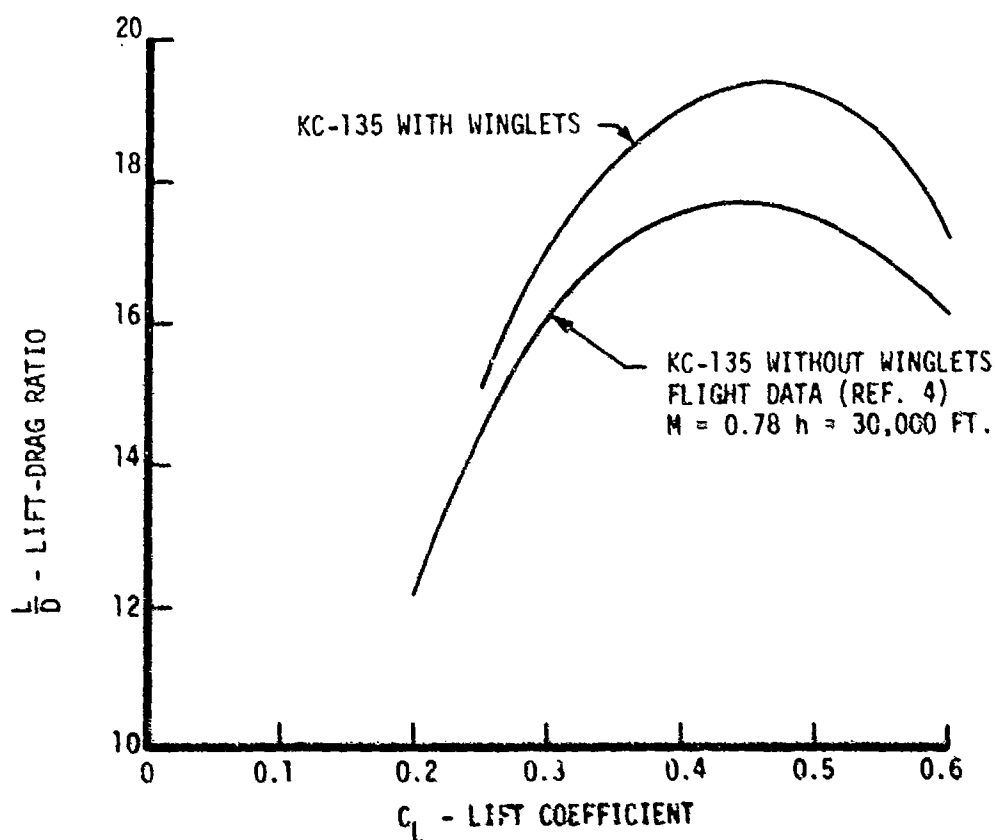


Figure 78. Effect of Winglets on KC-135A Aircraft Lift-  
Drag Ratio at Cruise Flight Conditions

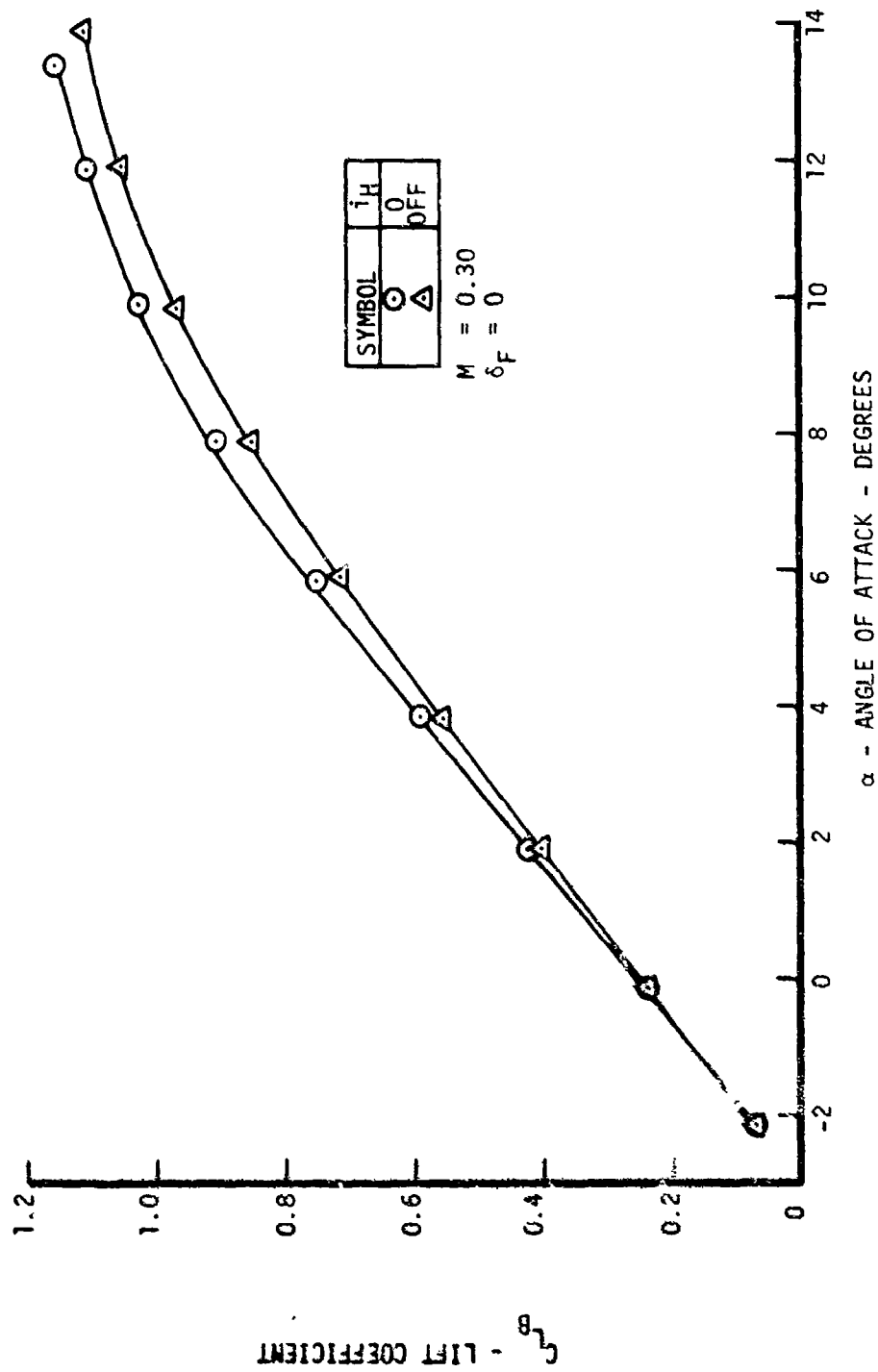


Figure 79. Variation of Lift of Basic KC-135A Model with Angle of Attack.  $M = 0.30$ .  $\delta_F = 0$

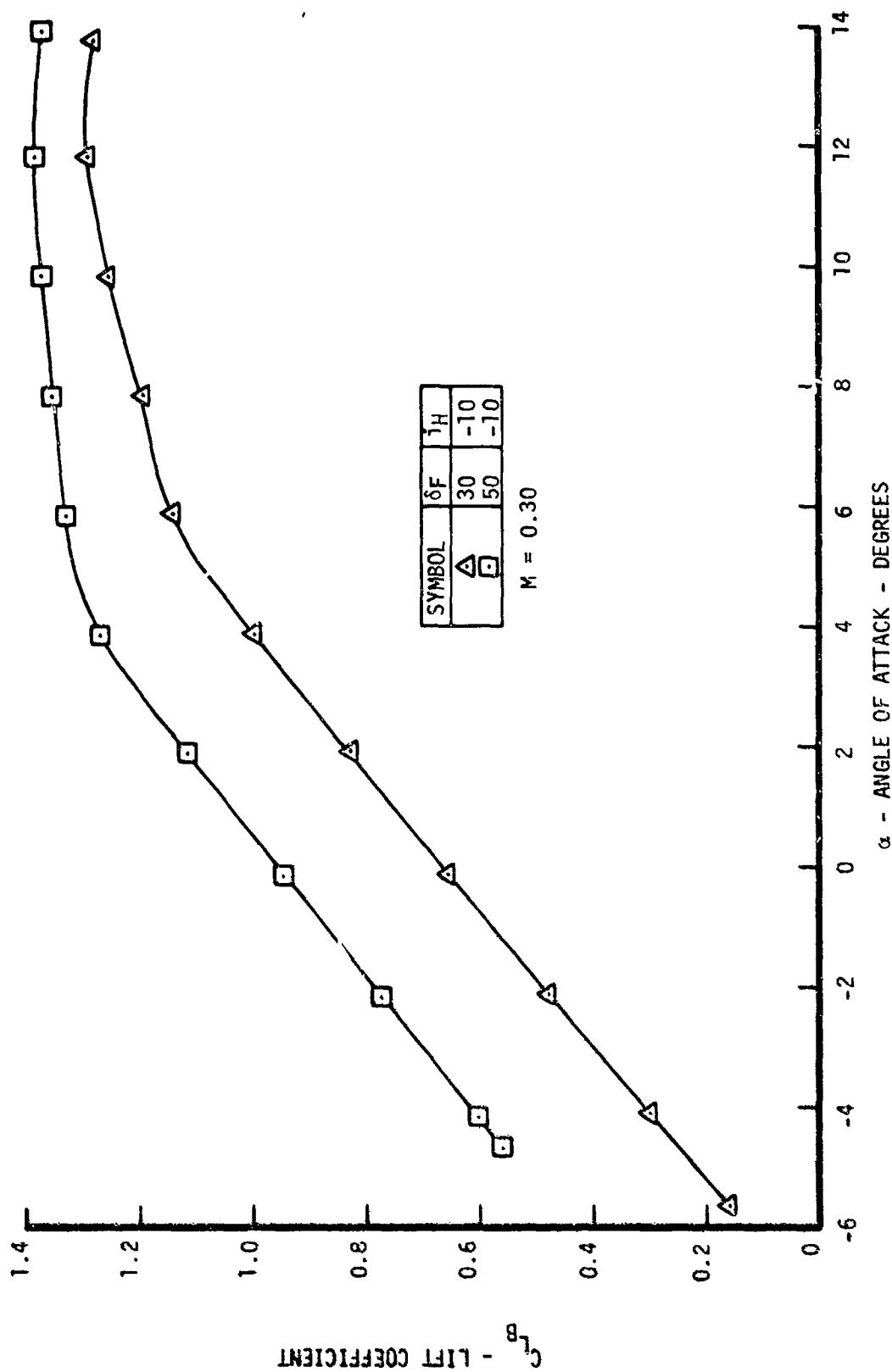


Figure 80. Variation of Lift of Basic KC-135A Model with Angle of Attack and Flap Deflection.  $M = 0.30$ .  $i_H = -10$  Degrees

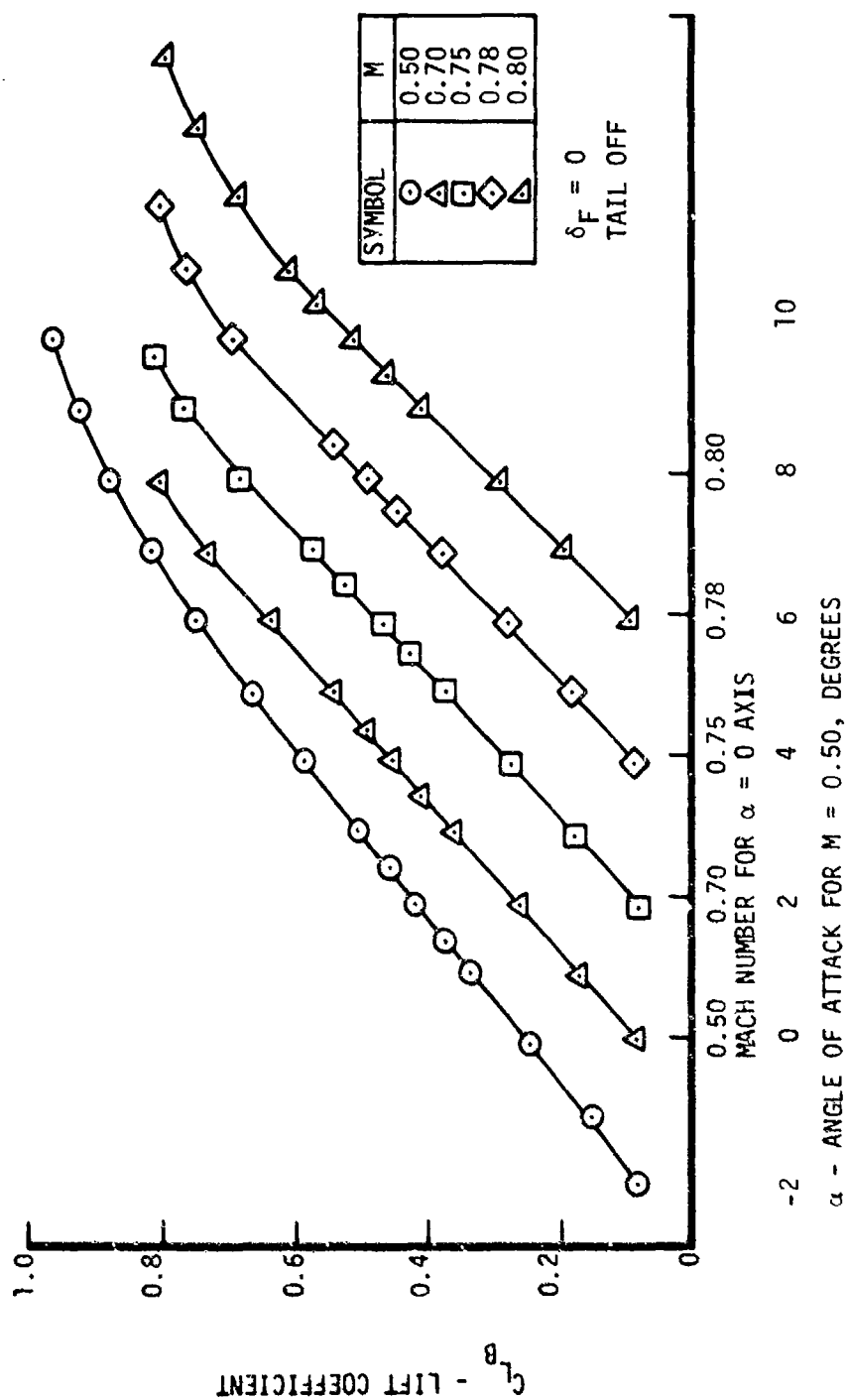


Figure 81. Variation of Lift of Basic KC-135A Model with Angle of Attack Near Cruise Conditions.  $\delta_F = 0$



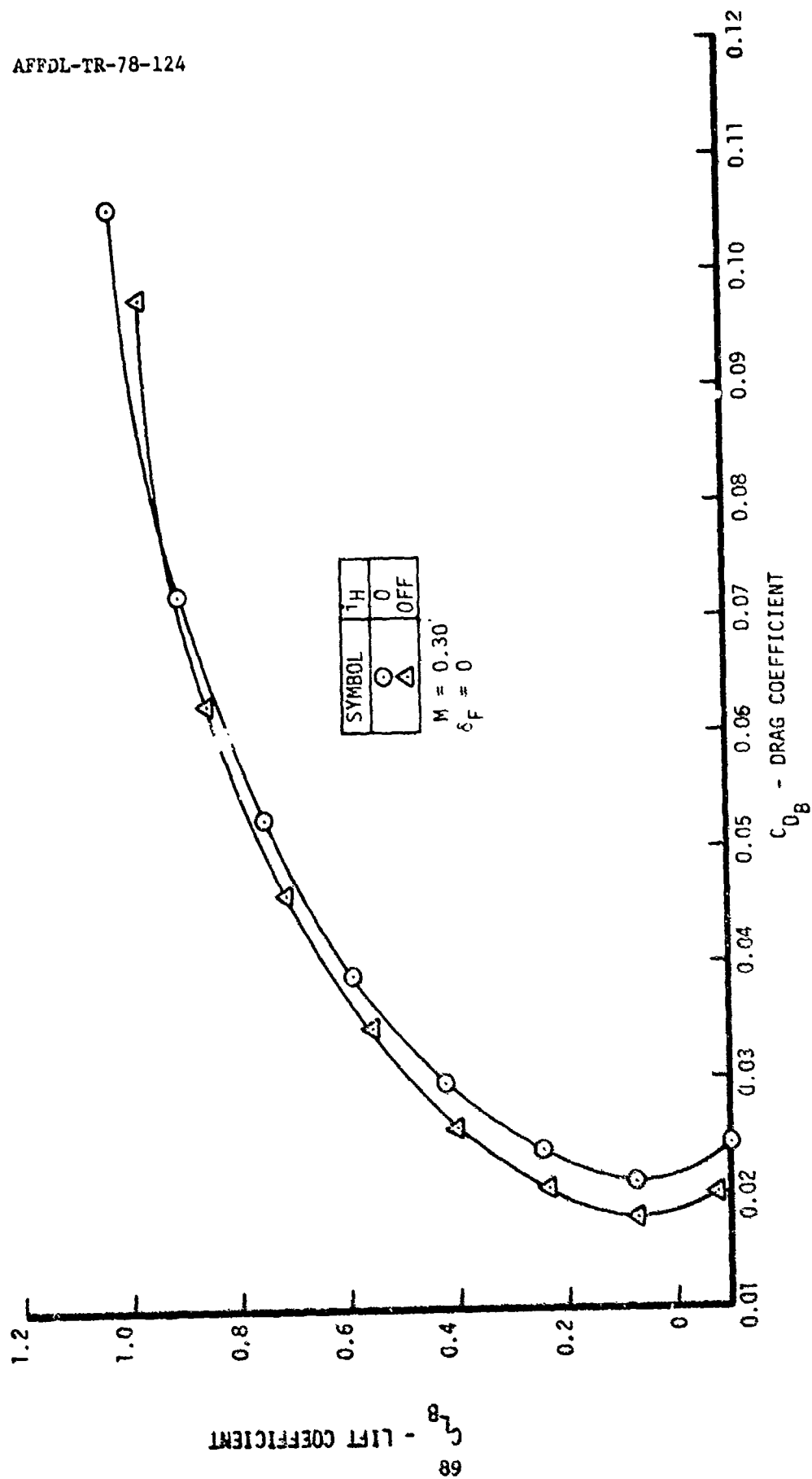


Figure 82. Variation of Drag of Basic KC-135A Model  
 with Lift.  $M = 0.30$ .  $\delta_P = 0$

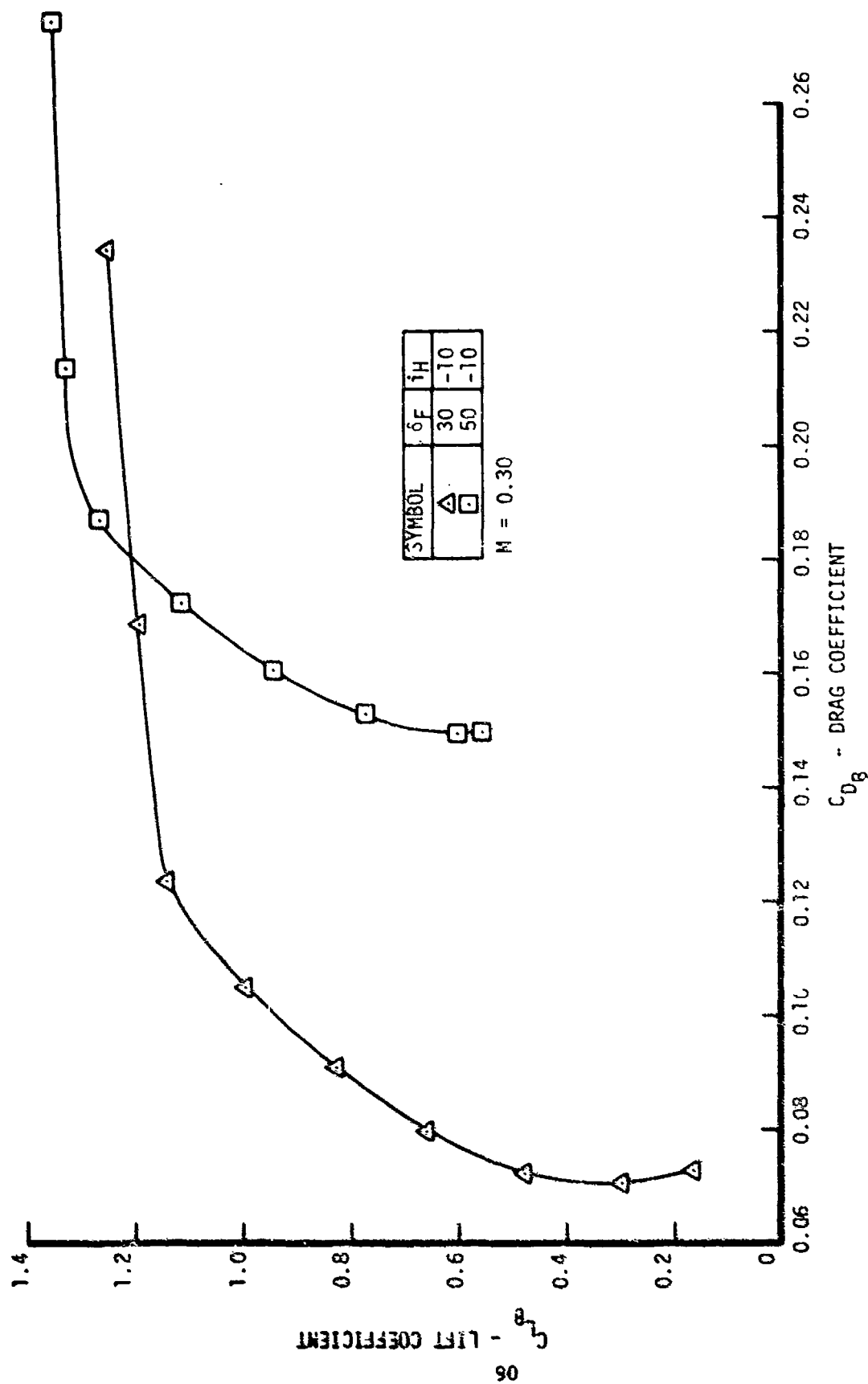


Figure 83. Variation of Drag of Basic KC-135A Model with Lift and Flap Deflection.  $M = 0.30$ .  $i_H = -10$  Degrees

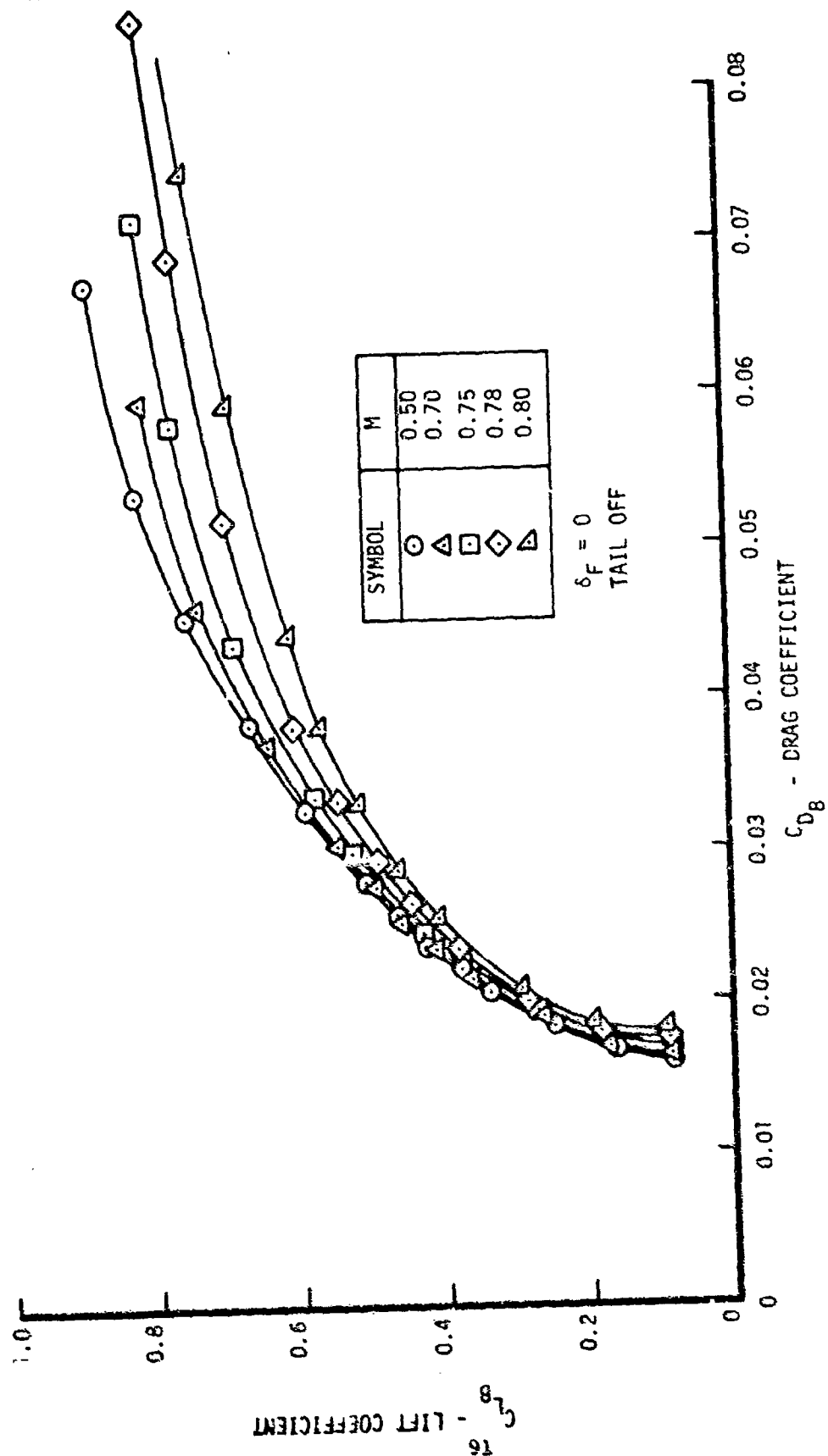


Figure 84. Variation of Drag of Basic KC-135A Model with Lift Near Cruise Condition.  $\delta_F = 0$

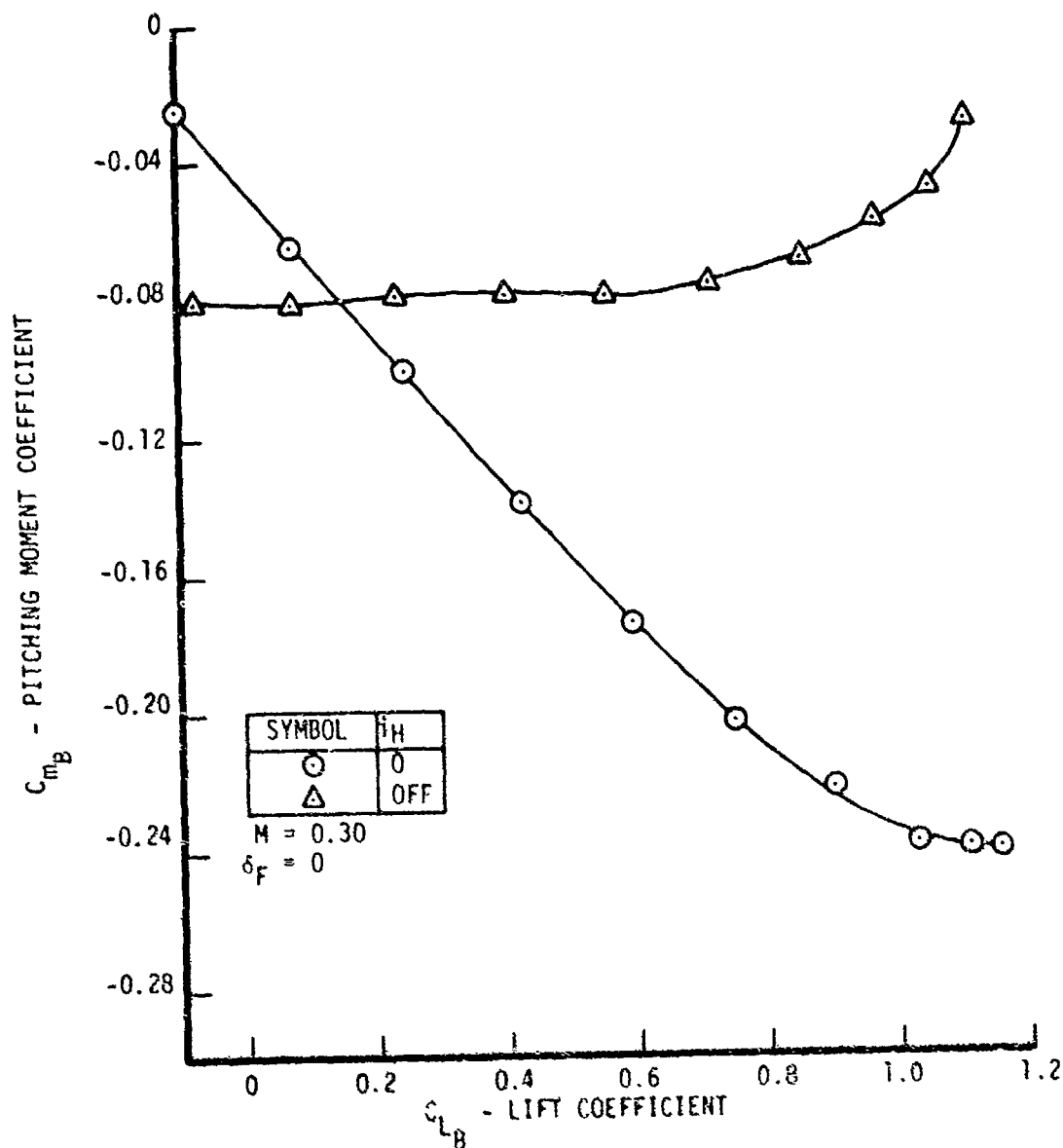


Figure 85. Variation of Pitching Moment of Basic KC-135A Model with Lift.  $M = 0.30$ .  $\delta_F = 0$

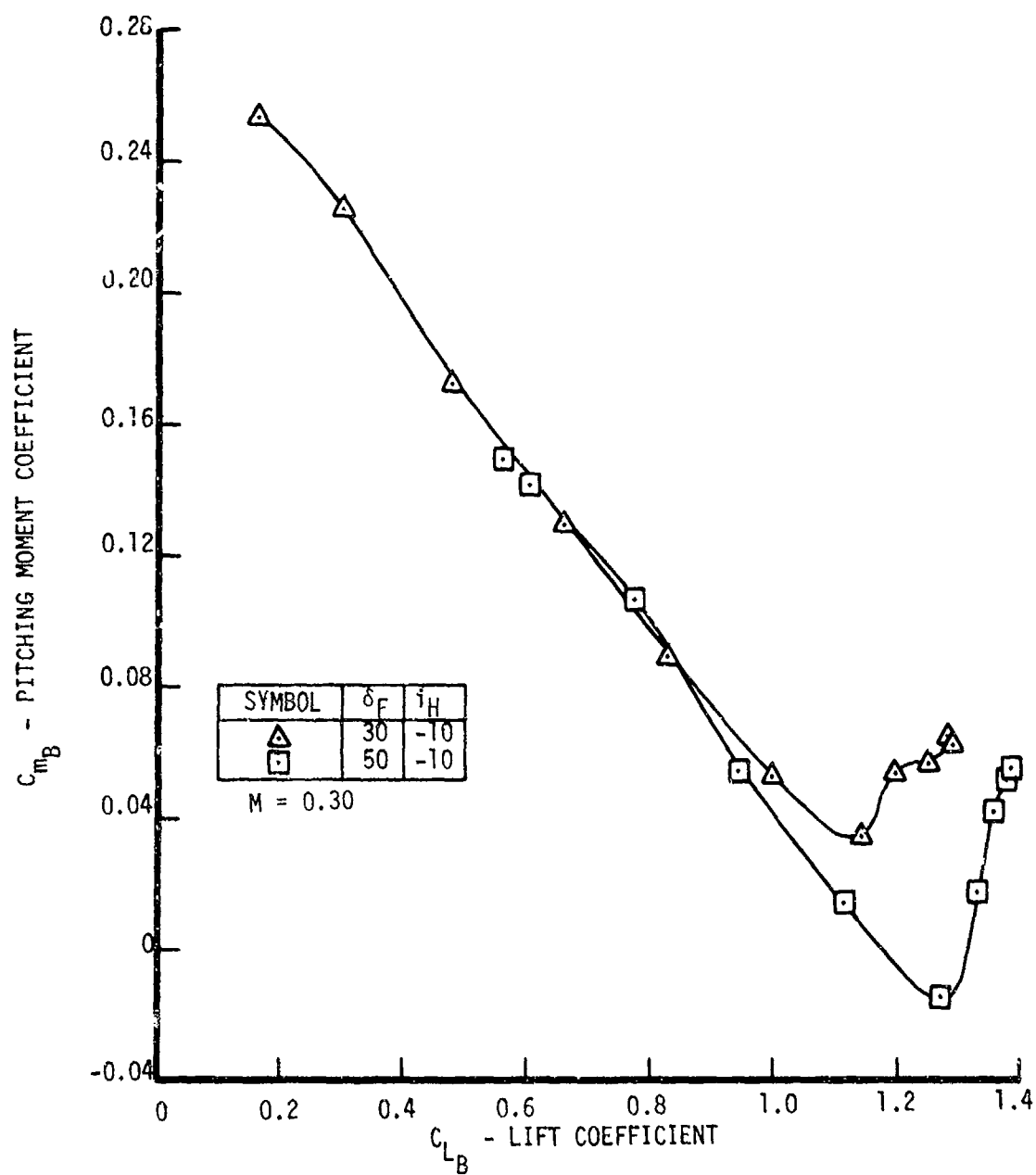


Figure 86. Variation of Pitching Moment of Basic KC-135A Model with Lift and Flap Deflection.  $M = 0.30$ .  $i_H = -10$  Degrees

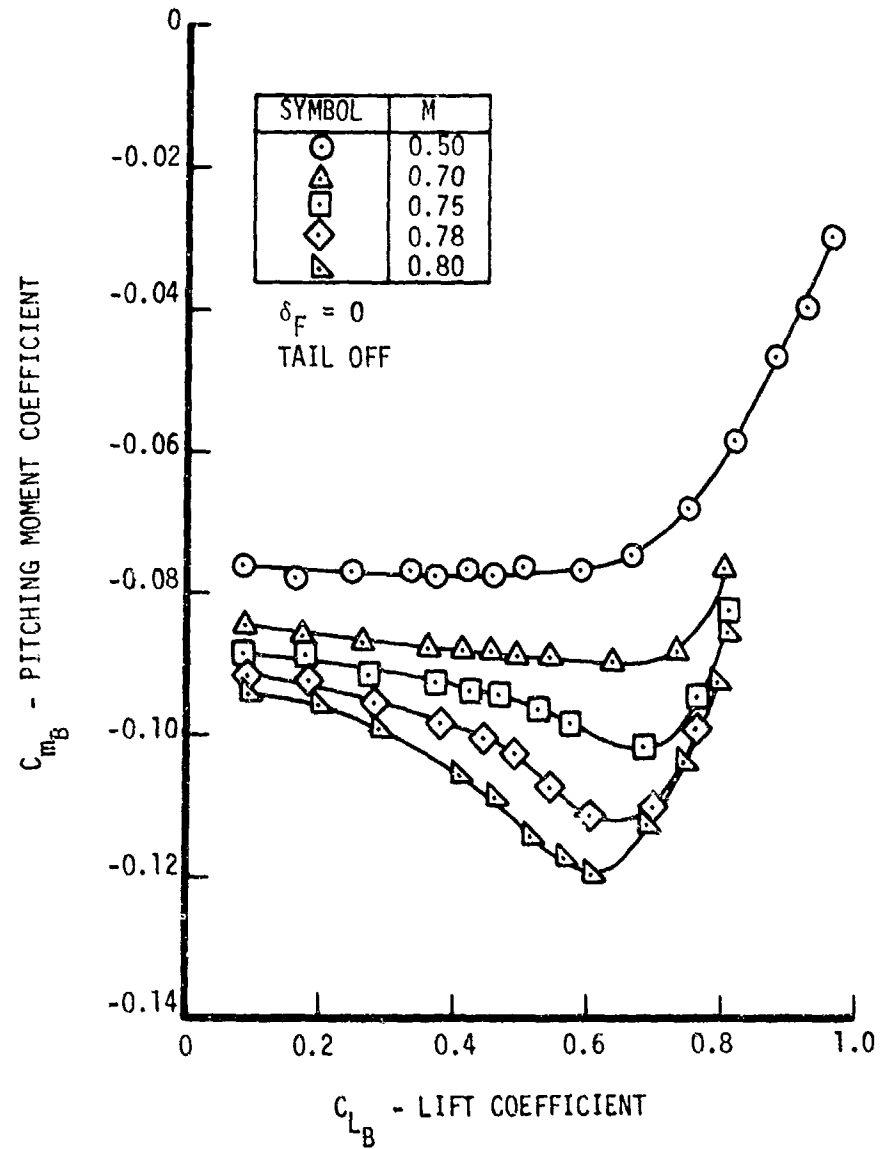


Figure 87. Variation of Pitching Moment of Basic KC-135A Model with Lift Near Cruise Conditions.  $\delta_F = 0$

AFFDL-TR-78-124

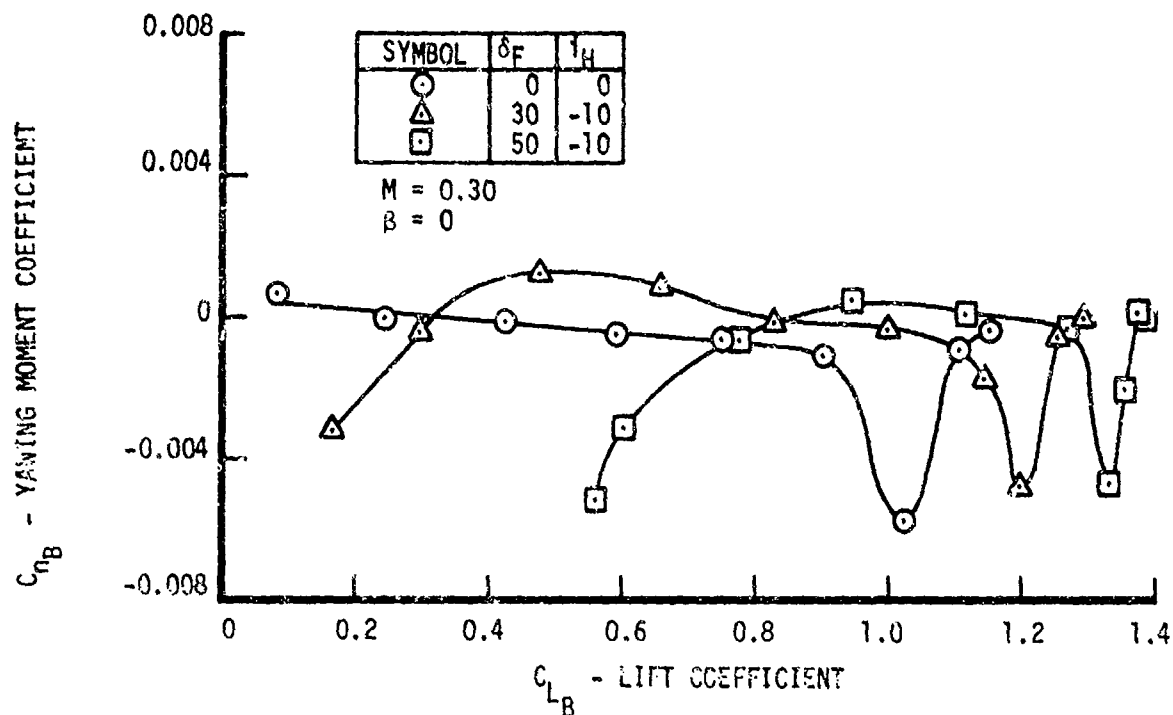


Figure 88. Variation of Yawing Moment of Basic KC-135A Model with Lift and Flap Deflection.  $M = 0.30$ .  
 $\beta = 0$

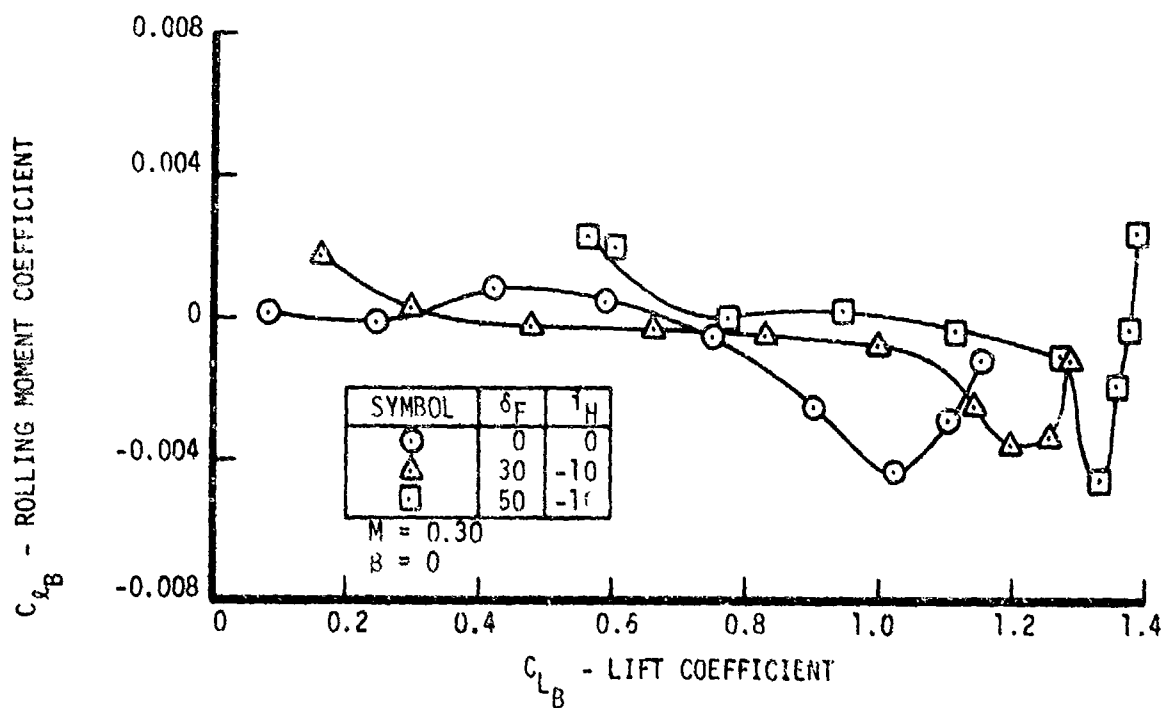


Figure 89. Variation of Rolling Moment of Basic KC-135A Model with Lift and Flap Deflection.  $M = 0.30$ .  
 $\beta = 0$

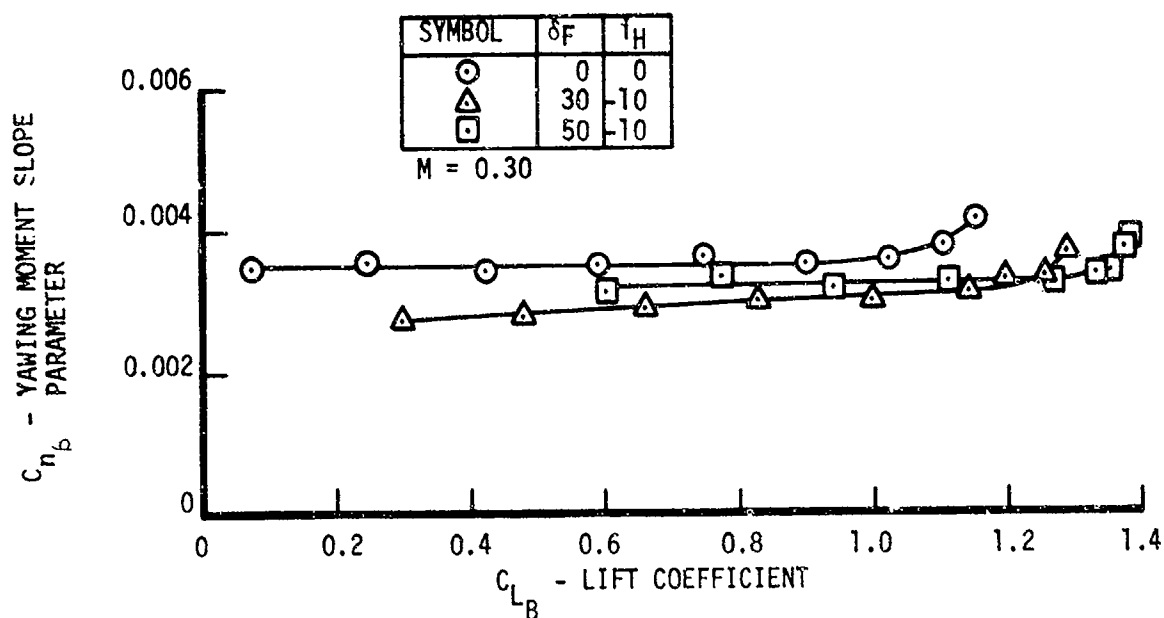


Figure 90. Variation of Yawing Moment Slope Parameter of Basic KC-135A Model with Lift and Flap Deflection.  $M = 0.30$

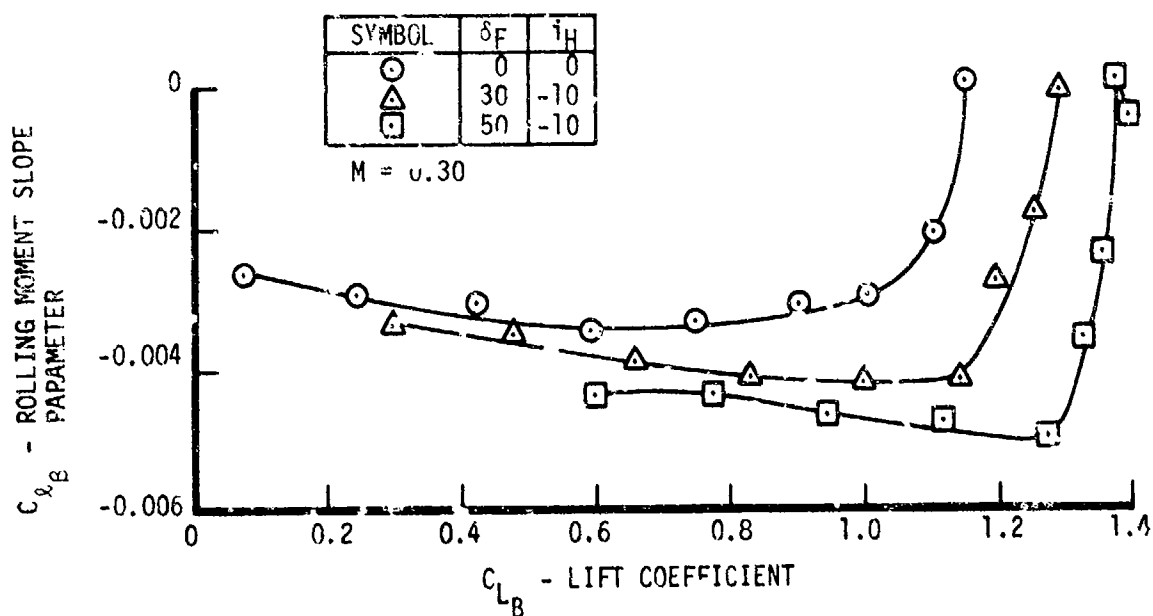


Figure 91. Variation of Rolling Moment Slope Parameter of Basic KC-135A Model with Lift and Flap Deflection.  $M = 0.30$



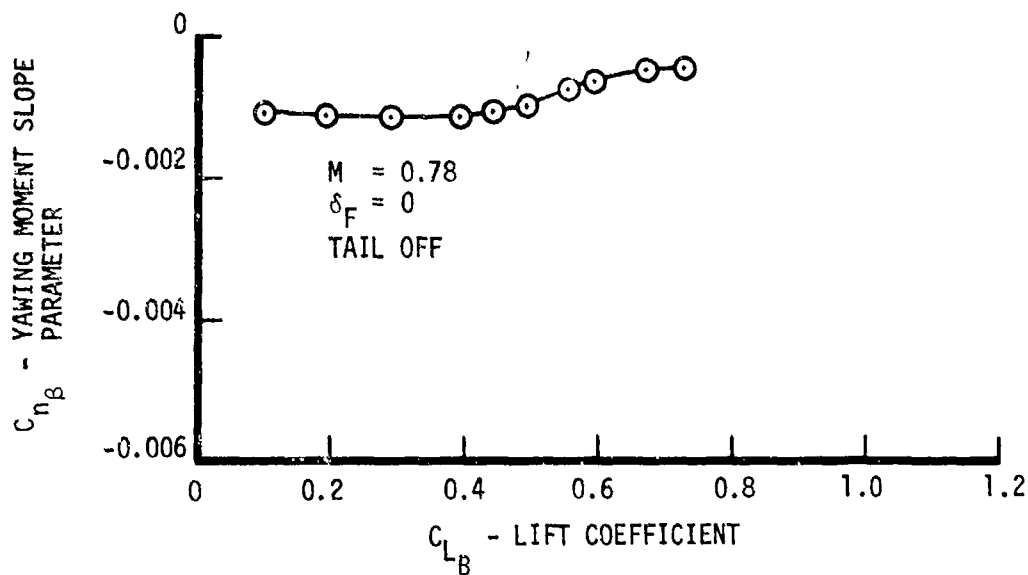


Figure 92. Variation of Yawing Moment Slope Parameter of Basic KC-135A Model with Lift Near Cruise Conditions.  $\delta_F = 0$

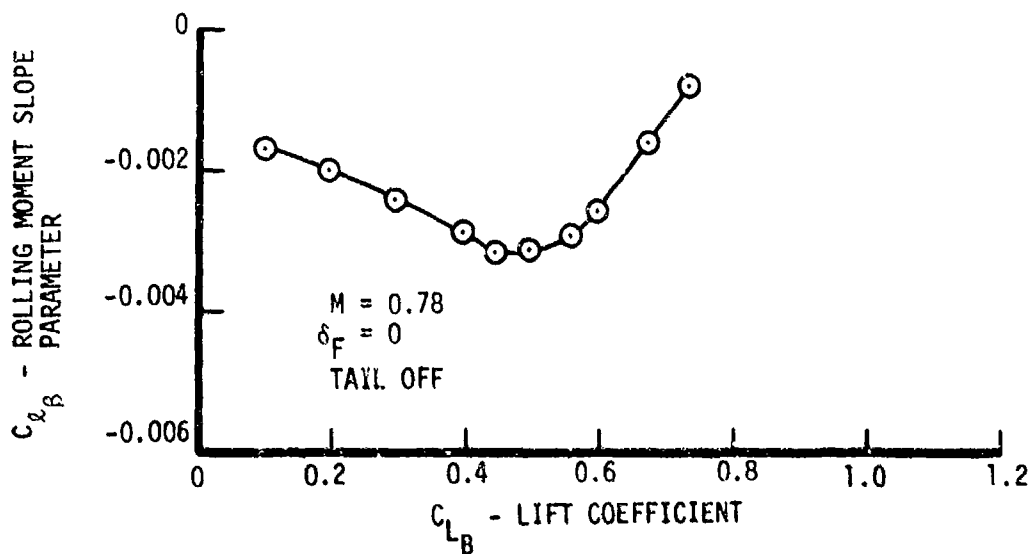


Figure 93. Variation of Rolling Moment Slope Parameter of Basic KC-135A Model with Lift Near Cruise Condition.  $\delta_F = 0$

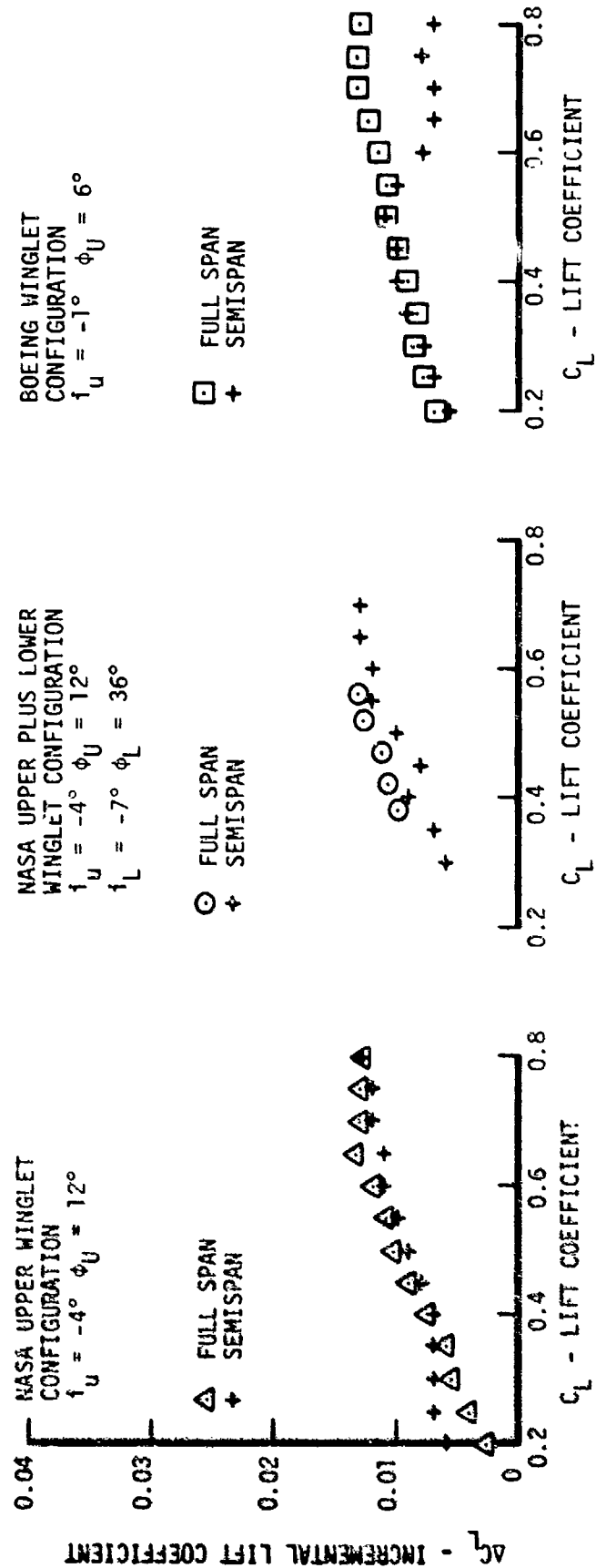


Figure 94. Comparison of Full-Span and Semispan Model Incremental Lift.  $M = 0.70$

Figure 95. Comparison of Full-Span and Semispan Model Incremental Lift.  $M = 0.78$

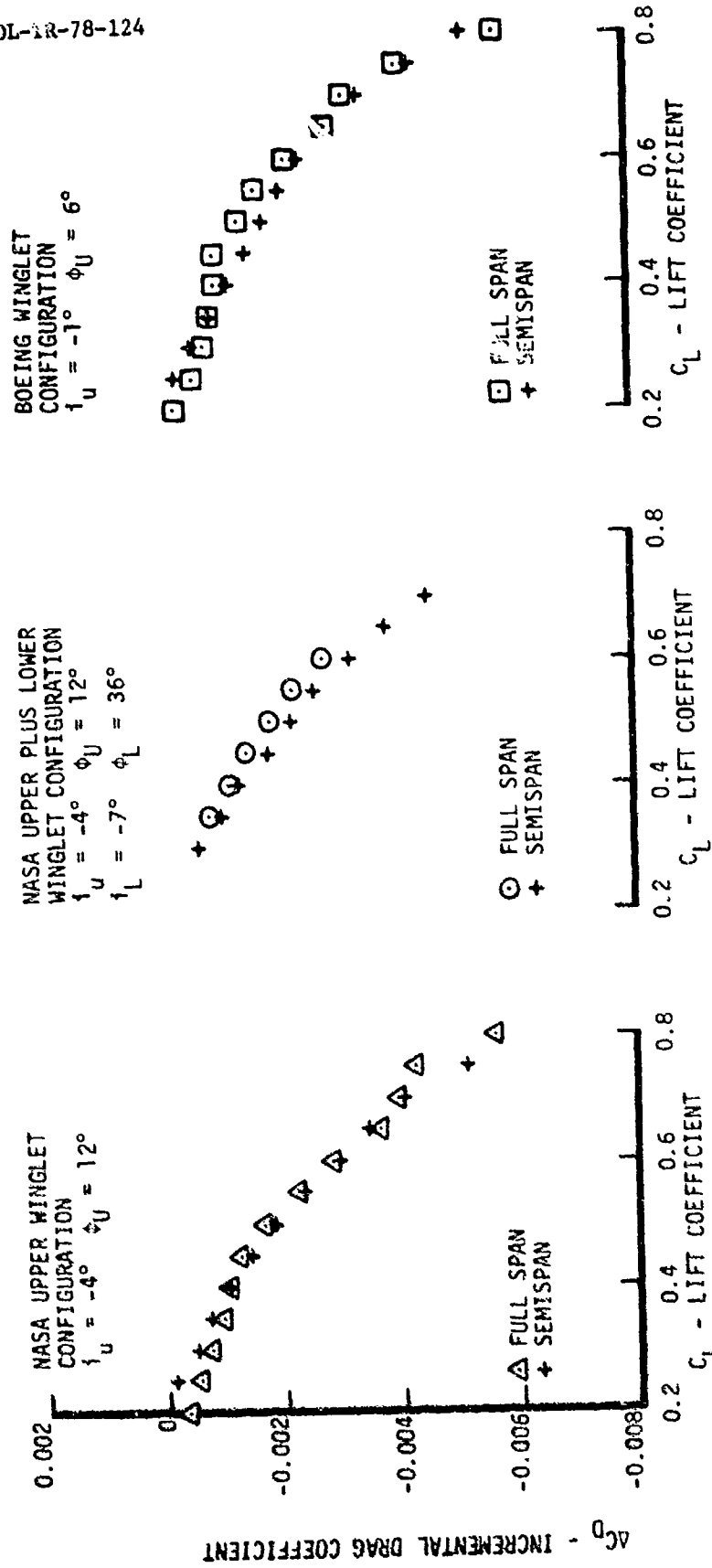


Figure 96. Comparison of Full-Span and Semispan Model Incremental Drag.  $M = 0.70$

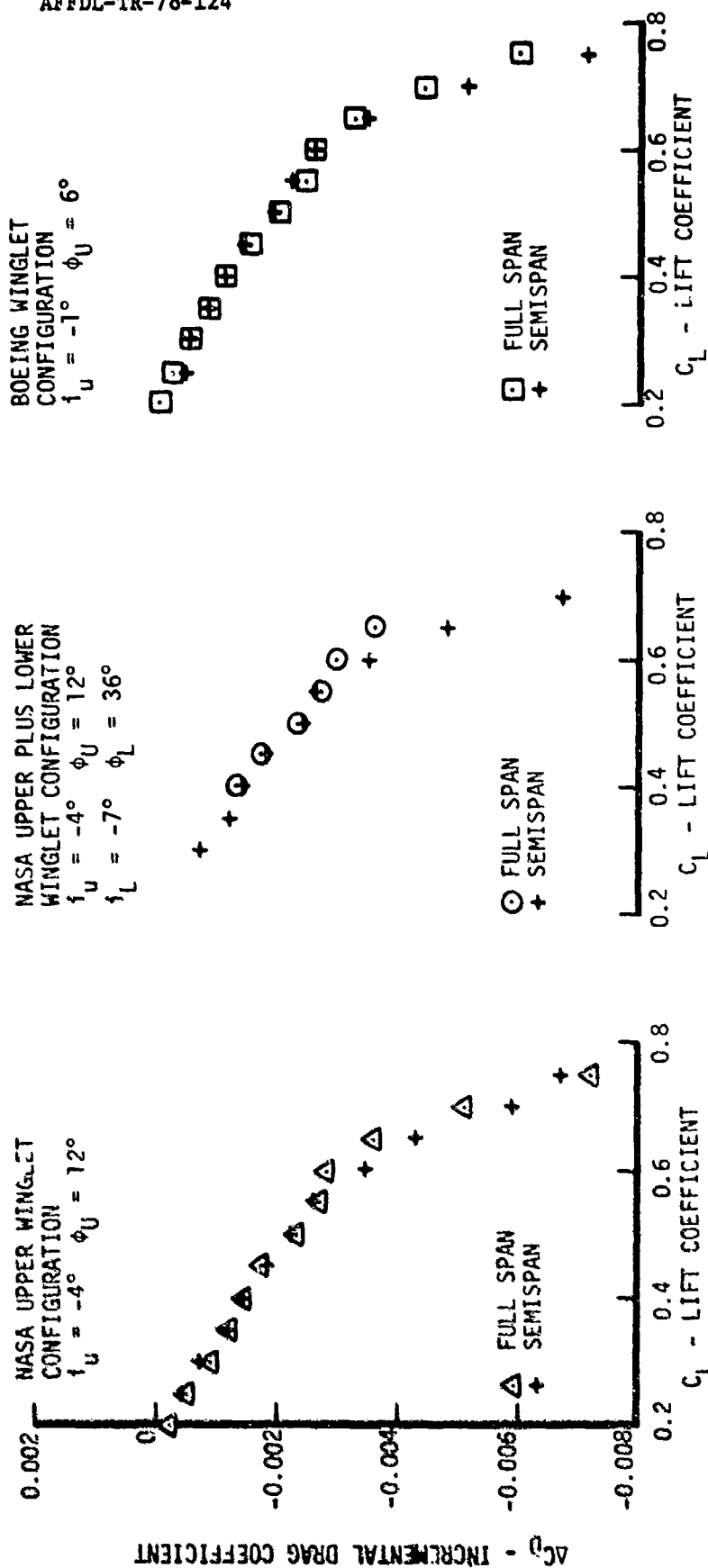


Figure 97. Comparison of Full-Span and Semispan Model Incremental Drag.  $M = 0.78$

#### REFERENCES

1. Ishimitsu, K. K., Van Devender, N., Dodson, R., et al, "Design and Analysis of Winglets for Military Aircraft," AFFDL-TR-76-6, February 1976.
2. Goldhammer, M. I., "Nonplanar Lifting Systems Method," Douglas Aircraft Company Report MDC J 6985, January 1976.
3. Whitcomb, Richard T., "A Design Approach and Selected Wind Tunnel Results at High Subsonic Speeds for Wing Tip Mounted Winglets," NASA TN D-8260, July 1976.
4. Ramlow, H. D., "Substantiation Data for the KC-135A Flight Manual," Boeing Document D6-5599, December 1964.